

The dilute A_L models and the $\Phi_{1,2}$ perturbation of unitary minimal CFTs.

J. Suzuki*

*Department of Physics,
Faculty of Science, Shizuoka University
Ohya 836, Shizuoka
Japan*

Abstract

Motivated by recent studies by Dorey, Pocklington and Tateo[24, 25] for unitary minimal models perturbed by $\phi_{1,2}$, we examine the thermodynamics of one dimensional quantum systems, whose counterparts in the 2D classical model are the dilute A_L models in regime 2. The functional relations for arbitrary values of L are established. Guided by numerical evidences, we obtain a set of coupled integral equations from the established relations, which yields the evaluation of the free energy at arbitrary temperature. In the scaling limit, the integral equations coincide with the thermodynamic Bethe ansatz equations (TBA) proposed in [25], thereby support their results. The new Fermionic representations of the Virasoro characters are shortly remarked.

*e-mail: sjsuzuk@ipc.shizuoka.ac.jp

1 Introduction

The Andrews-Baxter Forrester model [1] has been a prototype in the studies of integrable lattice models as well as the integrable $\Phi_{1,3}$ perturbation of the minimal unitary CFT.

The dilute A_L model proposed in [2, 3] deserves the same attention, as it represents a lattice analogue of the $\phi_{1,2}$ and $\phi_{2,1}$ perturbations of the minimal unitary CFT.

Especially, there are abundant research results on the dilute A_3 model in regime 2, which corresponds to the model of high interest, $M_{3,4} + \Phi_{1,2}$ theory. The latter belongs to the same universality class as the Ising model in a magnetic field at T_c , and is characterized by the famous E_8 structure[4]-[12]. There are several evidences for this coincidence, the central charge[2, 3], surface exponents [13] universal amplitude ratio [14, 15, 16] scaling dimensions[17] and excitation spectra [18]. The most impressive demonstration may be presented in [19], which confirms the hidden E_8 structure behind the thermodynamic Bethe ansatz equation (TBA, for short) of the dilute A_3 model. See also [20, 21].

Similarly, $M_{4,5} + \Phi_{1,2}(M_{6,7} + \Phi_{1,2})$ theory has the hidden $E_7(E_6)$ structure behind [4]. In spite of lack of relevant string hypothesis, the technique of the quantum transfer matrix (QTM) and the fusion relations make it possible to manifest the desired Lie algebraic structure in the TBA of the dilute $A_{3,4,6}$ in regime 2[22, 23].

The aim of the present report is to extend the result further; we will establish a closed set of fusion relations of the dilute A_L model for *arbitrary* L . From these relations, we derive the nonlinear integral equations (TBA) which yields the evaluation of the free energy of the corresponding 1D quantum model at arbitrary temperatures. This is obviously motivated by the recent progress in the study of the models as perturbed conformal field theories [24, 25]. The perturbation theory by an operator $\Phi_{1,2}$ or $\Phi_{2,1}$ encountered serious technical difficulties. The systematic studies on the bootstrap procedure on S matrix have been initiated in [26] and [27]. See also [28, 29]. The latter approach bases on the scaling q – state Potts field theory and will be relevant in our view point. It is only recently that the closed bootstrap procedure, associated to the Potts field theory, has been obtained for a set of S – matrices for a wide range of parameters by Dorey, Pocklington and Tateo[24]. The check of the results against a finite size system however, again poses a challenging problem because of the non-diagonal nature of the scattering theory. In [25], a set of involved TBA is conjectured by ingenious insights from special cases which have similarity to the TBA for the sine-Gordon model. They prepare pieces of TBA equations, one of which comes from Z_n models[30], then glue them together by respecting symmetries and by physical requirements. The resultant equations pass several nontrivial checks, however, lack firm grounds. It is thus interesting to see if it is possible to recover the Y – system [31, 32, 33], the algebraic version of the TBA, from the fusion relations of the dilute A_L model.

The functional relations among transfer matrices (the T – system) are determined by the fusion relations[34, 36]. The decomposition of the product of two modules at the singular points of the Boltzmann weight rules the latter. Thus the problem seems to be straightforward, at the first sight. This is, unfortunately, not true. There are often infinitely many functional relations for a given model. One thus has to choose a subset

which offers the closed $T-$ system with finitely many entries. Moreover, among the sets, the only those of which both sides contain fusion transfer matrices with good analytic properties (to be specified) will be relevant for the TBA. Therefore the problem of finding the relevant functional relations so as to reach the TBA is far from trivial.

It is well known that the dilute A_L model has $U_q(A_2^{(2)})$ symmetry at the critical point. The off-critical extension, deformed Virasoro algebra $\mathcal{V}_{x,r}(A_2^{(2)})$ plays a role in the vertex operator approach [37]. This elegant result, however, is not of our direct relevance. The crucial fact for the present study is, rather, that the fusion structure which is valid even away from criticality [38]; it possesses the fusion structures similar to $U_q(A_1^{(1)})$ and $U_q(A_2^{(1)})$. We will relate the former to breathers while the latter to the pseudo-particles constituting ladders in their TBA diagrams. In addition, we will introduce a set of objects which we call "magnon-like", characterized by similar diagrams to those associated with simply-laced Lie algebra (A, D and E). It turns out that they constitute closed functional relations with the good analyticity. They are three almost independent relations but for one common object T_{B_3} , which plays the role of glue. Thus the construction employed here makes the meaning of gluing in [25] very explicit.

We will introduce auxiliary functions, fusion transfer matrices,¹ labelled by skew Young diagrams[39, 40, 41, 42]. In view of the latter diagrams, proofs of the functional relations seem to be similar to those of the decomposition rules in the symmetric group. There are, however, extra complication due to the fact that our coupling constant in a sense lies at a "root of unity". Sometimes two (or even more) diagrams, with completely different disguise, correspond to an identical fusion transfer matrix. One must choose relevant expressions (diagrams) case by case in order to obtain suitable decompositions. This makes the proof of the functional relations simple but lengthy, unfortunately. There are four families of functional relations depending on the values of L and they need separate treatment at the present stage.

The validity of the obtained algebraic equations does not necessary legitimate the integral equations (TBA). We need another step to clarify the analytic structure of $Y-$ functions. This remains an important issue to be understood. In this report, we employ the direct numerical calculation by various range of parameters and adopt a simple conjecture on the analyticity. With the established functional relations and the assumption on the analyticity, it is then straightforward to transform the $T-$ system into $Y-$ system and then $Y-$ system into coupled integral equations[35]. In the scaling limit, the TBA proposed in [25] is recovered from them. A simple ansatz, suggested by numerics, on the zeros of fusion transfer matrices remarkably leads to the correct mass ratio of the particles determined by $S-$ matrix poles.

This paper is organized as follows. In the next section, we give a brief review on the dilute A_L models and the QTM method. Some obvious consistency of the lattice models and the CFT perturbed by $\Phi_{1,2}$ will be remarked. Section 3 is devoted to the discussion on fusion transfer matrices which are parameterized by skew Young diagrams. We introduce

¹We expect them to be the eigenvalues of transfer matrices of which fusion types are described by the diagrams. This is however yet to be proved. As our argument does not rely on whether this coincidence is true or not, we simply call the auxiliary functions as (eigenvalues of) fusion transfer matrices.

there important kinds of objects in section 4, 5 and 6. The first object introduced in section 4 seems to correspond to the breathers in [24] while the second one in section 5 is responsible for the ladder structure in the Y –system diagram in [25]. The section 6 is divided into 4 subsections, each is devoted to the discussion on "magnon-like" objects. In case of the dilute A_L model, L even, a fundamental role seems to be played by a "kink" transfer matrix, which is introduced in section 7. We will give a remark on the "reality property" of the magnon-like objects in section 8. Once fusion relations, the T –system, are established, it is readily transformed into Y –system. The explicit procedure will be discussed in section 9. The proofs of the T –system (or the "magnon-like" t –system) are simple but lengthy. Those for L even (odd) are somewhat similar. For brevity, we thus present the proof for $L = 4k + 2$ in the section 10 and $L = 4k + 1$ in the appendix F. In section 11, it will be shown that the conjectured TBA is naturally restored in a scaling limit. We conclude the paper with brief summary and discussion in section 12. A new fermionic formula for the Virasoro character found for $M_{5,6}$ is briefly commented.

2 The dilute A_L models and the quantum transfer matrix

The dilute A_L model is proposed in [2] as an elliptic extension of the Izergin-Korepin model [43]. The model is of the restricted SOS type with local variables $\in \{1, 2, \dots, L\}$. The variables $\{a, b\}$ on neighboring sites should satisfy the adjacency condition, $|a - b| \leq 1$, which is often described by a graph in fig.1. The following RSOS weights are found in [2]

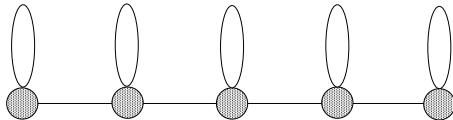


Figure 1: An incidence diagram for the dilute A_5 model. The local states corresponding to connected nodes can be located to nearest neighbor sites on a square lattice.

which satisfy the Yang-Baxter relation. They are parameterized by the spectral parameter u , the elliptic nome $q = e^{-\tau}$.

$$\begin{aligned}
a \boxed{u} a &= \frac{\theta_1(6-u)\theta_1(3+u)}{\theta_1(6)\theta_1(3)} - \frac{\theta_1(u)\theta_1(3-u)}{\theta_1(6)\theta_1(3)} \times \\
&\quad \left(\frac{S_{a+1}}{S_a} \frac{\theta_4(2a-5)}{\theta_4(2a+1)} + \frac{S_{a-1}}{S_a} \frac{\theta_4(2a+5)}{\theta_4(2a-1)} \right), \\
a \pm 1 \boxed{u} a &= a \boxed{u} a = \frac{\theta_1(3-u)\theta_4(\pm 2a+1-u)}{\theta_1(3)\theta_4(\pm 2a+1)}, \\
a \pm 1 \boxed{u} a &= a \boxed{u} a \pm 1 = \left(\frac{S_{a\pm 1}}{S_a} \right)^{1/2} \frac{\theta_1(u)\theta_4(\pm 2a-2+u)}{\theta_1(3)\theta_4(\pm 2a+1)}, \\
a \boxed{u} a \pm 1 &= a \pm 1 \boxed{u} a \pm 1 = \left(\frac{\theta_4(\pm 2a+3)\theta_4(\pm 2a-1)}{\theta_4^2(\pm 2a+1)} \right)^{1/2} \frac{\theta_1(u)\theta_1(3-u)}{\theta_1(2)\theta_1(3)}, \\
a \pm 1 \boxed{u} a \mp 1 &= \frac{\theta_1(2-u)\theta_1(3-u)}{\theta_1(2)\theta_1(3)}, \\
a \pm 1 \boxed{u} a \mp 1 &= - \left(\frac{S_{a-1}S_{a+1}}{S_a^2} \right)^{1/2} \frac{\theta_1(u)\theta_1(1-u)}{\theta_1(2)\theta_1(3)}, \\
a \pm 1 \boxed{u} a \pm 1 &= \frac{\theta_1(3-u)\theta_1(\pm 4a+2+u)}{\theta_1(3)\theta_1(\pm 4a+2)} \\
&\quad + \frac{S_{a\pm 1}}{S_a} \frac{\theta_1(u)\theta_1(\pm 4a-1+u)}{\theta_1(3)\theta_1(\pm 4a+2)}, \quad \text{for } \pm 4a+2 \neq 0, \\
&= \frac{\theta_1(3+u)\theta_1(\pm 4a-4+u)}{\theta_1(3)\theta_1(\pm 4a-4)} \\
&\quad + \left(\frac{S_{a\mp 1}\theta_1(4)}{S_a\theta_1(2)} - \frac{\theta_4(\pm 2a-5)}{\theta_4(\pm 2a+1)} \right) \frac{\theta_1(u)\theta_1(\pm 4a-1+u)}{\theta_1(3)\theta_1(\pm 4a-4)}, \text{ otherwise .(1)}
\end{aligned}$$

Here $\theta_{1,4}(x) = \vartheta_{1,4}(\lambda x, \tau)$,

$$\begin{aligned}
\vartheta_1(x, \tau) &= 2q^{1/4} \sin x \prod_{n=1}^{\infty} (1 - 2q^{2n} \cos 2x + q^{4n})(1 - q^{2n}), \\
\vartheta_4(x, \tau) &= \prod_{n=1}^{\infty} (1 - 2q^{2n-1} \cos 2x + q^{4n-2})(1 - q^{2n}), \\
S_a &= (-1)^a \frac{\theta_1(4a)}{\theta_4(2a)}.
\end{aligned}$$

Note an important property, the standard initial condition, that only those weights with identical variables on the NE and the SW diagonal remain nonzero when $u \rightarrow 0$.

The crossing parameter λ needs to be a function of L for the restriction. The model exhibits four different physical regimes depending on parameters[2, 3],

- regime 1. $0 < u < 3$, $\lambda = \frac{\pi L}{4(L+1)}$, $L \geq 2$
- regime 2. $0 < u < 3$, $\lambda = \frac{\pi(L+2)}{4(L+1)}$, $L \geq 3$

- regime 3. $3 - \frac{\pi}{\lambda} < u < 0$, $\lambda = \frac{\pi(L+2)}{4(L+1)}$, $L \geq 3$
- regime 4. $3 - \frac{\pi}{\lambda} < u < 0$, $\lambda = \frac{\pi L}{4(L+1)}$, $L \geq 2$.

In the low temperature limit, the ground states correspond to ferromagnetic ordered states in regime 1 and 2 in which we are interested.

As usual, we define the row to row transfer matrix $T_{\text{RTR}}(u)$ by

$$(T_{\text{RTR}}(u))_{\{a\}}^{\{b\}} = \prod_{j=1}^M b_j \boxed{u}_{a_j} b_{j+1}.$$

Denoting its largest eigenvalue by the same symbol, $T_{\text{RTR}}(u)$, the free energy per site of the 2D classical model in thermodynamic limit reads, $\beta f = -\lim_{M \rightarrow \infty} \frac{1}{M} \log T_{\text{RTR}}(u)$. Several other quantities other than the free energy have been evaluated for the models. For example, we mention the explicit one point functions elaborated in [17].

We are not dealing with the dilute A_L model directly but its one dimensional quantum counterpart.

The Hamiltonian for the latter is defined by

$$\mathcal{H} = -2 \frac{\partial}{\partial u} \ln T_{\text{RTR}}(u)|_{u=0} \quad (2)$$

as in [19]. The explicit form of the Hamiltonian is not needed in the following argument.

We are interested in the free energy of the 1D model at finite temperatures. The success in the previous studies on the thermodynamics of 1D quantum systems depends on the efficient conjectures on the dominant solutions of the Bethe ansatz equation in the thermodynamic limit, the string hypothesis. It seems too difficult to perform the same procedure for arbitrary L . Instead, we apply another machinery, the method of the quantum transfer matrix (QTM)[44]-[48].

The quantity of our interest is the partition function of the 1D model,

$$Z_{\text{1D}} = \text{tr} e^{-\beta \mathcal{H}}.$$

The first step is to rewrite this as the partition function of the 2D model, defined on $M \times N$ square lattice by a simple trick,

$$Z_{\text{1D}} = \lim_{N \rightarrow \infty} \text{tr} (e^{-\frac{\beta}{N} \mathcal{H}})^N = \lim_{N \rightarrow \infty} \text{Tr} (\mathcal{T}^\vee)^N = \lim_{N \rightarrow \infty} \text{Tr} Z_{\text{2D}}. \quad (3)$$

The fictitious dimension, N , is referred to as the Trotter number. \mathcal{T}^\vee is a kind of transfer matrix, composed of matrix elements of $e^{-\frac{\beta}{N} \mathcal{H}}$.

In order to relate \mathcal{T}^\vee to the row to row transfer matrix above, we introduce a rotated transfer matrix, $\tilde{T}_{\text{RTR}}(u)$,

$$(\tilde{T}_{\text{RTR}}(u))_{\{a\}}^{\{b\}} = \prod_{j=1}^M b_j \boxed{z}_{a_j} b_{j+1}.$$

Thank to (2) and the standard initial condition, we immediately see,

$$T_{\text{RTR}}(u) \sim P_R e^{-\frac{u}{2}\mathcal{H}+O(u^2)}, \quad \tilde{T}_{\text{RTR}}(u) \sim P_L e^{-\frac{u}{2}\mathcal{H}+O(u^2)},$$

where $P_R(P_L)$ is the right (left) shift operator, commuting with the Hamiltonian and $P_L P_R = P_R P_L =$ the identity operator. Then the desired expression for \mathcal{T}^\vee is obtained

$$\mathcal{T}^\vee = T_{\text{RTR}}\left(\frac{\beta}{N}\right)\tilde{T}_{\text{RTR}}\left(\frac{\beta}{N}\right)$$

where the limit $N \rightarrow \infty$ is assumed in the both sides. The eigenvalues of \mathcal{T}^\vee are highly degenerated in $N \rightarrow \infty$, which makes the summation in the partition function difficult to perform. The intriguing observation [44] is that if one defines yet another transfer matrix \mathcal{T} , the quantum transfer matrix (QTM), propagating in the horizontal direction, then there is a gap in between the largest and the second largest eigenvalues which remains non vanishing in the limit $N \rightarrow \infty$. Now that $Z_{1D} \sim \text{Tr} \mathcal{T}^M$ and $M \rightarrow \infty$, the *only* largest eigenvalue of \mathcal{T} is necessary in the evaluation of (3).

In the most sophisticated formulation[49], the QTM is defined with one further variable x ,

$$(T_{\text{QTM}}(u, x))_{\{a\}}^{\{b\}} = \prod_{j=1}^{N/2} \frac{b_{2j-1}}{a_{2j-1}} \begin{array}{|c|} \hline u+ix \\ \hline \end{array}^{b_{2j}}_{a_{2j}} \frac{b_{2j}}{a_{2j}} \begin{array}{|c|} \hline \begin{array}{c} z \\ \downarrow \\ \bar{z} \end{array} \\ \hline \end{array}^{b_{2j+1}}_{a_{2j+1}}.$$

By taking $x = 0$ one recovers \mathcal{T} .

The commutative property of QTMs with fixed u is crucial in the QTM formulation,

$$[T_{\text{QTM}}(u, x), T_{\text{QTM}}(u, x')] = 0.$$

It represents the existence of infinitely many conserved quantities commuting with QTM, which may be a key in the exact enumeration of the free energy at arbitrary temperatures. Since we will adopt identical value for $u = \frac{\beta}{N}$ for commuting QTM, it will be dropped afterwards.

Let us explicitly write again that the free energy per site is represented *only* by the largest eigenvalue of T_{QTM} with $x = 0$ and $u = \frac{\beta}{N}$

$$\begin{aligned} \beta f &= -\lim_{M \rightarrow \infty} \frac{1}{M} \ln \text{Tr} \exp(-\beta \mathcal{H}) \\ &= -\lim_{N \rightarrow \infty} \ln \left(\text{the largest eigenvalue of } T_{\text{QTM}}(x=0) \right). \end{aligned}$$

Our aim is thus to evaluate the largest eigenvalue of QTM. This is again not so simple problem as it seems at the first sight. The coupling constant u depends on the fictitious system size, Trotter number, which makes it difficult to take the limit $N \rightarrow \infty$.

Our strategy is to introduce auxiliary transfer matrices (fusion transfer matrices) commuting with QTM and to explore functional relations among them [22, 23, 50, 51, 52, 53]. We find the latter relations, if suitable subset is chosen, are efficient enough to yields the

evaluation of the largest eigenvalue of T_{QTM} for arbitrary N : The functional relations can be transformed into coupled integral equations whose solution yields the desired quantity. The resultant equations admit to take the limit $N \rightarrow \infty$ without any difficulty.

In the next section, we will introduce the fusion transfer matrices. Before doing so, we mention a simple evidence that the dilute A_L model (or its 1D analogue) is a lattice analogue of the minimal unitary model perturbed by $\Phi_{1,2}$ or $\Phi_{2,1}$ operator. In TBA formulation, the dressed energy function ϵ and $Y = \exp(\epsilon)$ are main objects. It is pointed out in [54] that, within framework of TBA, it seems too difficult to show analytically that the small r expansion coincides with the result from the conformal perturbation theory. The hidden periodicity of the Y –system, found by a brute-force substitution, partially resolves the problem [31].

We will show, within our formalism, Y is expressible by ratios of fusion transfer matrices. Therefore in our view point, the periodicity of Y (and ϵ) is a consequence of the periodicity of the original Boltzmann weights. In view of the rapidity variable $\theta \equiv \frac{x\pi}{3}$, the periods read

$$P_\theta = \begin{cases} \frac{4(L+1)\pi}{3L}, & \text{for regime 1} \\ \frac{4(L+1)\pi}{3(L+2)}, & \text{for regime 2.} \end{cases} \quad (4)$$

From this one can read off the scaling dimension of the perturbed field by $\Delta = 1 - \frac{\pi}{P_\theta}$, explicitly,

$$\Delta = \begin{cases} \frac{p+3}{4p}, & \text{for regime 1} \\ \frac{p-2}{4(p+1)}, & \text{for regime 2.} \end{cases} \quad (5)$$

Note that we adopted a different identification,

$$p = \begin{cases} L+1 & \text{for regime 1} \\ L & \text{for regime 2.} \end{cases} \quad (6)$$

They coincide with the scaling dimensions $\Delta_{2,1}$ and $\Delta_{1,2}$ in the unitary model $M_{p,p+1}$. This thus supports the hypothesis that the dilute A_L models in regime 1 (regime 2) are lattice regularizations of perturbed minimal models $M_{p,p+1}$ under the identification (6).

From now on, we restrict our argument to the regime 2. As is announced, the fusion transfer matrices will be examined in the next section.

3 The fusion transfer matrices and quantum Jacobi-Trudi formula

Any model integrable in the sense of the Yang-Baxter relation offers a systematic way of generalizations, the fusion procedure. It utilizes the singular values of spectral parameter at which the Boltzmann weights reduce to projectors to a subspace. In [38], a detailed description is given for the explicit procedures to obtain "generalized" Boltzmann weights.

The explicit construction of these weights for various fusion types is not of issue in this report. Rather, the main objects of our interest are functional relations which involves QTM. In the following we introduce several auxiliary functions which generalizes QTM. We expect that they corresponds to eigenvalues of transfer matrices made by the fusion procedure. We, however, do not attempt to prove this, as it is not necessary for the evaluation of free energy.

The most important building block in our argument is the following expression for the (any) eigenvalues of QTM, which we will denote by $T_1(x)$,

$$\begin{aligned}
T_1(x) &= w\phi(x + \frac{3}{2}i)\phi(x + \frac{1}{2}i)\frac{Q(x - \frac{5}{2}i)}{Q(x - \frac{1}{2}i)} + \phi(x + \frac{3}{2}i)\phi(x - \frac{3}{2}i)\frac{Q(x - \frac{3}{2}i)Q(x + \frac{3}{2}i)}{Q(x - \frac{1}{2}i)Q(x + \frac{1}{2}i)} \\
&+ w^{-1}\phi(x - \frac{3}{2}i)\phi(x - \frac{1}{2}i)\frac{Q(x + \frac{5}{2}i)}{Q(x + \frac{1}{2}i)}, \\
Q(x) &:= \prod_{j=1}^N h[x - x_j] \\
\phi(x) &:= \left(\frac{h[x + (\frac{3}{2} - u)i]h[x - (\frac{3}{2} - u)i]}{h[2i]h[3i]} \right)^{\frac{N}{2}}, \quad h[x] := \theta_1(ix),
\end{aligned} \tag{7}$$

where $w = \exp(i\frac{\pi\ell}{L+1})$ and $\ell = 1$ for the largest eigenvalue sector. It is often referred to as the dressed vacuum form.

The parameters, $\{x_j\}$ are solutions to "Bethe ansatz equation" (BAE)[19],

$$w\frac{\phi(x_j + i)}{\phi(x_j - i)} = -\frac{Q(x_j - i)Q(x_j + 2i)}{Q(x_j + i)Q(x_j - 2i)}, \quad j = 1, \dots, N. \tag{8}$$

We introduce

$$P = \begin{cases} \frac{4(L+1)}{L}, & \text{for regime 1} \\ \frac{4(L+1)}{L+2}, & \text{for regime 2.} \end{cases} \tag{9}$$

Then the periodicity $T_1(x) = T_1(x + Pi)$ follows obviously from the above expression.

We represent the three terms in eigenvalue of the quantum transfer matrix by three boxes with letter 1,2 and 3 suffixed by the spectral parameter .

$$\begin{aligned}
T_1(u, x) &= \boxed{1}_x + \boxed{2}_x + \boxed{3}_x, \\
\boxed{1}_x &:= w\phi(x + \frac{3}{2}i)\phi(x + \frac{1}{2}i)\frac{Q(x - \frac{5}{2}i)}{Q(x - \frac{1}{2}i)} \\
\boxed{2}_x &:= \phi(x + \frac{3}{2}i)\phi(x - \frac{3}{2}i)\frac{Q(x - \frac{3}{2}i)Q(x + \frac{3}{2}i)}{Q(x - \frac{1}{2}i)Q(x + \frac{1}{2}i)} \\
\boxed{3}_x &= w^{-1}\phi(x - \frac{3}{2}i)\phi(x - \frac{1}{2}i)\frac{Q(x + \frac{5}{2}i)}{Q(x + \frac{1}{2}i)}.
\end{aligned} \tag{10}$$

These boxes are analogue to those for Young tableaux and play a fundamental role in the following.

3.1 The symmetric fusion structure

In the bootstrap procedure of the $S-$ matrix, ϕ^3 property is most essential. The similar feature, referred to as the $a_2^{(2)}$ fusion structure, as been discussed in the dilute A_L model [38]. This comes from the singularity of the RSOS weights at $u = \pm 2$.

Due to the fusion procedure, the eigenvalue of a fusion QTM can be represented by sum over products of "boxes" with different letters and spectral parameters. The point is that the sum of such boxes can be identified with Semi-Standard Young Tableaux (SST) for sl_3 . Let us present a simple example. See [39, 41, 40, 38, 55] for details. By the fusion procedure, one can construct a transfer matrix of which auxiliary space acts on a symmetric subspace of $V \times V$. We associate this to the set of the SST, $\boxed{i_1 i_2}$, ($i_1 \leq i_2$). The eigenvalue of the transfer matrix is then represented by,

$$\sum_{i_1 \leq i_2} \boxed{i_1}_{x-i} \boxed{i_2}_{x+i}.$$

In a same manner, one can introduce fusion models based on general Young diagrams, of which eigenvalues are specified by their shapes. On each diagram, the spectral parameter changes by $+2i$ from left to right and $-2i$ from top to the bottom.

First, we argue QTMs associated to rectangular shape diagrams. Although they are simpler, some of the properties below are crucial for the discussion for QTMs associated to complex Young diagrams. First, due to identities,

$$\boxed{\begin{matrix} 1 \\ 2 \end{matrix}}_{x-i}^{x+i} = \phi_2(x) \boxed{1}_x, \quad \boxed{\begin{matrix} 1 \\ 3 \end{matrix}}_{x-i}^{x+i} = \phi_2(x) \boxed{2}_x$$

$$\boxed{\begin{matrix} 2 \\ 3 \end{matrix}}_{x-i}^{x+i} = \phi_2(x) \boxed{3}_x, \quad \phi_2(x) := \phi(x \pm \frac{5}{2}i) \quad (11)$$

$$\boxed{\begin{matrix} 1 \\ 2 \\ 3 \end{matrix}}_{x-2i}^{x+2i} = \phi_3(x) := \prod_{j=1}^3 \phi(x \pm (\frac{9}{2} - j)i), \quad (12)$$

the QTMs from $2 \times m$ ($3 \times m$) Young diagram can be reduced to those from $1 \times m$ (or just scalars). Hereafter we adopt abbreviations for any function f ,

$$f(x \pm ia) := f(x + ia)f(x - ia).$$

The first three relations brings additional symmetry besides sl_3 , and make the $a_2^{(2)}$ symmetry explicit. We call this the $a_2^{(2)}$ structure hereafter.

Second, the eigenvalues of $1 \times m$ fusion QTMs have the "duality" in the following sense. Let us denote a renormalized $1 \times m$ fusion QTMs by $T_m(x)$;

$$T_m(x) = \frac{1}{f_m(x)} \sum \boxed{i_1 \ i_2 \ \cdots \ i_3} \quad (13)$$

where the semi-standard (SS) condition $i_1 \leq i_2 \leq \cdots \leq i_m$ is imposed on the summation. The spectral parameters are assigned $x - i(m-1) \cdots x + i(m-1)$ from left to right. The renormalization factor, which is the common factor of the expressions from tableaux of length m , is given by

$$f_m(x) := \prod_{j=1}^{m-1} \phi(x \pm i(\frac{2m-1}{2} - j)),$$

such that the resultant T_m 's are all degree $2N$ w.r.t. $h[x + \text{shift}]$. For later convenience, we also denote by $T_m^{\text{non}}(x)$, the un-renormalized $T_m(x)$, namely, the object without the factor $f_m(x)$ in (13). Obviously, we have a periodicity due to Boltzmann weights;

$$T_m(x + Pi) = T_m(x). \quad (T_m^{\text{non}}(x + Pi) = T_m^{\text{non}}(x))$$

where P is defined in (9).

Hereafter, we frequently use functions of which argument is shifted by the half period in the imaginary direction, i.e., $x + i\frac{P}{2}$. We shall denote them by a symbol \vee . For example,

$$T_m^\vee(x) = T_m(x + \frac{P}{2}i).$$

The following functional relations are direct consequence of the $a_2^{(2)}$ structure.

$$T_m(x - i)T_m(x + i) = g_m(x)T_m(x) + T_{m+1}(x)T_{m-1}(x), \quad m \geq 1 \quad (14)$$

$$\begin{aligned} g_m(x) &= \phi(x \pm i(m + \frac{3}{2})), \\ T_{-1}(x) &:= 0 \\ T_0(x) &:= f_2(x). \end{aligned} \quad (15)$$

The scalar function $g_m(x)$ satisfies,

$$g_{2L-1-m}(x) = \begin{cases} g_m(x), & \text{if } L \text{ is even} \\ g_m^\vee(x), & \text{if } L \text{ is odd.} \end{cases}$$

The adjacency condition leads to $T_{2L}(x) = T_{2L+1}(x) = 0$. Thus one deduces the duality relations,

$$T_m(x) = \begin{cases} T_{2L-1-m}(x), & m = 0, \dots, 2L \quad \text{for } L \text{ even} \\ T_{2L-1-m}^\vee(x), & m = 0, \dots, 2L \quad \text{for } L \text{ odd} \end{cases} \quad (16)$$

for the solutions to eq.(14). Note that this duality is not valid for $T_m^{\text{non}}(x)$; obviously $T_{2L-1-m}^{\text{non}}(x)$ and $T_m^{\text{non}}(x)$ have different order in $h[x]$. These relations can be in principle proved by using explicit fusion weights. We have at least checked this numerically and assume the validity in this report.

The duality brings about many relations. It thus happens seemingly quite different equations are identical; an identical object can have (infinitely) many equivalent expressions. It sometimes makes the proof of the functional relations quite involved.

Before closing this section, we make a comment.

The simple relation (14) suggests a choice of Y function,

$$Y_m(x) = \frac{T_{m+1}(x)T_{m-1}(x)}{g_m(x)T_m(x)} \quad (m = 1, \dots, 2L-2). \quad (17)$$

This leads to a set of simple equations (the Y -system)[55]

$$\mathcal{Y}_m(x-i)\mathcal{Y}_m(x+i) = \frac{(1+\mathcal{Y}_{m+1}(x))(1+\mathcal{Y}_{m-1}(x))}{1+\mathcal{Y}_m(x)}. \quad (18)$$

The relations seem to be tractable and they indeed work well in a nonunitary case [57]. This is not the case for the unitary models. The transformation of the Y -system into a simple set of integral equations requires the both sides to be Analytic and NonZero and to have Constant asymptotic behavior as $|x| \rightarrow \infty$ (ANZC) in certain strips.

As is demonstrated numerically in appendix in the case of $L = 8$ in appendix G, this requirement is not satisfied for (18). Therefore we must seek for alternatives, which may not be found only among symmetric fusion transfer matrices.

In the next subsection, we thus consider a much wider class of skew Young diagrams.

3.2 The quantum Jacobi-Trudi formula

Let μ and λ be a pair of Young diagrams satisfying $\mu_i \geq \lambda_i, \forall i$. We subtract a diagram λ from μ . The resultant "narrower" one, consisted of $(\mu_1 - \lambda_1, \mu_2 - \lambda_2, \dots)$ boxes is called a skew Young diagram $\mu - \lambda$. (The usual Young diagram is the special case that λ is empty, and we will omit λ in the case hereafter.)

Consider a set of semi-standard skew Young table of the shape $\mu - \lambda$. The spectral parameters are assigned to boxes in a table such that they change by $+2i$ from left to right and $-2i$ from top to the bottom. The spectral parameters of the head (left-top) and the tail (right-bottom) are fixed to be $x + i(\mu_1 + \mu'_1 - 2)$ and $x - i(\mu_1 + \mu'_1 - 2)$ where μ'_1 denotes the depth of the diagram. One identifies each box in a table with an expression under the rule (10) with a shift of the spectral parameter. Then the product over all constituting boxes yields the desired expression for a table. We then have the following theorem which is a quantum analogue to Jacobi-Trudi formula for the Schur function.

Theorem 1. *Let $\mathcal{T}_{\mu/\lambda}(x)$ be the sum over the resultant expressions divided by a common factor, $\prod_{j=1}^{\mu'_1} f_{\mu_j - \lambda_j}(x + i(\mu'_1 - \mu_1 + \mu_j + \lambda_j - 2j + 1))$. Then the following equality holds[39, 40].*

$$\mathcal{T}_{\mu/\lambda}(x) = \det_{1 \leq j, k \leq \mu'_1} (T_{\mu_j - \lambda_k - j + k}(x + i(\mu'_1 - \mu_1 + \mu_j + \lambda_k - j - k + 1))) \quad (19)$$

where $T_{m<0} := 0$.

$\mathcal{T}_{\mu/\lambda}(x)$ may be naturally identified with the eigenvalue of QTM corresponding to fusion $\mu - \lambda$, although this is yet to be proved. We note that the pole-free property of $\mathcal{T}_{\mu/\lambda}(x)$, obvious from the quantum Jacobi-Trudi formula.

Due to the semi-standard condition, products of $\mathcal{T}_{\mu/\lambda}(x)$ enjoy the decomposition similar to that of the products of Young diagrams. This observation is crucial in the proving the functional relations below. One, should, however note that each box can only stay at positions with identical spectral parameter. Therefore, the product of two \mathcal{T} shows non-trivial decomposition only when corresponding diagrams are situated at proper relative positions specified by their spectral parameters.

For illustration, let us prove (14) diagrammatically. We consider $T_m^{\text{non}}(x+i)T_m^{\text{non}}(x-i)$. The spectral parameters are assigned for each box, $x - (m-2)i, \dots, x + mi$ from the left to the right for $T_m^{\text{non}}(x+i)$, and $x - mi, \dots, x + (m-2)i$ for $T_m^{\text{non}}(x-i)$. Thus two diagrams are situated so that these two width m rectangles piled vertically (fig. 2). @

We consider a particular assignment of letters, i_1, \dots, i_m for the upper and j_1, \dots, j_m for the lower diagram. $T_m^{\text{non}}(x+i)T_m^{\text{non}}(x-i)$ is obtained by the sum over tableaux under the condition, $i_1 \leq i_2 \leq \dots \leq i_m$ and $j_1 \leq j_2 \leq \dots \leq j_m$, respectively.

i_1	i_2	i_3	i_4	i_5	i_6	i_7	i_8
j_1	j_2	j_3	j_4	j_5	j_6	j_7	j_8

Figure 2: A typical table in the product $T_m^{\text{non}}(x+i)T_m^{\text{non}}(x-i)$. Hereafter, disjoint diagrams represent their product.

The first term in the lhs of (14) comes from the configurations, $i_k < j_k$, ($k = 1, \dots, m$). The resultant table is of the shape $2 \times m$ and satisfy the semi-standard condition. Due to the reduction (11), it is a member of $T_m^{\text{non}}(x)$ times $\prod_{j=1}^m \phi_2(x - i(m+1) + 2ij)$. The second term comes from the configurations which breaks the condition (fig. 3). By $i_\alpha \geq j_\alpha$, we mean the first pairs breaking the condition from the left end. Then the ordering within i 's and j 's concludes that the new sequences $j_1, \dots, j_\alpha, i_\alpha, i_{\alpha+1}, \dots, i_m$ and $i_1, \dots, i_{\alpha-1}, j_{\alpha+1}, \dots, j_m$ satisfies the semi-standard condition. One can also check that the new sequences satisfy the proper spectral parameter assignment, namely increment of the spectral parameter by $2i$ from the left to right. Thus after the recombination of sequences, we obtain $T_{m+1}^{\text{non}}(x)T_{m-1}^{\text{non}}(x)$. Finally, by dividing the both sides by the factor $f_m(x \pm i)$, one arrives at (14).

The above procedure is formally interpreted as follows. Place two diagrams properly according to their spectral parameters. We just join them or recombine them such that the total set of spectral parameters is conserved.

The case studies for $L = 3, 4, 6$, however, suggest that $\mathcal{T}_{\mu/\lambda}(x)$ is not the right object in the discussion of functional relations. Instead, we should introduce $\Lambda_{\mu/\lambda}(x)$, which is analytic under BAE, from $\mathcal{T}_{\mu/\lambda}(x)$ by putting $T_{m \geq 2L}(x) = 0$ in the latter,

$$\Lambda_{\mu/\lambda}(x) := \mathcal{T}_{\mu/\lambda}(x) / \{T_{m \geq 2L}(x) = 0\}. \quad (20)$$

The pole-free property of $\Lambda_{\mu/\lambda}(x)$ is obvious from (19).

The diagrammatic decomposition applies to $\mathcal{T}_{\mu/\lambda}(x)$ but not to $\Lambda_{\mu/\lambda}(x)$ in a strict sense. Therefore the above decomposition rules, demonstrated above, may not seem to

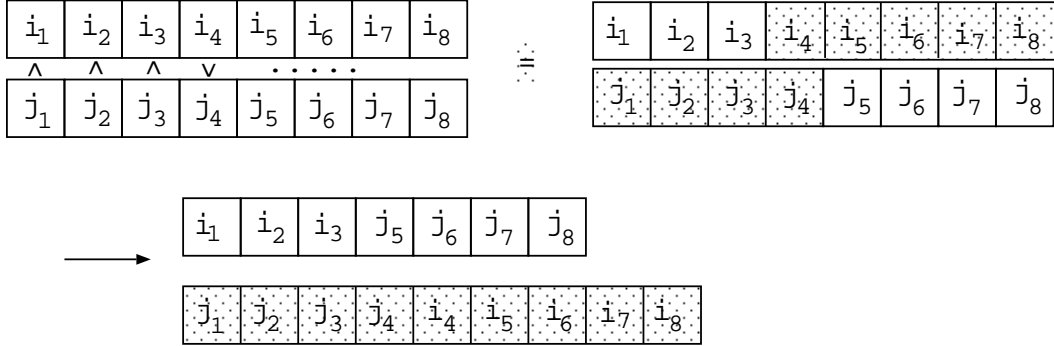


Figure 3: The pair (i_4, j_4) is the first from the left which breaks the semi-standard condition. Then the recombination of tableaux occurs there, into hatched and unhatched ones.

be helpful in our discussion. For most of case which we treat below, however, the skew diagram $\mu - \lambda$ is no so huge and Λ and \mathcal{T} coincide. Thus the above rules are quite often applicable and play significant roles ; as already remarked, there are plenty of expressions for an identical object. Therefore it is sometimes crucial to choose "the most" relevant expression among many. The above graphical decomposition provides hints on the optimal candidate in proving the functional relations .

Before closing the section, we mention an important diagrammatic symmetry of $\Lambda_{\mu/\lambda}$

Corollary 1. *Let Y and \widehat{Y} be skew diagrams. \widehat{Y} is obtained from Y after 180° rotation. The following relation is a consequence of the eq (19)*

$$\mathcal{T}_Y(x) = (\mathcal{T}_{\widehat{Y}}(x^*))^* \quad (21)$$

where the asterisk stands for complex conjugations.

The proof is direct; one substitutes $\widehat{Y}_i = (\mu_1 - \lambda_{d+1-i}) - (\mu_1 - \mu_{d+1-i})$ for $Y = \mu - \lambda$ and $\mu'_1 = d$.

This corollary is crucial in establishing a property of the transfer matrices (see section 8). It will be also used implicitly in the proof of functional relations in the following.

After these preparations, we introduce the first of our three ingredients in the closed functional relations, the Breather $T-$ system in the next section.

4 Breather $T-$ system

The RSOS weights possesses a singularity at $u = \pm 3$ besides the $u = \pm 2$ singularity related to $a_2^{(2)}$ structure [38]. It is shown that the singularity at $u = \pm 3$ signifies the "hidden" sl_2 structure behind the model. The breather type relation originates from this sl_2 structure.

We define the "breather" transfer matrices for the dilute A_L model in regime 2.

$$\begin{aligned} T_{B_1}(x) &= T_1(x) \\ T_{B_3}(x) &= \begin{cases} \frac{1}{\phi^\vee(x)} \Lambda_{2L-2,1}(x - \frac{5}{2}i), & \text{for } L \text{ odd} \\ \frac{1}{\phi^\vee(x)} \Lambda_{2L-2,1}^\vee(x - \frac{5}{2}i), & \text{for } L \text{ even} \end{cases} \\ T_{B_5}(x) &= \frac{1}{\phi(x \pm \frac{3}{2}i)} \Lambda_{(4L-5,2L-2,2L-2)/(2L-3,2L-3)}(x) \end{aligned}$$

One immediately verifies the validity of the following functional relations,

$$T_{B_1}(x \pm i \frac{L-2}{2(L+2)}) = T_0(x \pm i \frac{L+6}{2(L+2)}) + \phi^\vee(x) T_{B_3}(x) \quad (22)$$

$$T_{B_3}(x \pm i \frac{L-2}{2(L+2)}) = T_0(x)T_0(x \pm i \frac{4}{(L+2)}) + T_{B_1}(x)T_{B_5}(x). \quad (23)$$

Proof. Proof utilizes the duality (16). For (22), we first consider the multiplication of $T_1(x)(=T_{B_1})$ by its dual $T_{2L-2}(x + (2L-1)i)$. See fig. 4 for a case $L=5$.

Figure 4: The multiplication of $T_1(x)(=T_{B_1})$ by $T_{2L-2}(x + (2L-1)i)$. The letter a in a box implies its spectral parameter $x + ia$.

The spectral parameters are assigned so that they align horizontally. For L even (odd) $T_{2L-2}(x + (2L-1)i)$ is equal to $T_{B_1}(x + (2L-1)i)$ ($T_{B_1}(x + (2L-1)i + \frac{P}{2}i)$). Thus the product is equivalent to that of two T_{B_1} . It is decomposed into two terms; the first is T_{2L-1} and the second is T_{B_3} (with some shifts in spectral parameters and with coefficients.) By the duality, T_{2L-1} is replaced by T_0 . Then one arrives (22) after the shift in the spectral parameter and taking account of proper coefficients.

The second relation is shown similarly. One only should notice that dual of the diagram $(2L-1, 1)$ is given by a skew diagram $(2L-1, 2L-1) - (2L-2)$. The case $L = 5$ is depicted in fig. 5.

The diagram illustrates the decomposition of a 10x1 rectangle into two 5x1 rectangles and a 2x2 square. The top row shows a 10x1 rectangle divided into a 5x1 rectangle and a 5x2 rectangle. The bottom row shows the 5x2 rectangle further divided into a 5x1 rectangle and a 2x2 square.

Figure 5:

Despite its disguise, the first diagram in the rhs corresponds to the products of T_0 due to (19). Then it is straightforward to verify (23). \square

By noticing $3 = -\frac{(L-2)}{(L+2)} \pmod{\frac{4(L+1)}{L+2}}$, we understand the above relation stems from the singularity of the RSOS weight at $u = \pm 3$ related to sl_2 structure.

The following representation of $T_{B_3}(x)$ and $T_{B_5}(x)$ will be useful in the following argument for the regime 2

$$T_{B_3}(x - \frac{L-2}{2(L+2)}i) = \frac{1}{\phi(x - \frac{5}{2}i)} \Lambda_{(2,1)}(x+i) \quad (24)$$

$$T_{B_5}(x) = \Lambda_{(3,2)/(1)}(x). \quad (25)$$

Proof. The first equation utilizes the representation of $T_{B_1}(x)$ by the height 2 diagram.

$$T_{B_1}(x)T_{B_1}(x+3i) = \frac{f_2(x+2i)}{\phi_2(x)} \Lambda_{(2,1)}(x+i) + \frac{\phi_3(x+i)}{\phi_2(x)} \quad (26)$$

See (11) and (12) for $\phi_{2,3}$.

$$\begin{array}{c} \boxed{1} \quad \boxed{3} \\ \hline -1 \end{array} = \begin{array}{c} 3 \\ \hline 1 \\ \hline -1 \end{array} + \begin{array}{c} \boxed{1} \quad \boxed{3} \\ \hline -1 \end{array}$$

Figure 6: A graphical representation of (26). The letter a in a box implies its spectral parameter $x + ia$

We present graphically eq.(26) in fig. 6. By noticing $3 = -\frac{(L-2)}{(L+2)} \pmod{\frac{4(L+1)}{L+2}}$, and comparing the above with (22) (after trivial shift in x), one concludes (24).

To prove the second, we consider $\mathcal{T}_{(4L-5,2L-2,2L-2)/(2L-3,2L-3)}^{\text{non}}(x)$ instead of $\Lambda_{(4L-5,2L-2,2L-2)/(2L-3,2L-3)}(x)$ in the definition of T_{B_5} . Note their difference, (20). From theorem 1, $\mathcal{T}_{(4L-5,2L-2,2L-2)/(2L-3,2L-3)}^{\text{non}}(x)$ decomposed into 3 pieces as in the case of usual Young diagrams.

$\mathcal{T}_{(4L-5,2L-2,2L-2)/(2L-3,2L-3)}^{\text{non}}(x) = T_{2L-3}^{\text{non}}(x \pm 2iL) \phi_3(x) = T_2(x \pm 2i) \phi_3(x) f_{2L-3}(x \pm 2iL)$ where the duality relation (16) is used in the second equality. $\phi_3(x)$ is defined in (12). After proper normalizations, it reads,

$$\mathcal{T}_{(4L-5,2L-2,2L-2)/(2L-3,2L-3)}(x) = T_2(x \pm 2i). \quad (27)$$

On the other hand, the formula (19) leads to

$$\mathcal{T}_{(4L-5,2L-2,2L-2)/(2L-3,2L-3)}(x) = \Lambda_{(4L-5,2L-2,2L-2)/(2L-3,2L-3)}(x) + T_0(x \pm i) T_{4L-3}(x). \quad (28)$$

Note $T_{4L-3}(x) = T_4(x)$, which is derived in parallel to the duality. Then the comparison (27) and (28) leads to

$$\Lambda_{(4L-5,2L-2,2L-2)/(2L-3,2L-3)}(x) = T_2(x \pm 2i) - T_0(x \pm i) T_4(x) = \Lambda_{(3,2)/(1)}(x),$$

where (19) is applied in the last equality. In this manner, one verifies (25). \square

The transformation of the T system to the "breather" $Y-$ system is standard[35, 36, 52]. We define,

$$\begin{aligned} Y_{B_1}(x) &:= \frac{\phi^\vee(x)T_{B_3}(x)}{T_0(x \pm i\frac{L+6}{2(L+2)})} \\ Y_{B_3}(x) &:= \frac{T_{B_1}(x)T_{B_5}(x)}{T_0(x)T_0(x \pm i\frac{4}{(L+2)})}. \end{aligned}$$

Then the following "breather" $Y-$ system is directly derived with the help of the "breather" functional relation (23).

$$Y_{B_1}(x \pm i\frac{L-2}{2(L+2)}) = (1 + Y_{B_3})(x). \quad (29)$$

The main goal in this report is to evaluate the largest eigenvalue of $T_1(u, 0)$ or $T_{B_1}(0)$ in the Trotter limit. For this, our strategy is to utilize a set of closed functional relations, including $T_{B_1}(x)$. The sl_2 originated functional relations are indeed enough to obtain the desired relations in the case of $M_{3,4} + \phi_{1,2}$. This is no longer valid for general case. In the next sections, we introduce further objects and relations to achieve the goal.

5 The sl_3 type functional relations

As is mentioned in the preceding section, there is another structure analogous to the sl_3 models. Let $W_m^{(a)}$, ($a = 1, 2$. $m \in \mathbb{Z}_{\geq 0}$) be a Yangian module corresponding to $m\Lambda_a$ as a classical sl_3 module. We associate a transfer matrix $T_m^{(a)}(x)$ to $W_m^{(a)}$. Then the following functional relations hold,

$$T_m^{(a)}(x \pm i\gamma) = T_m^{(a+1)}(x)T_m^{(a-1)}(x) + T_{m+1}^{(a)}(x)T_{m-1}^{(a)}(x)$$

where γ is a parameter related to a singularity in R matrix. $T_0^{(a)}$, $T_m^{(0)}$ and $T_m^{(3)}$ are given by trivial scalar factors times an identity operator. Thus when multiplied on a common eigenspace of the commuting transfer matrices, they amount to known trivial scalar functions. The above relation can be graphically represented as follows. Consider a product of two rectangles of the shape $a \times m$. It decomposed into two subsets. The one is the products of two rectangles of the shape $(a+1) \times m$ and the shape $(a-1) \times m$ and the other is the products of rectangles, $a \times (m+1)$ and $a \times (m-1)$.

We turn back to the dilute A_L models in regime 2. The above relations among rectangular can not hold ; due to the $a_2^{(2)}$ symmetry, the $2 \times m$ rectangle is always reduced to the rectangle of $1 \times m$. Nevertheless, an analogue can be still found . Let us denote

$$T_{D_j}(x) = \Lambda_{(j+1,j)/(1)}(x).$$

In this notation, which is adopted hereafter, $T_{B_5}(x)$ in the preceding section is identical to $T_{D_2}(x)$. Note also that $T_{D_1}(x) = T_1(x \pm 2i)$ and $T_{D_0}(x) = T_0(x \pm 2i)$.

Lemma 1. *The following functional relations, similar to sl_3 type, hold.*

$$T_{2j}(x \pm 2i) = T_{2(j+1)}(x)T_{2(j-1)}(x) + T_{D_{2j}}(x) \quad (30)$$

$$T_{D_{2j}}(x \pm 2i) = \begin{cases} T_{D_{2(j+1)}}(x)T_{D_{2(j-1)}}(x) + T_{2j}(x)T_{B_3}(x \pm i\frac{L-2-4j}{2L+4}) & j \text{ even} \\ T_{D_{2(j+1)}}(x)T_{D_{2(j-1)}}(x) + T_{2j}(x)T_{B_3}^\vee(x \pm i\frac{L-2-4j}{2L+4}) & j \text{ odd.} \end{cases} \quad (31)$$

The similarity is clearer by writing $T_j^{(1)}(x) = T_{2j}(x)$ and $T_j^{(2)}(x) = T_{D_{2j}}(x)$. The difference lies in that fact that $T_j^{(3)}(x)$, which amounts to a known scalar for the sl_3 case, remains non trivial; it is given by a product of T_{B_3} .

Proof. The first equality (30) is trivial shown by the quantum Jacobi-Trudi formula. The second one needs one step further. First, one uses the following relation, proved by the quantum Jacobi-Trudi formula,

$$T_{D_{2j}}(x \pm 2i) - T_{D_{2(j+1)}}(x)T_{D_{2(j-1)}}(x) = T_{2j}(x)\mathcal{T}_{(2j+2,2j+1,2j)/(2,1)}(x). \quad (32)$$

From the tableaux rule, a hatched part of the diagram in $\mathcal{T}_{(2j+2,2j+1,2j)/(2,1)}(x)$ reduces to product of scalars, see fig. 7.

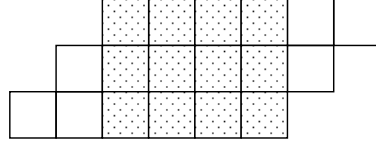


Figure 7: $\mathcal{T}_{(2j+2,2j+1,2j)/(2,1)}(x)$ for $j = 3$.

The resultant two pieces of diagrams represents the products of $\Lambda_{(2,1)}(x + (2j+1)i)$ and $\Lambda_{(2,2)/(1)}(x - (2j+1)i)$ apart from normalization factors. Note that $2j \equiv \frac{4j}{2L+4} \pmod{P}$ for j even and $2j \equiv \frac{4j}{2L+4} + \frac{P}{2} \pmod{P}$ for j odd. Then from the expression (24), one finds for the first piece,

$$\Lambda_{(2,1)}(x + (2j+1)i) = \phi(x + (2j - \frac{5}{2})i)T_{B_3}(x - \frac{L-2-4j}{2L+4}i).$$

The second piece, $\Lambda_{(2,2)/(1)}(x - (2j+1)i)$, equals to $(\Lambda_{(2,1)/(1)}(x + (2j+1)i))^*$ by corollary 1. Therefore, after taking account of proper normalization factors and using the property $(T_{B_3}(x))^* = T_{B_3}(x^*)$, one finds,

$$T_{B_3}(x \pm \frac{L-2-4j}{2L+4}i) = \begin{cases} \mathcal{T}_{(2j+2,2j+1,2j)/(2,1)}(x) & j \text{ even,} \\ \mathcal{T}_{(2j+2,2j+1,2j)/(2,1)}^\vee(x) & j \text{ odd.} \end{cases} \quad (33)$$

Thus the second relation is proved from (32) and (33). \square

For $L = 4k - 1, 4k$ and $4k + 1$, we introduce

$$Y_j^{(1)}(x) := \begin{cases} \frac{T_{D_{2(j+1)}}(x)}{\frac{T_{2j}(x)T_{2(j+2)}(x)}{T_{D_{2(j+1)}}(x)}}, & j \text{ even} \\ \frac{T_{D_{2(j+1)}}(x)}{\frac{T_{2j}^{\vee}(x)T_{2(j+2)}^{\vee}(x)}{T_{2j}(x)T_{2(j+2)}(x)}}, & j \text{ odd} \end{cases} \quad 0 \leq j \leq k-3 \quad (34)$$

$$Y_j^{(2)}(x) := \begin{cases} \frac{T_{2(j+1)}^{\vee}(x)T_{B_3}(x \pm \frac{L-2-4(j+1)}{2L+4})}{T_{D_{2j}}^{\vee}(x)T_{D_{2(j+2)}}^{\vee}(x)}, & j \text{ even} \\ \frac{T_{2(j+1)}(x)T_{B_3}(x \pm \frac{L-2-4(j+1)}{2L+4})}{T_{D_{2j}}(x)T_{D_{2(j+2)}}(x)}, & j \text{ odd} \end{cases} \quad 0 \leq j \leq k-3. \quad (35)$$

while these do not show up for $L = 4k + 2$.

By noticing $2 \equiv \frac{4}{2L+4} + \frac{P}{2}$, one immediately obtains the following $Y-$ system,

$$Y_j^{(1)}(x \pm \frac{4}{2L+4}i) = \frac{1 + Y_j^{(2)}(x)}{(1 + \frac{1}{Y_{j+1}^{(1)}(x)})(1 + \frac{1}{Y_{j-1}^{(1)}(x)})} \quad (36)$$

$$Y_j^{(2)}(x \pm \frac{4}{2L+4}i) = \frac{1 + Y_j^{(1)}(x)}{(1 + \frac{1}{Y_{j+1}^{(2)}(x)})(1 + \frac{1}{Y_{j-1}^{(2)}(x)})} \quad 1 \leq j \leq k-3. \quad (37)$$

These are desired relations. See the $Y-$ system in the appendix A.

The sl_2 $T-$ system is not itself closed. Here we find it connected to the sl_3 like $T-$ system through $T_{B_3}(x) = T_{D_2}(x)$. The latter system is, however, neither closed. In the next section, other functional relations are introduced, referred to as "magnon-like", which turns out to "close" the total $T-$ systems.

6 The magnon-like $t-$ system and the Dynkin like diagrams

The above transfer matrices are not enough to obtain sets of closed functional relations, which are necessary to derive TBA. We have to introduce further objects separately depending on four families. They are related to the magnon-like $Y-$ system introduced in [25, 30]. A magnon-like $Y-$ system is associated to a diagram of the Dynkin type. Although they can be classified into the four families, the diagrams are all different depending on values of L . Consequently, the magnon-like Y system are all distinct for different L .

Here the situation is slightly unified. The diagrams we have to deal with are "tails" of those in [25, 30], independent of L , except for the dilute A_{4k+2} models.

Before starting discussions on individual cases, we shall make remarks. A blank node in each Dynkin like diagram indicates its different character from the rests. To node a in the diagram, we associate $t_m^{(a)}(x)$, where m takes an integer value from a finite set. Our magnon-like $t-$ system is a set of functional relations among $t_m^{(a)}(x)$, which should be described separately for four families. The most crucial observation below will be that $t_m^{(a)}$ associated to a blank node is always expressed by (product of) T_{B_3} .

The dilute A_{4k-1} model and the dilute A_{4k+1} model share a same diagram but possess different $t-$ system. The only "L" depending diagram for A_{4k+2} ($L = 4k + 2$) remarkably coincides with the Dynkin diagram for D_{k+2} .

Below we take x to be real. As usual, the symbol $a \sim b$ means that nodes a and b are adjacent on the diagram.

6.1 The magnon-like $t-$ system for A_{4k-1}

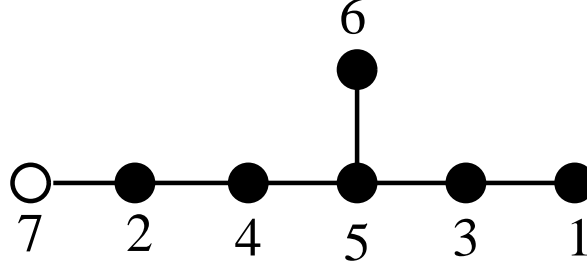


Figure 8: Dynkin like diagram for A_{4k-1}

We define a magnon-like $t-$ system associated to fig. 8,

$$t_m^{(a)}(x \pm \frac{i}{2L+4}) = t_{m-1}^{(a)}(x)t_{m+1}^{(a)}(x) + \prod_{b \sim a} t_m^{(b)}(x), \quad a = 1 \sim 6, \quad m = 1, 2 \quad (38)$$

$$t_0^{(a)} = 1 \quad (a = 1 \sim 6), \quad t_3^{(a)} = 0, \quad (a = 3 \sim 6) \\ t_1^{(7)}(x \pm \frac{i}{2L+4}) = t_2^{(7)}(x). \quad (39)$$

This is not a set of closed functional relation. We, however, note its affinity to the E_6 related $T-$ system [36]. Indeed if $t_1^{(7)}(x) = 1$ and $t_3^{(1)}(x) = t_3^{(2)}(x) = 0$, the above functional relation coincides with the $T-$ system for level 3 RSOS model, corresponding to the coset $(E_6^{(1)})_2 \times (E_6^{(1)})_1 / (E_6^{(1)})_3$. Our interpretation is as follows. The nontrivial $t_1^{(7)}(x)$ makes the $t_3^{(1)}(x)$ and $t_3^{(2)}(x)$ non zero and connects the E_6 level 3 $T-$ system to others. Thus $t_1^{(7)}(x)$ plays a role of "glue". This seems to be quite parallel to the sl_3 like T system, which is connected to sl_2 T system by nontrivial T_{B_3} . Here the situation is indeed the same; we will see below $t_1^{(7)}(x) = T_{B_3}$. T_{B_3} thus plays a role in gluing the sl_3 , the E_6 and the sl_2 $T-$ systems.

We shall define "gauge invariant" functions for later discussions.[36, 56]

$$\begin{aligned}
Y_{k-1}^{(a)}(x) &:= \frac{\prod_{b \sim a} t_1^{(b)}(x)}{t_2^{(a)}(x)}, \quad a = 1 \sim 6 \\
Y_{k-2}^{(1)}(x) &:= \frac{t_2^{(3)}(x)}{t_1^{(1)}(x)t_3^{(1)}(x)} \\
Y_{k-2}^{(2)}(x) &:= \frac{t_2^{(4)}(x)t_2^{(7)}(x)}{t_1^{(2)}(x)t_3^{(2)}(x)}.
\end{aligned}$$

6.2 The magnon-like $t-$ system for A_{4k}

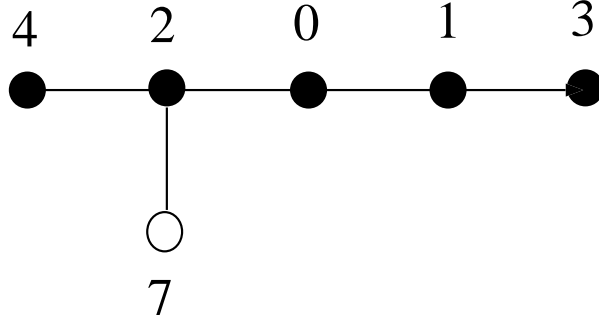


Figure 9: Dynkin like diagram for A_{4k}

Associated to fig. 9 we propose a magnon-like $t-$ system for this case,

$$\begin{aligned}
t_m^{(a)}(x \pm \frac{i}{L+2}) &= t_{m-1}^{(a)}(x)t_{m+1}^{(a)}(x) + \prod_{b \sim a} t_m^{(b)}(x), \quad a = 1 \sim 6, \quad m = 1, 2, \\
t_0^{(a)} &= 1 \quad (a = 1 \sim 6), \quad t_3^{(a)}(x) = 0 \quad (a = 0, 3, 4), \\
t_1^{(7)}(x \pm \frac{i}{L+2}) &= t_2^{(7)}(x).
\end{aligned}$$

Again, this is not a set of closed functional relation. In this case we note its similarity to the $T-$ system for level 3 RSOS model, corresponding to the coset $(A_5^{(1)})_2 \times (A_5^{(1)})_1 / (A_5^{(1)})_3$ [36]. As in the preceding case, $t_1^{(7)}(x)$ will turn out to be equal to $T_{B_3}(x)$. Thus the interpretation is the same; $t_1^{(7)}$ connects the $T-$ system for level 3 A_5 RSOS model, the sl_3 and the sl_2 $T-$ systems.

Y functions for this case read,

$$Y_{k-1}^{(a)}(x) := \frac{\prod_{b \sim a} t_1^{(b)}(x)}{t_2^{(a)}(x)}, \quad a = 1 \sim 6 \quad (40)$$

$$Y_{k-2}^{(1)}(x) := \frac{t_2^{(0)}(x)t_2^{(3)}(x)}{t_1^{(1)}(x)t_3^{(1)}(x)} \quad (41)$$

$$Y_{k-2}^{(2)}(x) := \frac{t_2^{(0)}(x)t_2^{(4)}(x)t_2^{(7)}(x)}{t_1^{(2)}(x)t_3^{(2)}(x)}. \quad (42)$$

6.3 The magnon-like $t-$ system for A_{4k+1}

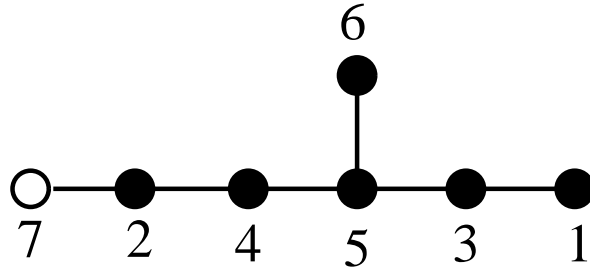


Figure 10: Dynkin like diagram for A_{4k+1}

Although it shares the same diagram with the case A_{4k-1} , a magnon-like $t-$ system takes a slightly different form,

$$\begin{aligned} t_1^{(a)}(x \pm \frac{i}{2L+4}) &= t_2^{(a)}(x) + \prod_{b \sim a} t_1^{(b)}(x), \quad a = 3, 4, 5, 6 \\ t_1^{(1)}(x \pm \frac{4i}{2L+4}) &= t_2^{(1)}(x) + t_1^{(2)}(x) \\ t_1^{(2)}(x \pm \frac{4i}{2L+4}) &= t_2^{(2)}(x) + t_1^{(1)}(x)t_1^{(7)}(x) \\ t_1^{(7)}(x \pm \frac{i}{2L+4}) &= t_2^{(7)}(x) \\ t_2^{(a)}(x \pm \frac{i}{2L+4}) &= \prod_{b \sim a} t_2^{(b)}(x) \quad a = 5, 6 \\ t_2^{(3)}(x \pm \frac{i}{2L+4}) &= t_1^{(3)}(x)t_3^{(3)}(x) + t_2^{(5)}(x)t_1^{(1)}(x \pm \frac{i}{2L+4}) \\ t_2^{(4)}(x \pm \frac{i}{2L+4}) &= t_1^{(4)}(x)t_3^{(4)}(x) + t_2^{(5)}(x)t_1^{(2)}(x \pm \frac{i}{2L+4}). \end{aligned}$$

They are analogous to the $T-$ system for level 3 RSOS model, corresponding to the coset $(D_4^{(1)})_2 \times (D_4^{(1)})_1 / (D_4^{(1)})_3$ [36], which is clear by setting $t_1^{(1)} = t_1^{(2)} = t_1^{(7)} = 1$ and

$t_3^{(3)} = t_3^{(4)} = 0$. In this case, $t_1^{(7)}$ will turn out to be a product of T_{B_3} , $t_1^{(1)}$ and $t_1^{(2)}$ are shown to be originated from the sl_3 structure. Again, our interpretation is that non-trivial T_{B_3} glues the D_4 , the sl_3 and the sl_2 $T-$ systems.

Y functions are defined by,

$$\begin{aligned} Y_{k-1}^{(a)}(x) &:= \frac{t_2^{(a)}(x)}{\prod_{b \sim a} t_1^{(b)}(x)}, \quad a = 3 \sim 6 \\ Y_{k-1}^{(1)}(x) &:= \frac{t_1^{(3)}(x)t_3^{(3)}(x)}{t_2^{(5)}(x)t_1^{(1)}(x \pm \frac{1}{2L+4}i)} \\ Y_{k-1}^{(2)}(x) &:= \frac{t_1^{(4)}(x)t_3^{(4)}(x)}{t_2^{(5)}(x)t_1^{(2)}(x \pm \frac{1}{2L+4}i)} \\ Y_{k-2}^{(1)}(x) &:= \frac{t_1^{(2)}(x)}{t_2^{(1)}(x)} \\ Y_{k-2}^{(2)}(x) &:= \frac{t_1^{(1)}(x)t_1^{(7)}(x)}{t_2^{(2)}(x)}. \end{aligned}$$

6.4 The magnon-like $t-$ system for A_{4k+2}

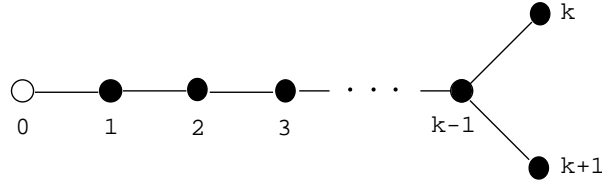


Figure 11: Dynkin like diagram for A_{4k+2}

Only in this case, the diagram depends on k . A magnon-like $t-$ system for the fig. 11 is defined as ,

$$t_m^{(a)}(x \pm \frac{2i}{L+2}) = t_{m-1}^{(a)}(x)t_{m+1}^{(a)}(x) + \prod_{b \sim a} t_m^{(b)}(x), \quad a = 1 \sim k+1 \quad m = 1, 2, 3 \quad (43)$$

$$\begin{aligned} t_0^{(a)} &= 1 \quad (a = 1 \sim k+1), \quad t_4^{(a)}(x) = 0 \quad (a = 2 \sim k+1) \\ t_1^{(0)}(x \pm \frac{2i}{L+2}) &= t_2^{(0)}(x), \quad t_2^{(0)}(x \pm \frac{2i}{L+2}) = t_1^{(0)}(x)t_3^{(0)}(x). \end{aligned} \quad (44)$$

In this case, the functional relations looks like the level 4 RSOS $T-$ system for D_{k+1} , instead of level 3.

The description of $Y_j^{(a)}$ can de done in the most systematic way among 4 categories,

$$Y_{a-1}^{(m)}(x) = \frac{t_{m+1}^{(a)}(x)t_{m-1}^{(a)}(x)}{\prod_{b \sim a} t_m^{(b)}(x)} \quad m = 1, 2 \quad 1 \leq a \leq k+1.$$

6.5 The solutions to magnon-like $t-$ system

The main finding in this report is that the solutions to the above magnon-like t system are expressible in terms of fusion transfer matrices appearing in dilute A_L models. We summarize the explicit solutions in appendix B. The proof requires several steps and rather lengthy, part of which will be given in section 10. Before going into such details, we would like draw attention to a general property of the solution and also its implication for the $Y-$ system . Firstly, we need to explain $T_K(x)$ appearing in the solutions for $L =$ even.

7 Kink transfer matrix

The case studies on $M_{4,5}, M_{6,7}$ [23] imply the necessity of the introduction of objects which are not produced from boxes by (19) . Generally, we find it possible to introduce the desired objects for the A_L model , L even.

The explicit procedure procedure to construct is as follows. Let $L = 2\ell$. and consider the model in regime 2, corresponding the perturbation $\phi_{1,2}$. Take

$$\omega^\ell \phi(x + \frac{\ell}{\ell+1}i) \frac{Q(x + \frac{\ell}{\ell+1}i)}{Q(x - \frac{1}{\ell+1}i)}$$

as the top term (or the highest term). Next, one adds a lower term

$$\omega^{\ell-1} \phi(x - \frac{\ell+2}{\ell+1}i) \frac{Q(x - \frac{\ell+2}{\ell+1}i)Q(x - \frac{2\ell+1}{\ell+1}i)}{Q(x - \frac{1}{\ell+1}i)Q(x + \frac{2\ell-1}{\ell+1}i)}$$

so that the singularity at $x = x_j + \frac{1}{\ell+1}i$ cancels due to the Bethe ansatz equation (8). Then we introduce another counter term so as to kill the singularity at $x = x_j - \frac{2\ell-1}{\ell+1}i$, and so on.

One observes that this procedure closes by finite steps and a pole-free object, consists of $2\ell + 1$ terms, results. We refer to this as an eigenvalue of "kink transfer matrix" , $T_K(x)$, although the corresponding transfer matrix is not yet found in the lattice model. For example,

$$\begin{aligned} T_K(x) = & w^4 \phi(x + \frac{4}{5}i) \frac{Q(x + \frac{4}{5}i)}{Q(x - \frac{1}{5}i)} + w^3 \phi(x - \frac{6}{5}i) \frac{Q(x - \frac{6}{5}i)Q(x - \frac{9}{5}i)}{Q(x - \frac{1}{5}i)Q(x + \frac{7}{5}i)} \\ & + w^2 \phi(x + \frac{2}{5}i) \frac{Q(x + \frac{2}{5}i)Q(x - \frac{9}{5}i)}{Q(x - \frac{3}{5}i)Q(x + \frac{7}{5}i)} + w \phi(x - \frac{8}{5}i) \frac{Q(x - \frac{8}{5}i)Q(x - \frac{9}{5}i)}{Q(x - \frac{3}{5}i)Q(x + i)} \\ & + \phi(x) \frac{Q(x)Q(x - \frac{9}{5}i)}{Q(x + i)Q(x - i)} + w^{-1} \phi(x + \frac{8}{5}i) \frac{Q(x + \frac{8}{5}i)Q(x + \frac{9}{5}i)}{Q(x + \frac{3}{5}i)Q(x - i)} \\ & + w^{-2} \phi(x - \frac{2}{5}i) \frac{Q(x - \frac{2}{5}i)Q(x + \frac{9}{5}i)}{Q(x + \frac{3}{5}i)Q(x - \frac{7}{5}i)} + w^{-3} \phi(x + \frac{6}{5}i) \frac{Q(x + \frac{6}{5}i)Q(x + \frac{9}{5}i)}{Q(x + \frac{1}{5}i)Q(x - \frac{7}{5}i)} \\ & + w^{-4} \phi(x - \frac{4}{5}i) \frac{Q(x - \frac{4}{5}i)}{Q(x + \frac{1}{5}i)} \end{aligned}$$

for the dilute A_8 model.

The numerical investigation on the largest eigenvalue indicates $(Q(x^*))^* = Q(x)$, which leads to an important property $(T_K(x^*))^* = T_K(x)$.

For our argument, it is not important whether it is a "real" transfer matrix or not, but significant are its pole-free property as well as functional relations among the products of kink transfer matrices and $T_m(x)$. One finds, for instance,

$$T_K(x \pm \frac{2k+1}{4k+2}i) = 2T_{4k-1}(x)$$

in the case of the dilute A_{4k} model.

These relations are summarized as lemma 7 in appendix C.

As mentioned there, although the explicit proof has been done only for smaller values of k , we assume the following.

Conjecture 1. *Lemma 7 holds for general k .*

The functional relations there play an important role in the proof of the magnon-like $t-$ system for $L = \text{even}$.

8 The reality property of magnon-like $t-$ functions

We remark the following significant property of our solutions to the T system.

Lemma 2. *Let $T(x)$ be an either solution of the magnon-like $t-$ system, the sl_3 like $T-$ system, or breather T system. Then, in "the largest eigenvalue sector",*

$$T(x) = (T(x^*))^* \quad (45)$$

which we call the reality property. Namely it assures the reality of $T(x)$ on the real axis.

As is commented in the previous section, $T_K(x)$ satisfies the reality property. One also verifies the property for most of $t_m^{(a)}(x)$ listed in the appendix B using the diagrammatic symmetry (21), immediately. It can be shown for the remaining $t_m^{(a)}(x)$, which takes "asymmetric" shape, with utilizing the magnon-like "t-" system which can be established without use of the reality property. We take the dilute A_{4k} case for example. Using the diagrammatic symmetry, $t_m^{(a)}(x)$ are shown to satisfy (45) except for $(a, m) = (0, 1)$ and $(a, m) = (4, 1)$. The one of the magnon-like $t-$ system,

$$t_1^{(1)}(x \pm i \frac{1}{2L+4}) - t_2^{(1)}(x) = t_1^{(0)}(x)t_3^{(0)}(x)$$

can be established independent of the property. Since all other entries other than $t_1^{(0)}(x)$ satisfy (45), it follows from the above relation that $t_1^{(0)}(x)$ also should satisfy (45). The case $(a, m) = (4, 1)$ can be treated similarly. There are, however, two exceptions, $t_1^{(3)}(x)$ and $t_1^{(4)}(x)$ for the dilute A_{4k+1} model. One still can devise other functional relations which explain the reality property of them. Since the proof is rather technical, we omit here.

9 The $Y-$ system and the $T-$ system

Several $Y-$ functions are already introduced for 4 categories by appropriate ratios of t or T functions. Thanks to the $T-$ system or the $t-$ system, one can easily check that the $Y-$ system is satisfied for the case in which the lhs are products of $Y_j^{(1)}$ or $Y_j^{(2)}(x)$ except for $j = k - 2$. One can verify the rest of the $Y-$ system by utilizing the explicit expressions of t in appendix B.

Our main message in this report is summarized as follows.

Proposition 1. *The four categories of the $Y-$ system proposed in [25] can be solved in terms of transfer matrices appeared in dilute A_L model, if x is real.*

Due to the different forms of $Y-$ system, the proof must be done separately for four categories. Below we shall concentrate on the case $L = 4k$. The other cases can be established with minor modifications.

Proof. Proposition 1 for $L = 4k$

Thanks to explicit relations between Y and t in (40) -(42) the "tail" part of the $Y-$ system (59) is shown to be a consequence of the magnon-like t system. Eq. (58) also follows from the sl_3 structure (36) except for $j = k - 2$. Consider the case $\alpha = 1$ and $j = k - 2$. By replacing the Y functions by $t_m^{(a)}$, one finds the lhs,

$$\frac{t_2^{(0)}(x \pm \frac{2}{L+2}i)t_2^{(3)}(x \pm \frac{2}{L+2}i)}{t_3^{(1)}(x \pm \frac{2}{L+2}i)t_1^{(1)}(x \pm \frac{2}{L+2}i)}$$

while the rhs reads

$$\frac{t_2^{(2)}(x \pm \frac{1}{L+2}i)}{t_3^{(2)}(x)t_1^{(1)}(x \pm \frac{2}{L+2}i)(1 + \frac{1}{Y_{k-3}^{(1)}(x)})}.$$

At this stage, the equality is not obvious. By the explicit forms of $Y_{k-3}^{(1)}(x)$ in (34), we rewrite

$$1 + \frac{1}{Y_{k-3}^{(1)}(x)} = \begin{cases} \frac{T_{2(k-2)}(x \pm 2i)}{T_{D_{2(k-2)}}(x)}, & k \text{ odd} \\ \frac{T_{2(k-2)}^{\vee}(x \pm 2i)}{T_{D_{2(k-2)}}^{\vee}(x)} = \frac{T_{2(k-2)}(x \pm \frac{2}{L+2}i)}{T_{D_{2(k-2)}}^{\vee}(x)}, & k \text{ even.} \end{cases}$$

By substituting further the explicit forms of $t_m^{(a)}$ in appendix B.2, one verifies the case $a = 1$ and $j = k - 2$; for example both sides reduce to

$$\frac{T_{D_{2(k-1)}}(x \pm \frac{2}{L+2}i)}{T_{2(k-2)}(x \pm \frac{2}{L+2}i)T_{2k}(x \pm \frac{2}{L+2}i)}$$

in case k even. The case $\alpha = 2$ and $j = k - 2$ can be shown in the same manner.

Since eq. (56) is already proved in (29), it remains to show eq. (57). We must treat the cases k even and odd separately. For $k = 2m + 1$, the product

$$\Xi_{k-1}^{(2)}(x) \prod_{\ell=0}^{k-2} \Xi_{\ell}^{(2)}(x \pm \frac{4k-4\ell-6}{2L+4}i) = \Xi_{k-1}^{(2)}(x) \prod_{\ell=1}^{k-1} \Xi_{k-\ell-1}^{(2)}(x \pm \frac{4\ell-2}{2L+4}i)$$

is written in terms of fusion transfer matrices using (35),

$$\begin{aligned} & \frac{T_{D_{2k}}(x \pm \frac{1}{L+2}i)}{T_{D_{2k-2}}^{\vee}(x \pm \frac{1}{L+2}i)} \prod_{\ell=1, \ell=\text{odd}}^{k-1} \frac{T_{D_{2k-2\ell}}^{\vee}(x \pm \frac{2\ell+1}{L+2}i) T_{D_{2k-2\ell}}^{\vee}(x \pm \frac{2\ell-3}{L+2}i)}{T_{D_{2k-2\ell-2}}(x \pm \frac{2\ell-1}{L+2}i) T_{D_{2k-2\ell+2}}(x \pm \frac{2\ell-1}{L+2}i)} \\ & \prod_{\ell=1, \ell=\text{even}}^{k-1} \frac{T_{D_{2k-2\ell}}(x \pm \frac{2\ell+1}{L+2}i) T_{D_{2k-2\ell}}(x \pm \frac{2\ell-3}{L+2}i)}{T_{D_{2k-2\ell-2}}^{\vee}(x \pm \frac{2\ell-1}{L+2}i) T_{D_{2k-2\ell+2}}^{\vee}(x \pm \frac{2\ell-1}{L+2}i)} \\ & = \frac{T_{D_{2k}}(x \pm \frac{1}{L+2}i)}{T_{D_{2k-2}}^{\vee}(x \pm \frac{1}{L+2}i)} \prod_{\ell'=1}^m \frac{T_{D_{2k-4(\ell'-1)-2}}^{\vee}(x \pm \frac{4(\ell'-1)-1}{L+2}i) T_{D_{2k-4\ell'}}(x \pm \frac{4\ell'+1}{L+2}i)}{T_{D_{2k-4(\ell'-1)-2}}^{\vee}(x \pm \frac{4\ell'-1}{L+2}i) T_{D_{2k-4(\ell'-1)}}(x \pm \frac{4(\ell'-1)+1}{L+2}i)} \\ & = \frac{T_{D_2}(x \pm \frac{2k-1}{L+2}i)}{T_0(x \pm \frac{2k-1}{L+2}i) T_0(x \pm \frac{2k-5}{L+2}i)} \end{aligned}$$

where we have used $T_{D_0}^{\vee}(x) = T_0^{\vee}(x \pm 2i) = T_0(x \pm \frac{2}{4k+2}i)$. Multiplying this by the remaining term in the rhs, $(1 + Y_{B_3}(x)) = T_{B_1}(x \pm \frac{2k-1}{L+2}i)/T_0(x \pm \frac{2k+3}{L+2}i)$, one reaches the expression identical to the lhs. Note $T_{D_2}(x) = T_{B_5}(x)$. The case k even can be treated analogously. \square

Once the solutions to magnon-like t system are proved to be given by those in the appendix B, the solutions to Y system immediately follow. It is thus vital to verify the solutions. The proofs for the $L =$ even cases and the odd cases are similar, respectively. We then present the proof for the case $L = 4k + 2$ in the next section, where it can be done most systematically. As a representative of the odd case, we supplement the outline of the proof for $L = 4k - 1$ case in the appendix E.

10 Proof of the magnon-like t -system for $L = 4k + 2$

We first prepare a few lemmas

Lemma 3.

$$\Lambda_{(m,m,1)/(m-1)}(x) = T_{D_{m-1}}(x) \phi(x \pm \frac{2m+5}{2}i)$$

This lemma holds not only for $L = 4k + 2$, but all L . The proof is direct by the $a_2^{(2)}$ property in (11). Although it is not used in this section, this lemma is frequently used in the proof of the magnon-like t -system. See appendix D for example.

Lemma 4. *The following equality holds by mod P*

$$-\frac{k}{2k+2} \equiv \begin{cases} 2k+3, & k: \text{ even} \\ 2k+3+\frac{P}{2}, & k: \text{ odd} \end{cases} \quad (46)$$

$$\frac{j}{2k+2} \equiv \begin{cases} 2j, & j: \text{ even} \\ 2j+\frac{P}{2}, & j: \text{ odd.} \end{cases} \quad (47)$$

They can be checked trivially.

Lemma 5.

$$(t_2^{(k)}(x))^2 = \begin{cases} T_{D_{2k}}^\vee(x), & k: \text{ even} \\ T_{D_{2k}}(x), & k: \text{ odd} \end{cases}$$

Lemma 6.

$$t_1^{(k)}(x)t_3^{(k)}(x) = \begin{cases} \frac{1}{2}(T_{D_{2k+2}}(x) - T_{D_{2k-2}}(x)), & k: \text{ even} \\ \frac{1}{2}(T_{D_{2k+2}}^\vee(x) - T_{D_{2k-2}}^\vee(x)), & k: \text{ odd} \end{cases} \quad (48)$$

The proofs of the above two lemmas are given in the appendix D.

With these preparations, we shall prove the magnon-like t system equation by equation. Consider first the case $m = 1$ in (43). For $a = 1, \dots, k-2$, by paying attention to (47) with $j = 1$, one immediately sees that the assertion is actually equivalent to (30). Thus only the cases $a = k, k-1$ need proofs. Using $t_1^{(k)}(x) = T_K(x)/2$ and the functional relation (101) with $j = k$, we find

$$t_1^{(k)}(x \pm \frac{1}{2k+2}i) = \begin{cases} T_{2k-2}^\vee(x) + \frac{1}{2}(T_{2k+2}^\vee(x) - T_{2k-2}^\vee(x)) & k: \text{ even} \\ T_{2k-2}(x) + \frac{1}{2}(T_{2k+2}(x) - T_{2k-2}(x)) & k: \text{ odd.} \end{cases}$$

The first and the second term in the rhs coincides with $t_1^{(k-1)}(x)$ and $t_2^{(k)}(x)$, respectively, which proves the case $a = k$ of (43). The $a = k-1$ case is less trivial. Substituting $a = k-1$ in (93) and using (30), one finds

$$t_1^{(k-1)}(x \pm \frac{1}{2k+2}i) = \begin{cases} T_{2k-2}(x \pm 2i) = T_{2k}(x)T_{2k-4}(x) + T_{D_{2k-2}}(x) & k \text{ even} \\ T_{2k-2}^\vee(x \pm 2i) = T_{2k}^\vee(x)T_{2k-4}^\vee(x) + T_{D_{2k-2}}^\vee(x) & k \text{ odd.} \end{cases} \quad (49)$$

The second term in the rhs is identified with $t_2^{(k-1)}(x)$.

We note

$$t_1^{(k)}(x)t_1^{(k+1)}(x) = (T_K(x)/2)^2 = \begin{cases} T_{2k}(x) & k \text{ even} \\ T_{2k}^\vee(x) & k \text{ odd} \end{cases}$$

where (101) with $j = k+1$ is used in the second equality. Since $T_{2k-4}(x) = t_1^{(k-2)}(x)$, the first term in (49) can be written as $t_1^{(k-2)}(x)t_1^{(k)}(x)t_1^{(k+1)}(x)$. Combining these observations,

we find that the rhs of (49) coincides with $t_2^{(k-1)}(x) + t_1^{(k-2)}(x)t_1^{(k)}(x)t_1^{(k+1)}(x)$, which proves (43) for $a = k - 1, m = 1$.

Next, consider the case $m = 2$ in (43). As in the case of $m = 1$, the relation is equivalent to (31) for $a = 1 \sim k - 2$. One only has to pay an attention,

$$T_{D_0}^\vee(x) = T_0(x \pm \frac{1}{2k+2}i) = t_2^{(0)}(x)$$

for $a = 1$. In the case of $a = k - 1$, the product of $t_2^{(k-1)}(x)$ reads,

$$t_2^{(k-1)}(x \pm \frac{1}{2k+2}i) = \begin{cases} T_{D_{2k-2}}^\vee(x \pm 2i) = T_{2k-2}^\vee(x)T_{B_3}(x \pm \frac{1}{2k+2}i) + T_{D_{2k}}^\vee(x)T_{D_{2k-4}}^\vee(x) & k \text{ even} \\ T_{D_{2k-2}}^\vee(x \pm 2i) = T_{2k-2}(x)T_{B_3}(x \pm \frac{1}{2k+2}i) + T_{D_{2k}}(x)T_{D_{2k-4}}(x) & k \text{ odd} \end{cases}$$

where (31) is again applied. The first term in the rhs is the product $t_1^{(k-1)}(x)t_3^{(k-1)}(x)$, while the second is $t_2^{(k)}(x)t_2^{(k+1)}(x)t_2^{(k-2)}(x)$. This comes from Lemma 5, as $t_2^{(k)}(x)t_2^{(k+1)}(x) = (t_2^{(k)}(x))^2$. Thus the case $a = k - 1, m = 2$ is proved.

The case $a = k, m = 2$ is the most non-trivial. We treat only the case k even for brevity. When taking the product $t_2^{(k)}(x \pm i\frac{1}{2k+2})$, we substitute two different expressions for $t_2^{(k)}(x)$. The first comes from the already proved relation, $t_2^{(k)}(x) = t_1^{(k)}(x \pm i\frac{1}{2k+2}) - t_1^{(k-1)}(x)$. The second is as listed in (94).

The first expression results, after applying (101),

$$\begin{aligned} & t_2^{(k)}(x \pm i\frac{1}{2k+2}) \\ &= \frac{1}{2} \left(T_{2k}(x)T_{2k-4}(x) + T_{2k}(x)T_{2k+4}(x) \right. \\ & \quad \left. - T_{2k-2}(x - \frac{1}{2k+2}i)T_{2k+2}^\vee(x + \frac{1}{2k+2}i) - T_{2k-2}^\vee(x + \frac{1}{2k+2}i)T_{2k+2}(x - \frac{1}{2k+2}i) \right) \\ &= \frac{1}{2} \left(T_{2k}(x)T_{2k-4}(x) + T_{2k}(x)T_{2k+4}(x) \right. \\ & \quad \left. - T_{2k-2}(x - 2i)T_{2k+2}(x + 2i) - T_{2k-2}(x + 2i)T_{2k+2}(x - 2i) \right). \end{aligned} \quad (50)$$

From the second expression, $t_2^{(k)}(x) = (T_{2k+2}^\vee(x) - T_{2k-2}^\vee(x))/2$, we find

$$\begin{aligned} t_2^{(k)}(x \pm i\frac{1}{2k+2}) &= \frac{1}{4} \left(T_{2k}(x)T_{2k-4}(x) + T_{2k}(x)T_{2k+4}(x) + T_{D_{2k-2}}(x) + T_{D_{2k+2}}(x) \right. \\ & \quad \left. - T_{2k-2}(x - 2i)T_{2k+2}(x + 2i) - T_{2k-2}(x + 2i)T_{2k+2}(x - 2i) \right) \end{aligned} \quad (51)$$

where (30) is used. Twice (51) and subtract (50), one arrives at,

$$t_2^{(k)}(x \pm i\frac{1}{2k+2}) = \frac{1}{2}(T_{D_{2k-2}}(x) + T_{D_{2k+2}}(x)) = T_{D_{2k-2}}(x) + \frac{1}{2}(T_{D_{2k+2}}(x) - T_{D_{2k-2}}(x)).$$

The first term in the rhs coincides with $t_2^{(k-1)}(x)$, while the second agrees with $t_1^{(k)}(x)t_3^{(k)}(x)$ due to Lemma 6. Thus the case $a = k, m = 2$ is established.

Finally consider the case $m = 3$. Except for the case $a = 1$, the relation is satisfied trivially. When $a = 1$, the lhs reads

$$\begin{aligned} t_3^{(1)}(x \pm \frac{1}{2k+2}i) &= T_{B_3}(x \pm \frac{k-2}{2k+2}i)T_{B_3}(x \pm \frac{k}{2k+2}i) \\ &= T_{B_3}(x \pm \frac{k-2}{2k+2}i)(T_0(x)T_0(x \pm \frac{2}{2k+2}i) + T_{B_1}(x)T_{B_5}(x)) \\ &= T_{B_3}(x \pm \frac{k-2}{2k+2}i)T_0(x)T_0(x \pm \frac{2}{2k+2}i) + T_{D_2}(x)T_{B_1}(x)T_{B_3}(x \pm \frac{k-2}{2k+2}i) \end{aligned}$$

where (23) is used in the second quality and $T_{D_2}(x) = T_{B_5}(x)$ is used in the last.

By noting $t_3^{(0)}(x) = T_0(x)T_0(x \pm \frac{2}{2k+2}i)$, one find the resultant expression coincides with $t_3^{(2)}(x)t_3^{(0)}(x) + t_2^{(1)}(x)t_4^{(1)}(x)$.

We thereby verified the magnon-like t system for $L = 4k + 2$.

11 Thermodynamic Bethe Ansatz in the scaling limit

11.1 Analytic properties

The $Y-$ systems are obtained in [25] by the simply Fourier transformation of the thermodynamic Bethe ansatz equation (TBA, for short), which is proposed in advance. In the present report, the $Y-$ system has been proved first, in the preceding sections. The (inverse) transformation of the $Y-$ system to TBA seems thus to be direct. This is, however, not necessary true. One needs further analytic properties of of $Y-$ functions as we shall see below.

The $Y-$ system typically assumes the following form. (See appendix A for notations.)

$$Y_m^{(a)}(x \pm i\alpha) = \prod_{b,j} \Xi_j^{(b)}(x \pm i\gamma_j^{(b)}) \prod_{c,k} \mathcal{L}_k^{(c)}(x \pm i\gamma_k^{(c)}) \quad (52)$$

We try to take the logarithm of both sides and take the Fourier transformation. For the necessary condition that the last transformation can be done simply, one must ensure that the lhs (rhs) is analytic and nonzero in the strip $\Im x \in [-\alpha, \alpha]$ ($\Im x \in [-\gamma_j^{(b)}, \gamma_j^{(b)}]$). Otherwise, one must take account of contributions from zeros in the strips.

As is already shown, complex combinations of "transfer matrices" solve the both sides. The explicit expressions for eigenvalues of transfer matrices thus enable the investigations of the analytic properties of the $Y-$ systems, once parameters, N, q, β are fixed. We have carried out numerical investigation for ranges of parameters, $L = 5, 7, 8, 9, 10, 4 \leq N \leq 10, 0 \leq q \leq 0.5, \beta = 0.04, 0, 05, \dots, 0.1$. Although our main interest is focus on the limit $N \rightarrow \infty$, our data suggests weak dependency on N . For illustration, appendix G presents some numerical data and graph showing locations of zeros for various transfer matrices

for the dilute A_8 model in regime 2. The analytic property of Y can be easily read off from these zeros.

To state our conclusion, we remark that the Y -system is invariant, for even N , if Y is replaced by \tilde{Y} , defined by

$$\tilde{Y}_{B_1}(x) = \begin{cases} \frac{Y_{B_1}(x)}{\kappa(x \pm i(1+u')\frac{L-2}{2(L+2)})} & \text{for } u < 0 \\ Y_{B_1}(x)\kappa(x \pm i(1-u')\frac{L-2}{2(L+2)}) & \text{for } u > 0 \end{cases}$$

and all other cases, $\tilde{Y} = Y$. The parameter u' stands for $\frac{2(L+2)}{L-2}u$. This is due to the definition of κ ,

$$\kappa(x) = \left(i \frac{\vartheta_1(i\frac{(L+2)}{2(L-2)}\pi x, \tau')}{\vartheta_2(i\frac{(L+2)}{2(L-2)}\pi x, \tau')} \right)^N$$

which satisfies $\kappa(x \pm i\frac{L-2}{2(L+2)}) = 1$. The elliptic nome $q' = \exp(-\tau')$, $\tau' = \frac{2(L+1)}{L-2}\tau$ is introduced so as to respect the periodicity of the Y function on the real direction of x . We refer the resultant functional relation to \tilde{Y} -system.

Our conjecture is as follows.

Conjecture 2. *The both sides of the \tilde{Y} -system are analytic and nonzero for appropriate strips, for any L, N, q, β .*

11.2 The coupled Integral equations

Once the conjecture 2 is taken for granted, the transformation of the \tilde{Y} -system into a set of integral equations is straightforward. When all \tilde{Y} functions are replaced by Y , only the integral equation for $\log Y_{B_1}(x)$ possesses a drive term. That is, for $u > 0$, with appropriate kernel functions $K_{B_1,a,m}$, it takes of the form,

$$\begin{aligned} \log Y_{B_1}(x) = & -\log \kappa(x \pm i(1-u')\frac{L-2}{2(L+2)}) + \sum_{(a,m)} \int_{-\tau''}^{\tau''} K_{B_1,a,m}(x-x') \log \Xi_m^{(a)}(x') dx' \\ & + \sum_{(a,m)} \int_{-\tau''}^{\tau''} K_{B_1,a,m}(x-x') \log \mathcal{L}_m^{(a)}(x') dx' \end{aligned} \quad (53)$$

where $\tau'' = \frac{(L-2)}{(L+2)}\frac{\tau'}{\pi}$. For $u < 0$, the driving term should be $\log \kappa(x \pm i(1+u')\frac{L-2}{2(L+2)})$.

The free-energy is evaluated from

$$\begin{aligned}
\log T_{B_1}(x) &= \log r_N(x) + \int_{-\tau''}^{\tau''} s(x - x') \log \varepsilon_N(x') dx' \\
&\quad + \int_{-\tau''}^{\tau''} s(x - x') \log(1 + Y_{B_1}(x')) dx' \\
r_N(x) &= \left(\frac{h(x \pm (\frac{2L-4}{2L+4} + u)i)h(x \pm (\frac{4L}{2L+4} + u)i)}{h(\pm(\frac{2L-4}{2L+4})i)h(\pm(\frac{4L}{2L+4})i)} \right)^{\frac{N}{2}} \\
\varepsilon_N(x) &= \left(\frac{h(x \pm (\frac{L-2}{2L+4} - u)i)h(x \pm (\frac{3L+2}{2L+4} - u)i)}{h(x \pm (\frac{L-2}{2L+4} + u)i)h(x \pm (\frac{3L+2}{2L+4} + u)i)} \right)^{\frac{N}{2}} \\
\widehat{s(k)} &= \frac{1}{2 \cosh \frac{L-2}{2(L+2)} k}.
\end{aligned} \tag{54}$$

Here we denote the Fourier transformation of $F(x)$ by $\widehat{F}(k)$,

$$\begin{aligned}
\widehat{F}(k) &= \int_{-\tau''}^{\tau''} F(x) e^{-ikx} dx \\
F(x) &= \frac{\delta}{2\pi} \sum_n \widehat{F}(k_n) e^{ik_n x}, \quad k_n = n\delta
\end{aligned}$$

and $\delta = \pi/\tau''$. The free energy is determined by the value of $T_{B_1}(x)$ at the origin, $\beta f = -\log T_{B_1}(0)$, thus we are only interested in $x \sim 0$ in (54).

All the above results are valid for any N . Now the Trotter limit can be performed analytically. The drive term in (53) becomes,

$$-\log \kappa(x \pm i(1 - u') \frac{L-2}{2(L+2)}) \rightarrow 4\beta\pi s(x)$$

while

$$\begin{aligned}
\log r_N(0) &\rightarrow \lambda\beta \left((\log \vartheta_1(\frac{L-2}{L+2}\lambda))' + (\log \vartheta_1(\frac{2L}{L+2}\lambda))' \right) \\
\log \varepsilon_N(x) &\rightarrow \lambda\beta \left((\log \frac{\vartheta_1(\lambda(ix - \frac{L-2}{2L+4}))}{\vartheta_1(\lambda(ix + \frac{L-2}{2L+4}))})' + (\log \frac{\vartheta_1(\lambda(ix - \frac{3L+2}{2L+4}))}{\vartheta_1(\lambda(ix + \frac{3L+2}{2L+4}))})' \right)
\end{aligned}$$

for $u = \beta/N$. The crossing parameter λ is set to be $\frac{\pi(L+2)}{4(L+1)}$.

11.3 Thermodynamic Bethe Ansatz equations

We consider the scaling limit $q \rightarrow 0, \beta \rightarrow \infty$ [19]. The precise tuning of these two parameters will be specified below. In order to take this limit, we conveniently rewrite the

integrals in the preceding subsection in such a form that "kernel function times small functions". The numerical calculation indicates, in the vicinity of the origin,

$$\begin{cases} |Y| \gg 1, & u > 0 \\ |Y| \ll 1, & u < 0. \end{cases}$$

if $\beta \gg 1$. In the connection with $M_{L,L+1} + \Phi_{1,2}$ theory, we are interested in the regime 2 ($u > 0$) case. Thus we first rewrite the Y system such that the relations involves only $(1 + \frac{1}{Y})$. Now the important contribution for the integral comes from "Fermi" surface $x' \sim \tau'$. Thus we are interested in the scaling function, $\lim_{q \rightarrow 0} y_{B_1}(x + \tau')$ etc and integral equations among them, TBA equation. To derive them, we take the logarithm of both sides of the transformed Y system above, take also the Fourier transform and find

$$\widehat{M} \begin{pmatrix} \widehat{\log Y_{B_1}} \\ \widehat{\log Y_{B_3}} \\ \vdots \end{pmatrix} = 4\pi\beta \begin{pmatrix} 1 \\ 0 \\ \vdots \end{pmatrix} + \widehat{K}_0 \begin{pmatrix} \widehat{L}_{B_1} \\ \widehat{L}_{B_3} \\ \vdots \end{pmatrix} \quad (55)$$

where $\widehat{L}_{B_1} = \widehat{\log}(1 + \frac{1}{Y_{B_1}})$ and similarly for others. Note that M and K_0 are asymmetric matrices. See appendix H for the example for $L = 5, 7$. By multiplying M^{-1} from the left, @the kernel matrix for TBA, $M^{-1}K_0$ turns out to be symmetric, remarkably. This property is crucial in applying the dilogarithm technique to evaluate the central charge. Its elements agree with the expression described in [25] in terms of S matrices, under identification $x = 3\theta/\pi$ in the limit $q \rightarrow 0$. Finally, we have checked that nonzero drive terms exist only for Y functions corresponding to Breathers and Kinks. For example, we consider $L = 5$. The explicit forms of the drive terms in the Fourier space read,

$$\begin{aligned} \widehat{d}_{B_1} &= \frac{8\pi\beta \cosh \frac{11}{14}k}{(2 \cosh \frac{2}{14}k - 1)D(k)} \\ \widehat{d}_{B_3} &= \frac{4\pi\beta(2 \cosh \frac{2}{14}k + 1)(2 \cosh \frac{4}{14}k - 1)}{D(k)} \\ \widehat{d}_{B_5} &= \frac{16\pi\beta \cosh \frac{1}{14}k \cosh \frac{4}{14}k}{(2 \cosh \frac{2}{14}k - 1)D(k)} \\ \widehat{d}_{B_2} &= \frac{8\pi\beta \cosh \frac{1}{14}k}{(2 \cosh \frac{2}{14}k - 1)D(k)} \\ \widehat{d}_{K_1} &= \frac{4\pi\beta}{(2 \cosh \frac{2}{14}k - 1)D(k)} \\ \widehat{d}_{K_2} &= \frac{8\pi\beta \cosh \frac{4}{14}k}{(2 \cosh \frac{2}{14}k - 1)D(k)}, \end{aligned}$$

where we denote by \widehat{d}_{B_1} for the drive term associated to $\widehat{\log Y_{B_1}}$ and so on. A common denominator $D(k)$ denotes

$$D(k) = 2 \cosh \frac{12}{14}k + 2 \cosh \frac{10}{14}k - 2 \cosh \frac{6}{14}k - 2 \cosh \frac{4}{14}k + 1.$$

When taking the inverse Fourier transformation, the nearest zero to the real axis of the denominator is relevant in the "scaling" limit, $q \rightarrow 0$. We have checked for various L that the zero of the common denominator $D(k)$ brings the nearest zero, and always, $k = \pm i\frac{\pi}{3}$.

Let us be more explicit for $L = 5$. As announced above, we are interested in the integral equation for $y(x) = \lim_{q \rightarrow 0} Y(x + \tau'')$. Thus the associated drive term reads,

$$d^{\text{scaling}}(x) := \lim_{q \rightarrow 0} d(x + \tau'') = \lim_{q \rightarrow 0} \frac{1}{2\pi} \sum_m \int_{-\infty}^{\infty} e^{2\pi i m \frac{k'}{\delta} + i(x + \tau'')k'} \hat{d}(k') dk'$$

where the Poisson's summation formula is applied. As $q \rightarrow 0$, δ, τ'' tends to be infinity, the only $m = 0, m = -1$ terms contribute,

$$d^{\text{scaling}}(x) \sim \lim_{q \rightarrow 0} \left(\frac{1}{2\pi} \int_{-\infty}^{\infty} e^{i(x + \tau'')k'} \hat{d}(k') dk' + \frac{1}{2\pi} \int_{-\infty}^{\infty} e^{-i(\tau'' - x)} \hat{d}(k') dk' \right).$$

We enclose the complex contour of the integration in the upper half plane for the first term and in the lower half plane for the second. For $\tau'' \rightarrow \infty$, the nearest poles $k = \pm i\pi/3$ bring the dominant contributions. We denote

$$\frac{1}{D(k)} \sim \frac{r}{(k - i\frac{\pi}{3})i},$$

then

$$d_{K_1}^{\text{scaling}}(x) = \frac{8\pi r}{2 \cos \frac{\pi}{21} - 1} e^{-\frac{4}{7}\tau} \cosh \frac{\pi}{3} x$$

for example. Let R be radius of compactification. Then we take $q \rightarrow 0, \beta \rightarrow \infty$ while m_k finite; $m_k R = \frac{8\pi\beta r}{2 \cos \frac{\pi}{21} - 1} q^{\frac{4}{7}}$. This is the precise meaning of our scaling limit. We write $\frac{\pi}{3}x = \theta$. Immediately, one verifies that all other drive terms also take the form $mR \cosh \theta$ and their mass ratio agree with those in [25].

$$\begin{aligned} m_{B_1} &= 2m_K \cos \frac{11}{42}\pi & m_{B_3} &= 4m_K \cos \frac{11}{42}\pi \cos \frac{3}{42}\pi \\ m_{B_5} &= 4m_K \cos \frac{1}{42}\pi \cos \frac{4}{42}\pi & m_{B_2} &= 2m_K \cos \frac{1}{42}\pi \\ m_{K_2} &= 2m_K \cos \frac{4}{42}\pi. \end{aligned}$$

We then write $y_a(\theta) = \exp(\epsilon(\theta))$, and verify that the TBA is recovered in the scaling limit.

We comment that for general L , the straightforward calculation shows $m_K \propto q^{\frac{2(L+1)}{3(L+2)}}$. This is consistent with scaling relation, $\xi = \frac{1}{2-2\Delta_{1,2}}$ for $m \propto q^\xi$. Indeed comparison of the result leads to proper scaling dimension, $\Delta = \frac{L-2}{4(L+1)}$.

It remains to check the expression for the scaling free energy.

The scaling limit of free energy comes from the contribution from the last term in (54) at $x = 0$.

$$\int_{-\infty}^{\infty} s(x') \log(1 + Y_{B_1}(x')) dx' = \int_{-\infty}^{\infty} s(x') \log Y_{B_1}(x') dx' + \int_{-\infty}^{\infty} s(x') \log L_{B_1} dx'.$$

We substitute the inverse transformed (55) into the first term in the rhs above to find,

$$\int_{-\infty}^{\infty} s(x') \log(1 + Y_{B_1}(x')) dx' = \int_{-\infty}^{\infty} s(x') d_{B_1}(x') dx' + \sum_{\ell} \int_{-\infty}^{\infty} \mathcal{K}_{\ell}(x') \log L_{\ell} dx'.$$

where \mathcal{K}_{ℓ} reads in the Fourier space,

$$\widehat{\mathcal{K}}_{\ell} = \widehat{s}(\widehat{M}^{-1})_{1,j} \widehat{D}_{j,\ell}.$$

and

$$\widehat{D}_{i,j} := \widehat{M}_{i,j} + (\widehat{K}_0)_{i,j}.$$

We adopt indices $y_{B_1} = y_1, y_{B_3} = y_2$, and so on.

The scaling free energy f_s , the contribution of excitations near the Fermi surface, is thus identified with

$$f_s = - \lim_{q \rightarrow 0} \frac{1}{\beta} \sum_{\ell} \int_{-\infty}^{\infty} \mathcal{K}_{\ell}(x' + \tau'') \log(1 + \frac{1}{y_{\ell}}(x')) dx'.$$

To perform the limit, we use a remarkable relation,

$$\widehat{\mathcal{K}}_{\ell} = \widehat{d}_{\ell}$$

which we checked case by case. Then one repeats the same argument in deriving the drive terms in TBA equation, and reaches

$$f_s = -\frac{1}{2\pi} \sum_{\ell} \int_{-\infty}^{\infty} m_{\ell} \cosh \theta \log(1 + \frac{1}{y_{\ell}}) d\theta, = -\frac{1}{2\pi} \sum_{\ell} \int_{-\infty}^{\infty} m_{\ell} \cosh \theta \log(1 + e^{-\epsilon(\theta)}) d\theta$$

under tuning $\beta = \sqrt{\frac{2\pi}{3}}R$. Therefore the field theoretical expression of the free energy is also reproduced.

12 Summary and discussions

In this report, we establish relevant functional relations of the dilute A_L models for *arbitrary* L , to analyze finite temperature property we demonstrate explicitly that TBA equations for $M_{L,L+1} + \phi_{1,2}$, conjectured by Dorey, Pocklington and Tateo [25], is realized in the scaling limit. The crucial idea is to introduce fusion transfer matrices associated to skew Young tableaux and to investigate the functional relations among them.

There are still many open problems. The explicit identification of string solutions would be definitely one of the most important. The complete study on this will shed some light on the way how to proceed for TBA in the case of perturbed nonunitary minimal models. We mention the first step in this direction in [57]. The minimal unitary theory perturbed by $\phi_{2,1}$ may be treated within the same framework. One only has to deal with the regime 1 instead of the regime 2. We already have some results about the "exceptional" cases in terminology of [25], however, they are omitted in this report for brevity. We hope to complete the program on the $\phi_{2,1}$ theory for arbitrary L in a subsequent report.

Before closing this paper, we comment on a possible link to Fermionic formulae of the Virasoro characters. In [58, 59, 60, 61, 62], remarkable results are reported on new representations of the Virasoro characters which originate from fermionic particle bases of the Bethe ansatz equations. See also combinatorial arguments in view of TBA[63, 64] and mathematical generalizations based on the combinatorial objects, the rigged configurations[65]-[69]. The Fermionic characters obtained in [58] -[64] seem to be connected to $\phi_{1,3}$ perturbation. In [70, 71], they also explicitly showed the different realization of Fermionic formulae which are related to $\phi_{2,1}$ or $\phi_{1,5}$ perturbations.

Since the TBA in [25] offers a description of the associated Hilbert space, it might be natural to expect that a new fermionic representation is possible based on the $\phi_{1,2}$ perturbation. There exists already positive results based on the simplest case, the dilute A_3 model [72]. It may be natural to expect the generalizations.

Indeed, we check up to $O(q^{200})$ that the following formula is valid,

$$\chi_{1,1}^{5,6} = \sum \frac{q^{\frac{1}{2}n_7 n_8}}{\prod_{i=1}^6 (q)_{n_i}} \begin{bmatrix} n_5 + n_6 + n_8 \\ 2 \end{bmatrix} \begin{bmatrix} n_7 \\ 2 \end{bmatrix} \begin{bmatrix} n_8 \\ 2 \end{bmatrix}$$

where

$$g = \begin{pmatrix} 4, & 6, & 8, & 4, & 2, & 4, & 0, & 0 \\ 6, & 12, & 16, & 8, & 4, & 8, & 0, & 0 \\ 8, & 16, & 24, & 12, & 6, & 12, & 0, & 0 \\ 4, & 8, & 12, & 8, & 4, & 6, & 0, & 0 \\ 2, & 4, & 6, & 4, & 3, & 3, & -\frac{1}{2}, & 0 \\ 4, & 8, & 12, & 6, & 3, & 7, & -\frac{1}{2}, & 0 \\ 0, & 0, & 0, & 0, & -\frac{1}{2}, & -\frac{1}{2}, & 1, & -\frac{1}{2} \\ 0, & 0, & 0, & 0, & 0, & 0, & -\frac{1}{2}, & 1 \end{pmatrix}.$$

The summation is taken under the condition, $n_7 \leq \frac{n_5 + n_6 + n_8}{2} \in \mathbb{Z}_{\geq 0}$, $n_8 \leq \frac{n_7}{2} \in \mathbb{Z}_{\geq 0}$. Note that g has its origin in the kernel functions of the TBA equation.

A similar formula for $\chi_{1,1}^{7,8}$ is checked up to $O(q^{100})$, which may imply the existence of Fermionic formulae for L odd case in general. We are not yet able to find such a simple expression for the L even case. We hope to clarify this in a future publication ².

Acknowledgements The author would like to thank P. Dorey and R. Tateo for many valuable comments, discussions, critical reading of the manuscript and collaborations at

²We have learnt that S.O. Warnaar has independently found polynomial version of these formulas corresponding to both $\Phi_{1,2}$ and $\Phi_{2,1}$ perturbations.

early stage. He also thanks S.O. Warnaar for correspondence, B.M. McCoy, P.A. Pearce and J. Shiraishi for conversations. A part of the present work has been reported at the APCTP focus program, 'Finite size technology in low dimensional quantum field theory'. The author thanks organizers for the kind invitation. This work has been supported by a Grant-in-Aid for Scientific Research from the Ministry of Education, Culture, Sports and Technology of Japan, no. 14540376.

A Y-system

As obtained in [25], Y system for the minimal unitary theories perturbed by $\Phi_{1,2}$ falls into 4 categories. Below we shall summarize their result with slight changes in notations. Instead of their rapidity variable θ , we use x as in the text. They are simply related by $x = \frac{3\theta}{\pi}$. By \mathcal{L} we mean $\mathcal{L} = \frac{1}{1+\frac{1}{Y}}$ for a Y function. In the section 11, an inverse function $L = 1 + \frac{1}{Y}$ is also introduced but it will not be utilized here. We understand indices associated with \mathcal{L} specify these for Y functions, e.g.,

$$\mathcal{L}_m^{(a)}(x) = \frac{1}{1 + \frac{1}{Y_m^{(a)}(x)}}$$

etc. Similarly $\Xi_m^{(a)}$ denotes

$$\Xi_m^{(a)}(x) = 1 + Y_m^{(a)}(x)$$

A.1 Case, ($L = 4k - 1, k \geq 2$):

The Y-system is

$$\begin{aligned} Y_{B_1}(x \pm \frac{L-2}{2L+4}i) &= \Xi_{B_3}(x) \\ Y_{B_3}(x \pm \frac{L-2}{2L+4}i) &= \Xi_{B_1}(x) \Xi_{k-1}^{(2)}(x) \prod_{\ell=0}^{k-2} \Xi_{\ell}^{(2)}(x \pm \frac{4k-4\ell-7}{2L+4}i) \\ Y_j^{(\alpha)}(x \pm \frac{4}{2L+4}i) &= [\Xi_{B_3}(x)]^{\delta_{j0}\delta_{\alpha2}} \Xi_j^{(\bar{\alpha})}(x) \prod_{\ell=0}^{k-2} \left(\mathcal{L}_{\ell}^{(\alpha)}(x) \right)^{I_{\ell,j}^{[A_{k-1}]}} \\ &\times \left[\mathcal{L}_{k-1}^{(4)}(x) \mathcal{L}_{k-1}^{(6)}(x) \mathcal{L}_{k-1}^{(5)}(x \pm \frac{1}{2L+4}i) \mathcal{L}_{k-1}^{(3)}(x \pm \frac{2}{2L+4}i) \mathcal{L}_{k-1}^{(1)}(x \pm \frac{3}{2L+4}i) \right]^{\delta_{j,k-2}\delta_{\alpha1}} \\ &\times \left[\mathcal{L}_{k-1}^{(3)}(x) \mathcal{L}_{k-1}^{(6)}(x) \mathcal{L}_{k-1}^{(5)}(x \pm \frac{1}{2L+4}i) \mathcal{L}_{k-1}^{(4)}(x \pm \frac{2}{2L+4}i) \mathcal{L}_{k-1}^{(2)}(x \pm \frac{3}{2L+4}i) \right]^{\delta_{j,k-2}\delta_{\alpha2}} \\ &\quad (\text{with } j = 0, \dots, k-2; \alpha = 1, 2 \text{ and } \bar{\alpha} = 3 - \alpha) \\ Y_{k-1}^{(\gamma)}(x \pm \frac{1}{2L+4}i) &= \left[\mathcal{L}_{k-2}^{(\gamma)}(x) \right]^{\delta_{\gamma1}+\delta_{\gamma2}} \prod_{\beta \sim \gamma} \left[\Xi_{k-1}^{(\beta)}(x) \right] \quad (\gamma = 1, \dots, 6) \end{aligned}$$

where the last product is taken over nodes on the E_6 Dynkin diagram, which is obtained from fig. 10 by deleting the node 7. $I^{[A_{k-1}]}$ stands for the incidence matrix for A_{k-1} , where nodes are indexed by 0 to $k-2$.

A.2 Case, ($L = 4k, k \geq 2$):

The Y-system is

$$Y_{B_1}(x \pm \frac{L-2}{2L+4}i) = \Xi_{B_3}(x) \quad (56)$$

$$Y_{B_3}(x \pm \frac{L-2}{2L+4}i) = \Xi_{B_1}(x) \Xi_{k-1}^{(2)}(x) \prod_{\ell=0}^{k-2} \Xi_{\ell}^{(2)}(x \pm \frac{4k-4\ell-6}{2L+4}i) \quad (57)$$

$$\begin{aligned} Y_j^{(\alpha)}(x \pm \frac{4}{2L+4}i) &= [\Xi_{B_3}(x)]^{\delta_{j0}\delta_{\alpha2}} \Xi_j^{(\bar{\alpha})}(x) \prod_{\ell=0}^{k-2} \left(\mathcal{L}_{\ell}^{(\alpha)}(x) \right)^{I_{\ell j}^{[A_{k-1}]}} \\ &\times \left[\mathcal{L}_{k-1}^{(0)}(x) \mathcal{L}_{k-1}^{(3)}(x) \mathcal{L}_{k-1}^{(1)}(x \pm \frac{2}{2L+4}i) \right]^{\delta_{j,k-2}\delta_{\alpha1}} \\ &\times \left[\mathcal{L}_{k-1}^{(0)}(x) \mathcal{L}_{k-1}^{(4)}(x) \mathcal{L}_{k-1}^{(2)}(x \pm \frac{2}{2L+4}i) \right]^{\delta_{j,k-2}\delta_{\alpha2}} \\ &\quad (\text{with } j = 0, \dots, k-2; \alpha = 1, 2 \text{ and } \bar{\alpha} = 3 - \alpha) \end{aligned} \quad (58)$$

$$Y_{k-1}^{(\gamma)}(x \pm \frac{2}{2L+4}i) = \left[\mathcal{L}_{k-2}^{(\gamma)}(s) \right]^{\delta_{\gamma1}+\delta_{\gamma2}} \prod_{\beta \sim \gamma} \left[\Xi_{k-1}^{(\beta)}(x) \right] \quad (\gamma = 0, \dots, 4) \quad (59)$$

where the last product is taken over nodes on the A_5 Dynkin diagram, which is obtained from fig. 9 by deleting the node 7.

A.3 Case, ($L = 4k + 1, k \geq 2$):

The Y-system is

$$\begin{aligned}
Y_{B_1}(x \pm \frac{(L-2)}{2L+4}i) &= \Xi_{B_3}(x) \\
Y_{B_3}(x \pm \frac{(L-2)}{2L+4}i) &= \Xi_{B_1}(x) \Xi_{k-1}^{(2)}(x) \prod_{\ell=0}^{k-2} \Xi_i^{(2)}(x \pm \frac{4k-4\ell-5}{2L+4}i) \\
Y_j^{(\alpha)}(x \pm \frac{4}{2L+4}i) &= [\Xi_{B_3}(x)]^{\delta_{j0}\delta_{\alpha2}} \Xi_j^{(\bar{\alpha})}(x) \prod_{\ell=0}^{k-2} \left(\mathcal{L}_\ell^{(\alpha)}(x) \right)^{I_{\ell,j}^{[A_{k-1}]}} \\
&\quad \times \left[\mathcal{L}_{k-1}^{(3)}(x) \mathcal{L}_{k-1}^{(1)}(x \pm \frac{1}{2L+4}i) \right]^{\delta_{j,k-2}\delta_{\alpha1}} \\
&\quad \times \left[\mathcal{L}_{k-1}^{(4)}(x) \mathcal{L}_{k-1}^{(2)}(x \pm \frac{1}{2L+4}i) \right]^{\delta_{j,k-2}\delta_{\alpha2}} \\
&\quad (\text{with } j = 0, \dots, k-2; \alpha = 1, 2 \text{ and } \bar{\alpha} = 3 - \alpha) \\
Y_{k-1}^{(1)}(x \pm \frac{2}{2L+4}i) &= \mathcal{L}_{k-2}^{(1)}(x) \Xi_{k-1}^{(4)}(x) \Xi_{k-1}^{(6)}(x) \Xi_{k-1}^{(5)}(x \pm \frac{1}{2L+4}i) \Xi_{k-1}^{(3)}(x \pm \frac{2}{2L+4}i) \\
Y_{k-1}^{(2)}(x \pm \frac{3}{2L+4}i) &= \mathcal{L}_{k-2}^{(2)}(0) \Xi_{k-1}^{(3)}(x) \Xi_{k-1}^{(6)}(x) \Xi_{k-1}^{(5)}(x \pm \frac{1}{2L+4}i) \Xi_{k-1}^{(4)}(x \pm \frac{2}{2L+4}i) \\
Y_{k-1}^{(3)}(x \pm \frac{1}{2L+4}i) &= \Xi_{k-1}^{(1)}(x) \mathcal{L}_{k-1}^{(5)}(x) \\
Y_{k-1}^{(4)}(x \pm \frac{1}{2L+4}i) &= \Xi_{k-1}^{(2)}(x) \mathcal{L}_{k-1}^{(5)}(x) \\
Y_{k-1}^{(5)}(x \pm \frac{1}{2L+4}i) &= \mathcal{L}_{k-1}^{(6)}(x) \mathcal{L}_{k-1}^{(3)}(x) \mathcal{L}_{k-1}^{(4)}(x) \\
Y_{k-1}^{(6)}(x \pm \frac{1}{2L+4}i) &= \mathcal{L}_{k-1}^{(5)}(x).
\end{aligned}$$

A.4 Case, ($L = 4k + 2, k \geq 2$):

$$\begin{aligned}
Y_{B_1}(x \pm \frac{L-2}{2L+4}i) &= \Xi_{B_3}(x) \\
Y_{B_3}(x \pm \frac{L-2}{2L+4}i) &= \Xi_{B_1}(x) \Xi_k^{(2)}(x) \prod_{\ell=0}^{k-1} \Xi_\ell^{(2)}(x \pm \frac{4k-4\ell-4}{2L+4}i) \\
Y_j^{(\alpha)}(x \pm \frac{4}{2L+4}i) &= [\Xi_{B_3}(x)]^{\delta_{j0}\delta_{\alpha2}} \Xi_j^{(\bar{\alpha})}(x) \prod_{\ell \sim j} \left[\mathcal{L}_\ell^{(\alpha)}(x) \right] \\
&\quad (\text{with } j = 0, \dots, k; \alpha = 1, 2 \text{ and } \bar{\alpha} = 3 - \alpha)
\end{aligned}$$

where the last product is taken over nodes on the D_{k+1} Dynkin diagram, which is obtained from fig. 11 by deleting the node 0.

B explicit solutions to magnon-like $t-$ system

Below, sets of explicit solutions to magnon-like $t-$ system are listed. There are, however, many equivalent expressions as remarked in the text. We write just representatives among them. When other expressions are convenient, some remarked will be made then.

B.1 solutions for $A_{L=4k-1}$

$$t_1^{(1)}(x) = \begin{cases} T_{2k}(x), & k \text{ even} \\ T_{2k}^\vee(x), & k \text{ odd} \end{cases} \quad (60)$$

$$t_1^{(2)}(x) = \begin{cases} T_{D_{2k}}^\vee(x), & k \text{ even} \\ T_{D_{2k}}(x), & k \text{ odd} \end{cases} \quad (61)$$

$$t_1^{(3)}(x) = \begin{cases} \Lambda_{(6k-2,2k)/(1)}(x - \frac{3}{2L+4}i), & k \text{ even} \\ \Lambda_{(6k-2,2k)/(1)}^\vee(x - \frac{3}{2L+4}i), & k \text{ odd} \end{cases} \quad (62)$$

$$t_1^{(4)}(x) = \begin{cases} \frac{1}{\phi^\vee(x+2ki+\frac{7}{2}i-\frac{i}{2L+4})} \Lambda_{(4k,4k,2k)/(4k-1,1)}^\vee(x - 2ki + i - \frac{i}{2L+4}), & k \text{ even} \\ \frac{1}{\phi(x+2ki+\frac{7}{2}i-\frac{i}{2L+4})} \Lambda_{(4k,4k,2k)/(4k-1,1)}(x - 2ki + i - \frac{i}{2L+4}), & k \text{ odd} \end{cases} \quad (63)$$

$$t_1^{(5)}(x) = \begin{cases} \Lambda_{(10k-4,6k-2,6k-3)/(4k-1,4k-2)}(x), & k \text{ even} \\ \Lambda_{(10k-4,6k-2,6k-3)/(4k-1,4k-2)}^\vee(x), & k \text{ odd} \end{cases} \quad (64)$$

$$t_1^{(6)}(x) = \frac{1}{\phi(x - (L+2)i - \frac{2i}{2L+4})} \Lambda_{(L,1)}(x - \frac{L+4}{2L+4}i) \quad (65)$$

$$t_1^{(7)}(x) = T_{B_3}(x). \quad (66)$$

For a guide to eye, corresponding diagrams are illustrated in fig. 12 for $k = 2$.

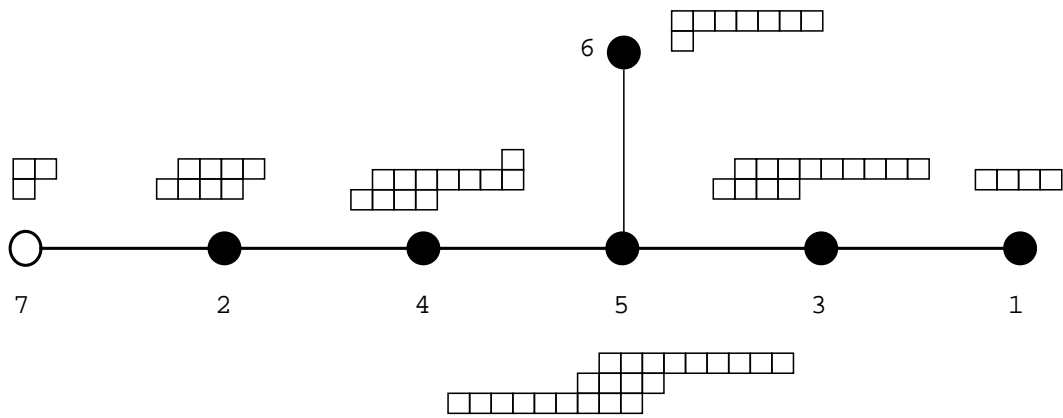


Figure 12: Young diagrams associated to $t_1^{(a)}(x)$ for $k = 2$.

For $t_2^{(a)}$,

$$t_2^{(1)}(x) = \begin{cases} T_{2k-2}^{\vee}(x \pm \frac{3}{2L+4}i), & k \text{ even} \\ T_{2k-2}(x \pm \frac{3}{2L+4}i), & k \text{ odd} \end{cases} \quad (67)$$

$$t_2^{(2)}(x) = \begin{cases} T_{D_{2k-2}}(x \pm \frac{3}{2L+4}i), & k \text{ even} \\ T_{D_{2k-2}}^{\vee}(x \pm \frac{3}{2L+4}i), & k \text{ odd} \end{cases} \quad (68)$$

$$t_2^{(3)}(x) = \begin{cases} T_{D_{2k-2}}(x)T_{2k-2}^{\vee}(x \pm \frac{2}{2L+4}i), & k \text{ even} \\ T_{D_{2k-2}}^{\vee}(x)T_{2k-2}(x \pm \frac{2}{2L+4}i), & k \text{ odd} \end{cases} \quad (69)$$

$$t_2^{(4)}(x) = \begin{cases} T_{D_{2k-2}}(x \pm \frac{2}{2L+4}i)T_{2k-2}^{\vee}(x), & k \text{ even} \\ T_{D_{2k-2}}^{\vee}(x \pm \frac{2}{2L+4}i)T_{2k-2}(x), & k \text{ odd} \end{cases} \quad (70)$$

$$t_2^{(5)}(x) = t_2^{(6)}(x \pm \frac{1}{2L+4}i) \quad (71)$$

$$t_2^{(6)}(x) = \begin{cases} T_{D_{2k-2}}(x)T_{2k-2}^{\vee}(x), & k \text{ even} \\ T_{D_{2k-2}}^{\vee}(x)T_{2k-2}(x), & k \text{ odd} \end{cases} \quad (72)$$

(73)

and

$$t_3^{(1)}(x) = \begin{cases} T_{2k-2}^{\vee}(x \pm \frac{2}{2L+4}i)T_{2k-4}(x), & k \text{ even} \\ T_{2k-2}(x \pm \frac{2}{2L+4}i)T_{2k-4}^{\vee}(x), & k \text{ odd} \end{cases} \quad (74)$$

$$t_3^{(2)}(x) = \begin{cases} T_{D_{2k-2}}(x \pm \frac{2}{2L+4}i)T_{D_{2k-4}}^{\vee}(x), & k \text{ even} \\ T_{D_{2k-2}}^{\vee}(x \pm \frac{2}{2L+4}i)T_{D_{2k-4}}(x), & k \text{ odd.} \end{cases} \quad (75)$$

(76)

B.2 solutions for $A_{L=4k}$

$$\begin{aligned} t_1^{(0)}(x) &= \begin{cases} t_1^{(3)}(x - \frac{2i}{L+2})T_{2k}(x + \frac{i}{L+2}) - t_1^{(3)}(x + \frac{2i}{L+2})T_{2k-2}^{\vee}(x - \frac{i}{L+2}), & k \text{ even} \\ t_1^{(3)}(x - \frac{2i}{L+2})T_{2k}^{\vee}(x + \frac{i}{L+2}) - t_1^{(3)}(x + \frac{2i}{L+2})T_{2k-2}(x - \frac{i}{L+2}), & k \text{ odd} \end{cases} \\ t_1^{(1)}(x) &= \begin{cases} T_{2k}(x), & k \text{ even} \\ T_{2k}^{\vee}(x), & k \text{ odd} \end{cases} \\ t_1^{(2)}(x) &= \begin{cases} T_{D_{2k}}^{\vee}(x), & k \text{ even} \\ T_{D_{2k}}(x), & k \text{ odd} \end{cases} \\ t_1^{(3)}(x) &= \frac{T_K(x)}{\sqrt{2}} \\ t_1^{(4)}(x) &= \frac{1}{\phi(x - \frac{2L}{L+2}i)}(t_1^{(3)}(x - \frac{L}{L+2}i)T_1(x + \frac{i}{2}) - t_1^{(3)}(x + \frac{L+4}{L+2}i)T_0(x - \frac{1}{2}i)) \\ t_1^{(7)}(x) &= T_{B_3}(x) \end{aligned}$$

Among $t_2^{(a)}(x)$, non-trivial are the cases $a = 3, 4$.

$$\begin{aligned} t_2^{(3)}(x) &= \begin{cases} T_{2k-2}^{\vee}(x), & k \text{ even} \\ T_{2k-2}(x), & k \text{ odd} \end{cases} \\ t_2^{(4)}(x) &= \begin{cases} T_{D_{2k-2}}(x), & k \text{ even} \\ T_{D_{2k-2}}^{\vee}(x), & k \text{ odd} \end{cases} \end{aligned}$$

and others are easily obtained from them due to the $t-$ system,

$$\begin{aligned} t_2^{(0)}(x) &= t_2^{(3)}(x)t_2^{(4)}(x) \\ t_2^{(1)}(x) &= t_2^{(3)}(x \pm \frac{i}{L+2}) \\ t_2^{(2)}(x) &= t_2^{(4)}(x \pm \frac{i}{L+2}). \end{aligned}$$

Finally,

$$\begin{aligned} t_3^{(1)}(x) &= \begin{cases} (T_{2k-2}^{\vee}(x))^2 T_{2k-4}(x), & k \text{ even} \\ (T_{2k-2}(x))^2 T_{2k-4}^{\vee}(x), & k \text{ odd} \end{cases} \\ t_3^{(2)}(x) &= \begin{cases} (T_{D_{2k-2}}(x))^2 T_{D_{2k-4}}^{\vee}(x), & k \text{ even} \\ (T_{D_{2k-2}}^{\vee}(x))^2 T_{D_{2k-4}}(x), & k \text{ odd.} \end{cases} \end{aligned}$$

B.3 solutions for $A_{L=4k+1}$

$$t_1^{(1)}(x) = \begin{cases} T_{2k-2}^{\vee}(x), & k \text{ even} \\ T_{2k-2}(x), & k \text{ odd} \end{cases} \quad (77)$$

$$t_1^{(2)}(x) = \begin{cases} T_{D_{2k-2}}(x), & k \text{ even} \\ T_{D_{2k-2}}^{\vee}(x), & k \text{ odd} \end{cases} \quad (78)$$

$$t_1^{(3)}(x) = \begin{cases} \Lambda_{(6k+2,2k)/(1)}(x - \frac{1}{2L+4}i), & k \text{ even} \\ \Lambda_{(6k+2,2k)/(1)}^{\vee}(x - \frac{1}{2L+4}i), & k \text{ odd} \end{cases} \quad (79)$$

$$t_1^{(4)}(x) = \frac{1}{\phi^{\vee}(x + (4k+3)i)} \Lambda_{(4k,4k,2k)/(4k-1,1)}^{\vee}(x + \frac{i}{2}), \quad (80)$$

$$t_1^{(5)}(x) = \begin{cases} \Lambda_{(10k+2,6k+2,6k+1)/(4k+1,4k)}^{\vee}(x), & k \text{ even} \\ \Lambda_{(10k+2,6k+2,6k+1)/(4k+1,4k)}(x), & k \text{ odd} \end{cases} \quad (81)$$

$$t_1^{(6)}(x) = \frac{1}{\phi(x - (L + \frac{3}{2})i + \frac{3L}{2L+4}i)} \Lambda_{(L,1)}(x + \frac{3L}{2L+4}i) \quad (82)$$

$$t_1^{(7)}(x) = T_{B_3}(x \pm \frac{3i}{2L+4}) \quad (83)$$

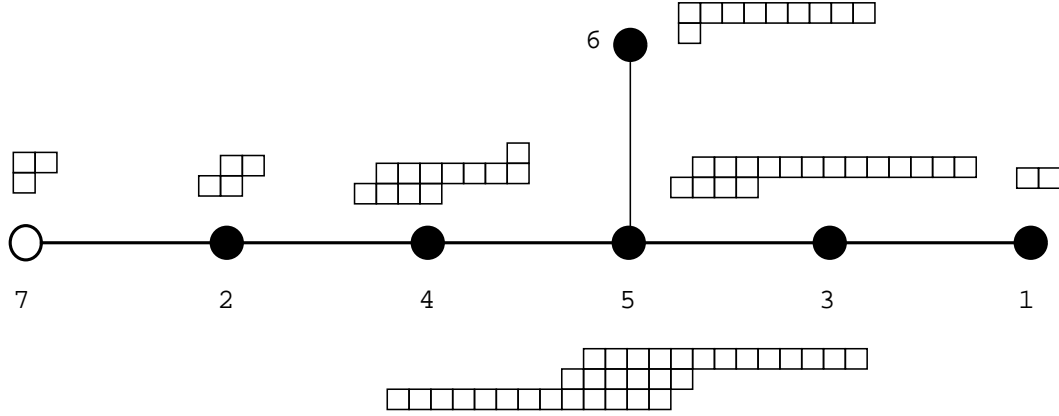


Figure 13: Young diagrams associated to $t_1^{(a)}(x)$ for $k = 2$.

The corresponding diagrams are illustrated in fig. 13 for $k = 2$. Notice their similarity to those in fig. 12.

For $t_2^{(a)}$,

$$t_2^{(1)}(x) = \begin{cases} T_{2k}(x)T_{2(k-2)}(x), & k \text{ even} \\ T_{2k}^\vee(x)T_{2(k-2)}^\vee(x), & k \text{ odd} \end{cases} \quad (84)$$

$$t_2^{(2)}(x) = \begin{cases} T_{D_{2k}}^\vee(x)T_{D_{2(k-2)}}^\vee(x), & k \text{ even} \\ T_{D_{2k}}(x)T_{D_{2(k-2)}}(x), & k \text{ odd} \end{cases} \quad (85)$$

$$t_2^{(3)}(x) = \begin{cases} T_{D_{2k}}^\vee(x)T_{2k}(x \pm \frac{2}{2L+4}i), & k \text{ even} \\ T_{D_{2k}}(x)T_{2k}^\vee(x \pm \frac{2}{2L+4}i), & k \text{ odd} \end{cases} \quad (86)$$

$$t_2^{(4)}(x) = \begin{cases} T_{D_{2k}}^\vee(x \pm \frac{2}{2L+4}i)T_{2k}(x), & k \text{ even} \\ T_{D_{2k}}(x \pm \frac{2}{2L+4}i)T_{2k}^\vee(x), & k \text{ odd} \end{cases} \quad (87)$$

$$t_2^{(5)}(x) = t_2^{(6)}(x \pm \frac{1}{2L+4}i) \quad (88)$$

$$t_2^{(6)}(x) = \begin{cases} T_{D_{2k}}^\vee(x)T_{2k}(x), & k \text{ even} \\ T_{D_{2k}}(x)T_{2k}^\vee(x), & k \text{ odd} \end{cases} \quad (89)$$

and the rests are found to be

$$t_3^{(3)}(x) = t_2^{(5)}(x) \quad (90)$$

$$t_3^{(4)}(x) = t_2^{(5)}(x)T_{B_3}(x). \quad (91)$$

B.4 solutions for $A_{L=4k+2}$

In this case, the eigenvalues of t associated to the tails, k and $k+1$, are identical.

$$t_1^{(k)}(x) = t_1^{(k+1)}(x) = \frac{T_K(x)}{2} \quad (92)$$

$$t_1^{(a)} = \begin{cases} T_{2a}(x), & a \text{ even} \\ T_{2a}^\vee(x), & a \text{ odd} \end{cases} \quad 0 \leq a \leq k-1 \quad (93)$$

$$t_2^{(k)}(x) = t_2^{(k+1)}(x) = \begin{cases} \frac{T_{2k+2}^\vee(x) - T_{2k-2}^\vee(x)}{2}, & k \text{ even} \\ \frac{T_{2k+2}(x) - T_{2k-2}(x)}{2}, & k \text{ odd} \end{cases} \quad (94)$$

$$t_2^{(a)}(x) = \begin{cases} T_{D_{2a}}^\vee(x), & a \text{ even} \\ T_{D_{2a}}(x), & a \text{ odd} \end{cases} \quad 0 \leq a \leq k-1 \quad (95)$$

(96)

$$t_3^{(k)}(x) = t_3^{(k+1)}(x) = T_{B_3}(x) \quad (97)$$

$$t_3^{(a)}(x) = T_{B_3}(x \pm \frac{k-a}{2k+2}i), \quad 1 \leq a \leq k-1 \quad (98)$$

$$t_4^{(1)}(x) = T_{B_1}(x)T_{B_3}(x \pm \frac{k-2}{2k+2}i). \quad (99)$$

C Functional relations for the kink transfer matrix

We verify the following lemma for relatively small values of k

Lemma 7. *The following functional relations among kink transfer matrices and T_m are valid for the dilute A_{4k} and A_{4k+2} models ($k = 1, 2, 3$ for the former and $k = 0 \sim 3$ for the latter) in regime 2. (corresponding to $M_{L,L+1} + \phi_{1,2}$)*

A_{4k} :

$$\begin{aligned} T_K(x \pm \frac{2k+1}{4k+2}i) &= 2T_{4k-1}(x) \\ T_K(x \pm \frac{2(k-j)+1}{4k+2}i) &= \begin{cases} 2(T_{2j-2}(x) + T_{4k-2j}^\vee(x)), & j : \text{ odd} \\ 2(T_{2j-2}^\vee(x) + T_{4k-2j}(x)), & j : \text{ even} \end{cases}, \quad j = 1, \dots, k \\ T_K(x \pm \frac{2(k+j)+1}{4k+2}i) &= \begin{cases} 2(T_{2j-1}(x) + T_{4k-2j-1}^\vee(x)), & j : \text{ odd} \\ 2(T_{2j-1}^\vee(x) + T_{4k-2j-1}(x)), & j : \text{ even} \end{cases}, \quad j = 1, \dots, k \end{aligned}$$

A_{4k+2} :

$$T_K(x \pm \frac{k+1}{2k+2}i) = 2T_{4k+1}^\vee(x) \quad (100)$$

$$T_K(x \pm \frac{k+1-j}{2k+2}i) = \begin{cases} 2(T_{2j-2}(x) + T_{4k-2j+2}(x)), & j : \text{odd} \\ 2(T_{2j-2}^\vee(x) + T_{4k-2j+2}^\vee(x)), & j : \text{even} \end{cases}, \quad j = 1, \dots, k+1 \quad (101)$$

$$T_K(x \pm \frac{k+1+j}{2k+2}i) = \begin{cases} 2(T_{2j-1}(x) + T_{4k-2j+1}(x)), & j : \text{odd} \\ 2(T_{2j-1}^\vee(x) + T_{4k-2j+1}^\vee(x)), & j : \text{even} \end{cases}, \quad j = 1, \dots, k+1 \quad (102)$$

We also note another functional relation for $T_K(x \pm i)$ of the A_{4k+2} case, indicating the ϕ^3 property

$$T_K(x \pm i) = \begin{cases} 2(\phi^\vee(x)T_K(x) + 2T_{2k-1}^\vee(x)), & k : \text{odd} \\ 2(\phi^\vee(x)T_K(x) + 2T_{2k-1}(x)), & k : \text{even}. \end{cases} \quad (103)$$

There are also relations obtained from the above by using the duality and the periodicity, omitted for brevity.

Proof. The proof is done by comparing the explicit dressed vacuum forms in the both sides. In most cases, this procedure, although simple enough in disguise, is not straightforward. For example, for the dilute A_{10} model, the product of two T_K with identical spectral parameters, decomposes as

$$T_K^2(x) = 3T_4(x) + T_{15}(x).$$

By the duality, $T_{15}(x) = T_4(x)$, one concludes (101), with $k = 2$ and $j = 3$. Similarly, consider

$$T_K^2(x \pm \frac{i}{6}) = 2T_2(x + \frac{11}{6}i) + T_6(x + \frac{11}{6}i) + T_{13}(x + \frac{11}{6}i).$$

The rhs is identical to $2(T_2(x + \frac{11}{6}i) + T_6(x + \frac{11}{6}i))$ due to the duality, which proves (101), with $k = 2$ and $j = 2$. The rests are also shown by using this kind of trick. \square

Corollary 2. For A_{4k+2} models, the kink transfer matrix is represented as

$$T_K(x) = \begin{cases} \frac{1}{\phi^\vee(x)}(T_{2k+1}^\vee(x) - T_{2k-1}^\vee(x)), & k : \text{odd} \\ \frac{1}{\phi^\vee(x)}(T_{2k+1}(x) - T_{2k-1}(x)), & k : \text{even}. \end{cases} \quad (104)$$

This is shown by comparing (102) with $j = k+1$ and (103).

For the dilute A_L models with odd L , we can also construct $T_K(x)$ following the above manner. The resulting pole-free object consists of $2L+2$ terms. It, however, proves to be identically zero under some assumption on analyticity. At the present, we do not know what is the implication of this.

D Proofs of Lemma 5 and 6

Proof. : Lemma 5

We use one of the magnon-like t system

$$t_1^{(k)}(x \pm i \frac{1}{2k+2}) = t_2^{(k)}(x) + t_1^{(k-1)}$$

which has been shown in the main text. Instead of using the solution for $t_2^{(k)}(x)$ in (94), we solve the above for $t_2^{(k)}(x)$ and take its square,

$$\begin{aligned} (t_2^{(k)}(x))^2 &= (t_1^{(k)}(x \pm i \frac{1}{2k+2}))^2 - 2t_1^{(k)}(x \pm i \frac{1}{2k+2})t_1^{(k-1)}(x) + (t_1^{(k-1)}(x))^2 \\ &= \frac{1}{4}(T_K(x + i \frac{1}{2k+2}))^2(T_K(x - i \frac{1}{2k+2}))^2 - \frac{1}{2}T_K(x \pm i \frac{1}{2k+2})t_1^{(k-1)}(x) \\ &\quad + (t_1^{(k-1)}(x))^2 \end{aligned}$$

where the solutions for $t_1^{(k)}$ is substituted. By further substituting the solutions for $t_1^{(k-1)}$ and making use of the functional relations for T_K (the cases $j = k$ and $j = k + 1$ in eq.(101)), one arrives

$$(t_2^{(k)}(x))^2 = \begin{cases} T_{2k}(x \pm \frac{1}{2k+2}i) - T_{2(k+1)}^\vee(x)T_{2(k-1)}^\vee(x), & k : \text{even} \\ T_{2k}^\vee(x \pm \frac{1}{2k+2}i) - T_{2(k+1)}(x)T_{2(k-1)}(x), & k : \text{odd}. \end{cases}$$

By noting the mod P relation (47) with $j = 1$ and using the sl_3 type relation (30), one concludes $(t_2^{(k)}(x))^2 = T_{D_{2k}}^\vee(x)$ for k even and $(t_2^{(k)}(x))^2 = T_{D_{2k}}(x)$ for k odd, which proves lemma 5. \square

Proof. : Lemma 6

Thanks to the ϕ^3 property (104), $t_1^{(k)}(x)$ has an expression,

$$t_1^{(k)}(x) = \frac{T_K(x)}{2} = \begin{cases} \frac{1}{2\phi^\vee(x)}(T_{2k+1}(x) - T_{2k-1}(x)), & k : \text{even} \\ \frac{1}{2\phi^\vee(x)}(T_{2k+1}^\vee(x) - T_{2k-1}^\vee(x)), & k : \text{odd}. \end{cases}$$

We solve (22) for $t_3^{(k)}(x) = T_{B_3}(x)$ and substitute the result into the product ,

$$t_1^{(k)}(x)t_3^{(k)}(x) = \begin{cases} \frac{1}{2(\phi^\vee(x))^2}(T_1(x \pm \frac{k}{2k+2}i)T_{2k+1}(x) - T_1(x \pm \frac{k}{2k+2}i)T_{2k-1}(x) \\ \quad - T_0(x \pm i \frac{k+2}{2k+2}i)T_{2k+1}(x) + T_0(x \pm i \frac{k+2}{2k+2}i)T_{2k-1}(x)) & k : \text{even} \\ \frac{1}{2(\phi^\vee(x))^2}(T_1(x \pm \frac{k}{2k+2}i)T_{2k+1}^\vee(x) - T_1(x \pm \frac{k}{2k+2}i)T_{2k-1}^\vee(x) \\ \quad - T_0(x \pm i \frac{k+2}{2k+2}i)T_{2k+1}^\vee(x) + T_0(x \pm i \frac{k+2}{2k+2}i)T_{2k-1}^\vee(x)) & k : \text{odd}. \end{cases} \quad (105)$$

We will show that the above expression coincide with the rhs of (48). For simplicity, only the case k even is considered below. Consider the second term in the rhs of (105) first. Noting the expression $T_1(x \pm \frac{k}{2k+2}i) = T_1(x \pm 2ki)$ due to (47) with $m = k$, we have

$$\begin{aligned} T_1(x \pm \frac{k}{2k+2}i)T_{2k-1}(x) &= T_0(x \pm \frac{k+2}{2k+2}i)T_{2k+1}(x) + \Lambda_{(2k-1,2k-1,1)/(2k-2)}(x) \\ &\quad + \frac{f_{2k}(x-i)}{f_{2k-1}(x)}\Lambda_{(2k,2k)/(2k-1)}(x) + \frac{f_{2k}(x+i)}{f_{2k-1}(x)}\Lambda_{(2k,1)}(x). \end{aligned} \quad (106)$$

The graphical representation in fig. 14 will be intuitively helpful. The second term in the

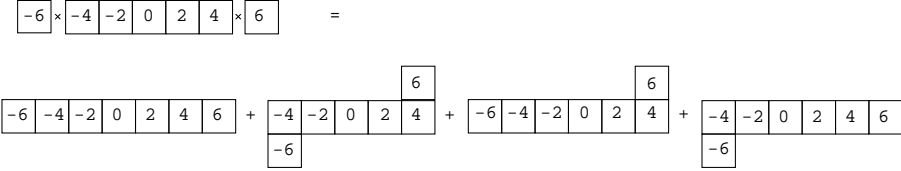


Figure 14: The graphical representation of eq.(106) for $k = 3$. A figure a in a box specifies its spectral parameter $x + ia$.

rhs of (106) is identical to $(\phi^\vee(x))^2 T_{D_{2k-2}}(x)$ due to Lemma 3 with $m = 2k - 1$. The third and the fourth term in the rhs of (106) can be further decomposed with the aid of the quantum Jacobi-Trudi formula and mod P relations in Lemma 4

$$\begin{aligned} &T_0(x - (2k-1)i)T_{2k}(x-i)T_1(x+2ki) - T_0(x \pm (2k-1)i)T_{2k+1}(x) \\ &= T_0(x + \frac{k+2}{2k+2}i)T_{2k}(x-i)T_1(x - (2k+3)i) - T_0(x \pm \frac{k+2}{2k+2}i)T_{2k+1}(x) \end{aligned}$$

for the third, and

$$\begin{aligned} &T_0(x + (2k+1)i)T_{2k}(x+i)T_1(x-2ki) - T_0(x \pm (2k-1)i)T_{2k+1}(x) \\ &= T_0(x - \frac{k+2}{2k+2}i)T_{2k}(x+i)T_1(x + (2k+3)i) - T_0(x \pm \frac{k+2}{2k+2}i)T_{2k+1}(x) \end{aligned}$$

for the fourth in (106). Next we consider the first term in the rhs of (105). To obtain a non trivial decomposition, we remark the following expression for $T_{2k+1}(x)$ due to the $a_2^{(2)}$ property,

$$T_{2k+1}(x) = \frac{1}{\phi(x \pm \frac{4k+5}{2}i)}\Lambda_{(2k+1,2k+1)}(x).$$

We also use the expression $T_1(x \pm \frac{k}{2k+2}i) = T_1(x \pm (2k+3)i)$ due to (46). By these tricks, three rectangles now set in the right position so that non trivial decomposition occurs.

$$\begin{aligned} T_1(x \pm \frac{k}{2k+2}i)T_{2k+1}(x) &= \phi(x \pm \frac{4k+3}{2}i)T_{D_{2k+2}}(x) + T_0(x \pm \frac{k+2}{2k+2}i)T_{2k-1}(x) \\ &\quad + n_c \Lambda_{(2k+1,2k)}^{\text{non}}(x+2i) + n_c^* \Lambda_{(2k+1,2k+1)/(1)}^{\text{non}}(x-2i). \end{aligned} \quad (107)$$

The scalar function of the first term in the rhs can be also written as $\phi(x \pm \frac{4k+3}{2}i) = (\phi^\vee(x))^2$.

The graphical representation in fig . 15 will be again helpful. The normalization factor

$$\begin{array}{c}
 \boxed{-7} \times \boxed{\begin{array}{|c|c|c|c|c|} \hline -3 & -1 & 1 & 3 & 5 \\ \hline -5 & -3 & -1 & 1 & 3 \\ \hline \end{array}} \times \boxed{7} = \\
 \\
 \boxed{-7} \times \boxed{\begin{array}{|c|c|c|c|c|c|} \hline -3 & -1 & 1 & 3 & 5 & 7 \\ \hline -5 & -3 & -1 & 1 & 3 & \\ \hline \end{array}} + \boxed{\begin{array}{|c|} \hline -3 \\ \hline -5 \\ \hline -7 \\ \hline \end{array}} \times \boxed{\begin{array}{|c|c|c|} \hline -1 & 1 & 3 \\ \hline -3 & -1 & 1 \\ \hline \end{array}} \times \boxed{\begin{array}{|c|} \hline 7 \\ \hline 5 \\ \hline 3 \\ \hline \end{array}} + \boxed{\begin{array}{|c|} \hline -3 \\ \hline -5 \\ \hline -7 \\ \hline \end{array}} \times \boxed{\begin{array}{|c|c|c|c|c|} \hline -1 & 1 & 3 & 5 & 7 \\ \hline -3 & -1 & 1 & 3 & \\ \hline \end{array}} + \boxed{\begin{array}{|c|c|c|c|c|} \hline -3 & -1 & 1 & 3 & \\ \hline -5 & -3 & -1 & 1 & \\ \hline \end{array}} \times \boxed{\begin{array}{|c|} \hline 7 \\ \hline 5 \\ \hline 3 \\ \hline \end{array}}
 \end{array}$$

Figure 15: The graphical representation of eq.(107) for $k = 2$. A figure a in a box specifies its spectral parameter $x + ia$.

n_c in the third and the fourth term in (107) reads,

$$n_c = \frac{\phi_3(x - i(2k+1))}{f_{2k+1}(x) \prod_{j=1}^{2k+1} \phi_2(x - 2(k+1)i + 2ji)}.$$

The upper index "non" in the third and the fourth term indicates the lack of their normalization factors. See (11) for ϕ_2 . The third term in (107) is further transformed with aid of the relation,

$$\begin{aligned}
 \Lambda_{(2k+1,2k)}^{\text{non}}(x+2i) &= \Lambda_{(2k,2k)}^{\text{non}}(x+i)T_1(x+(2k+3)i) - \Lambda_{(2k-1,2k-1,2k-1)/(2k-2)}^{\text{non}}(x+3i) \\
 &= f_{2k}(x+i) \prod_{j=1}^{2k} \phi_2(x - 2ki + 2ji) T_1(x + (2k+3)i) T_{2k}(x+i) \\
 &\quad - f_{2k-1}(x) \phi_3(x + (2k+1)i) \prod_{j=1}^{2k-1} \phi_2(x - 2ki + 2ji) T_{2k-1}(x)
 \end{aligned}$$

where we have used tableaux rule in the second equality. After taking account of normalization factors and mod P relations in Lemma 4 , the third term in (107) is given by

$$T_0(x - \frac{k+2}{2k+2}i) T_{2k}(x+i) T_1(x+(2k+3)i) - T_0(x \pm \frac{k+2}{2k+2}i) T_{2k-1}(x).$$

Similarly the fourth term reads,

$$T_0(x + \frac{k+2}{2k+2}i) T_{2k}(x-i) T_1(x-(2k+3)i) - T_0(x \pm \frac{k+2}{2k+2}i) T_{2k-1}(x).$$

Therefore the first two terms in the rhs of (105) add up to

$$\begin{aligned}
 &T_1(x \pm \frac{k}{2k+2}i) T_{2k+1}(x) - T_1(x \pm \frac{k}{2k+2}i) T_{2k-1}(x) \\
 &= (\phi^\vee(x))^2 (T_{D_{2k+2}}(x) - T_{D_{2k-2}}(x)) + T_0(x \pm \frac{k+2}{2k+2}i) (T_{2k+1}(x) - T_{2k-1}(x))
 \end{aligned}$$

Obviously the last two terms in the above cancel the third and the fourth term in (105). Thus we arrive

$$t_1^{(k)}(x)t_3^{(k)}(x) = \frac{1}{2}(T_{D_{2k+2}}(x) - T_{D_{2k-2}}(x)).$$

The case for odd k is done in parallel. □

E Proof of the magnon-like t system for $L = 4k + 1$

We summarize the proofs for the magnon-like t system, $L = 4k + 1$. Most of relations in (38), of which lhs takes the form $t_2^{(a)}(x \pm \frac{1}{2L+4}i)$, are shown without difficulty, thus they are omitted except for $a = 3, 4$.

Note the useful mod P relations

$$-\frac{1}{4k+3} \equiv (4k+1) + \frac{P}{2} \quad (108)$$

$$\frac{1}{4k+3} \equiv (4k+3) \quad (109)$$

$$\frac{4}{2L+4} = \frac{2}{4k+3} \equiv 2 - \frac{P}{2} \quad (110)$$

which will be used frequently below.

E.1 the proof for $t_1^{(1)}(x \pm \frac{4}{2L+4}i) = t_1^{(2)}(x) + t_2^{(1)}(x)$

Thanks to (110), the lhs equals to $T_{2(k-1)}(x \pm 2i)$ or $T_{2(k-1)}^\vee(x \pm 2i)$, depending on k even or odd. Then the sl_3 relation (30) proves the assertion.

E.2 the proof for $t_1^{(2)}(x \pm \frac{4}{2L+4}i) = t_1^{(1)}(x)t_1^{(7)}(x) + t_2^{(2)}(x)$

The proof is similar. One only has to apply (31).

E.3 the proof for $t_1^{(3)}(x \pm \frac{1}{2L+4}i) = t_1^{(1)}(x)t_1^{(5)}(x) + t_2^{(3)}(x)$

We consider the case k odd. Using the realness of $t_1^{(3)}(x)$, the mod P relation (108) and the diagrammatic symmetry, we rewrite the lhs as

$$\Lambda_{(6k+2,2k)/(1)}(x + (4k+1)i)\Lambda_{(6k+2,6k+1)/(4k+2)}(x - (4k+1)i),$$

while, thank to the duality, the second term in the rhs is given by

$$t_2^{(3)}(x) = T_{D_{2k}}(x)T_{6k+1}(x \pm (4k+3)i).$$

Then the quantum Jacobi Trudi formula leads to

$$\begin{aligned}
t_1^{(3)}(x \pm \frac{1}{2L+4}i) - t_2^{(3)}(x) = \\
T_{2(k-1)}(x) \left(T_{2k+2}(x)T_{6k+1}(x \pm (4k+3)i) + T_{2k-2}(x)T_{6k+3}(x \pm (4k+1)i) \right. \\
- T_{2k}(x-2i)T_{6k+1}(x+(4k+3)i)T_{6k+3}(x-(4k+1)i) \\
\left. - T_{2k}(x+2i)T_{6k+1}(x-(4k+3)i)T_{6k+3}(x+(4k+1)i) \right) \\
= T_{2(k-1)}(x)\Lambda_{(10k+2,6k+2,6k+1)/(4k+1,4k)}(x).
\end{aligned}$$

One can check the rhs of the above equation equals to $t_1^{(1)}(x)t_1^{(5)}(x)$.

E.4 the proof for $t_2^{(3)}(x \pm \frac{1}{2L+4}i) = t_1^{(1)}(x \pm \frac{i}{2L+4})t_2^{(5)}(x) + t_1^{(3)}(x)t_3^{(3)}(x)$

Again we treat the case k odd. Since $t_2^{(5)}(x) = t_3^{(3)}(x)$, the equality to prove is,

$$t_2^{(3)}(x \pm \frac{1}{2L+4}i) = t_3^{(3)}(x) \left(t_1^{(3)}(x) + t_1^{(1)}(x \pm \frac{i}{2L+4}) \right). \quad (111)$$

Substitute (86) and use (90) for $t_3^{(3)}(x)$, the lhs is given by

$$\begin{aligned}
t_2^{(3)}(x \pm \frac{1}{2L+4}i) &= t_3^{(3)}(x) \left(T_{2k}(x+(4k+1)i)T_{2k}(x+2i) \right) \Big|_{x \rightarrow x - \frac{i}{2L+4}} \\
&= t_3^{(3)}(x) \left(T_{2k}(x+(4k+1)i)T_{6k+1}(x+(8k+6)i) \right) \Big|_{x \rightarrow x - \frac{i}{2L+4}}
\end{aligned}$$

where the duality is used in the second equality. By the (19), it is readily shown that the rhs of the bracket above coincide with

$$t_3^{(3)}(x) \left(\Lambda_{(6k+2,2k)/(1)}^\vee(x - \frac{i}{2L+4}) + T_{2k-2}(x \pm \frac{i}{2L+4}) \right).$$

It is immediate to check that the above equation coincides with the rhs of (111)

E.5 the proof for $t_1^{(6)}(x \pm \frac{1}{2L+4}i) = t_1^{(5)}(x) + t_2^{(6)}(x)$

The first term in the rhs, $t_1^{(5)}(x)$ is identified with $\Lambda_{(10k+2,6k+2,6k+1)/(4k+1,4k)}(x)$ for k odd or $\Lambda_{(10k+2,6k+2,6k+1)/(4k+1,4k)}^\vee(x)$ for k even. We instead consider $\mathcal{T}_{(10k+2,6k+2,6k+1)/(4k+1,4k)}(x)$. See (20) for their difference. Due to the tableaux rule, it clearly decomposes into three parts. The "height-three" part reduces to the shifted product of $\phi_3(x)$ in (12). The remaining two parts are identified with the diagram for $t_1^{(6)}$ and its 180° rotation, referring to (82). See fig. 16. By the reality property of $t_1^{(6)}(x)$ and the diagrammatic symmetry

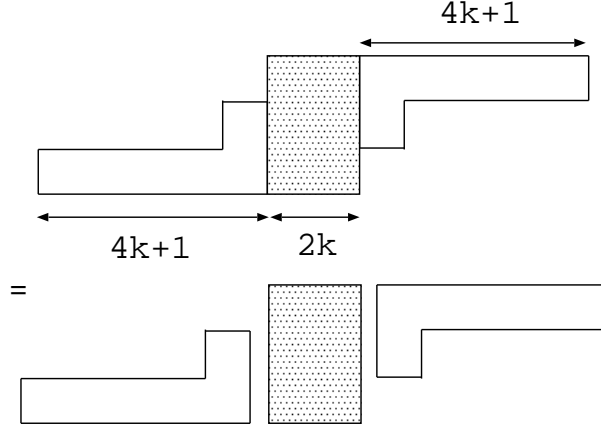


Figure 16: The decomposition of $\mathcal{T}_{(10k+2,6k+2,6k+1)/(4k+1,4k)}(x)$ into 3 parts. The hatched part reduces to a product of $\phi_3(x)$

(21), one finds

$$\mathcal{T}_{(10k+2,6k+2,6k+1)/(4k+1,4k)}(x) = \begin{cases} t_1^{(6)}(x \pm \frac{1}{2L+4}i) & k : \text{odd} \\ (t_1^{(6)})^\vee(x \pm \frac{1}{2L+4}i) & k : \text{even} \end{cases}$$

where the mod relation has been applied. On the other hand, the quantum Jacobi Trudi formula concludes

$$\begin{aligned} & \mathcal{T}_{(10k+2,6k+2,6k+1)/(4k+1,4k)}(x) - \Lambda_{(10k+2,6k+2,6k+1)/(4k+1,4k)}(x) \\ &= T_{10k+4}(x)T_{D_{2k}}(x) = T_{2k}^\vee(x)T_{D_{2k}}(x), \end{aligned}$$

which coincides with $t_2^{(6)}(x)((t_2^{(6)})^\vee(x))$ for k odd (even) in (89). Thus by comparing above due expressions, one concludes

$$t_1^{(6)}(x \pm \frac{1}{2L+4}i) = t_1^{(5)}(x) + t_2^{(6)}(x) \quad (112)$$

irrespective of k even or odd.

E.6 the proof for $t_1^{(4)}(x \pm \frac{1}{2L+4}i) = t_1^{(2)}(x)t_1^{(5)}(x) + t_2^{(4)}(x)$

We treat the case k even. First note the following representation of $t_1^{(4)}(x + \frac{1}{2L+4}i)$,

$$\begin{aligned} & t_1^{(4)}(x + \frac{1}{2L+4}i)\phi(x + (6k + \frac{9}{2})i) = \\ & \Lambda_{(4k-1,4k-1)/(4k-2)}(x + 2i)T_{2k}(x - (2k + 2)i) - \Lambda_{(4k+1,4k+1)/(4k)}(x)T_{2k-2}(x - 2ki). \end{aligned}$$

This relation is natural by its diagrammatic representation, and can be verified easily by (19). Again we use the reality property of $t_1^{(4)}(x)$ and the diagrammatic symmetry (21) to evaluate $t_1^{(4)}(x \pm \frac{1}{2L+4}i)\phi(x \pm (6k + \frac{9}{2})i)$.

After recombining the products of terms, it is found ,

$$\begin{aligned} t_1^{(4)}(x \pm \frac{1}{2L+4}i)\phi(x \pm (6k + \frac{9}{2})i) = \\ \{T_{2k-2}(x \pm 2i)\Lambda_{(6k+1,6k+1,4k+1,1)/(6k,2k)}(x) + (T_{2k}(x))^2\Lambda_{(6k+1,6k+1,4k-1,1)/(6k,2k+2)}(x) \\ - T_{2k}(x)T_{2k-2}(x-2i)\Lambda_{(6k+1,6k+1,4k-1,1)/(6k,2k)}(x) \\ - T_{2k}(x)T_{2k-2}(x+2i)\Lambda_{(6k+1,6k+1,4k+1,1)/(6k,2k+2)}(x)\} \\ + \{T_{2k-4}(x)T_{2k}(x) - T_{2k-2}(x \pm 2i)\}T_{2k}(x)\Lambda_{(6k+2,6k+2,1)/(6k+1)}(x). \end{aligned} \quad (113)$$

Thanks to (19), the content of the first curly bracket is equal to

$$\begin{aligned} T_{2k}(x)\mathcal{T}_{(6k,6k,4k,4k-1,1)/(6k-1,2k+1,2k)}(x) \\ + T_{D_{2k-2}}(x)\Lambda_{(L,1)}(x - (2k+2)i)\Lambda_{(L,L)/(L-1)}(x + (2k+2)i). \end{aligned} \quad (114)$$

The first term in the above is decomposed into three parts due to the tableaux rule as in the case of $t_1^{(6)}(x \pm \frac{1}{2L+4}i)$. An analogous argument leads to its expression,

$$\begin{aligned} \frac{1}{\phi(x \pm (2k - \frac{5}{2})i)}T_{2k}(x)\Lambda_{(2k+1,2k+1,1)/(2k)}(x \pm i(4k+1)) \\ = \phi(x \pm (6k + \frac{9}{2})i)T_{2k}(x)T_{D_{2k}}(x \pm (4k+1)i) = \phi(x \pm (6k + \frac{9}{2})i)t_2^{(4)}(x) \end{aligned}$$

where Lemma 3 and the mod P relation are used in the second equality.

The second term in (114) is identified with

$$\phi(x \pm i(6k + \frac{9}{2})i)T_{D_{2k-2}}(x)t_1^{(6)}(x \pm \frac{1}{2L+4}i)$$

by the reality property of $t_1^{(6)}(x)$ and (21) . Substituting the established relation, $t_1^{(6)}(x \pm \frac{1}{2L+4}i) = t_2^{(6)}(x) + t_1^{(5)}(x)$, we obtain the following expression for the first curly bracket term in (113) ,

$$\begin{aligned} \phi(x \pm i(6k + \frac{9}{2})i)\left(t_2^{(4)}(x) + T_{D_{2k-2}}(x)(t_1^{(5)}(x) + t_2^{(6)}(x))\right) \\ = \phi(x \pm i(6k + \frac{9}{2})i)(t_2^{(4)}(x) + t_1^{(2)}(x)t_1^{(5)}(x) + t_1^{(2)}(x)t_2^{(6)}(x)). \end{aligned}$$

The second curly bracket term in (113) is easily found to be

$$\begin{aligned} -T_{D_{2k-2}}(x)T_{2k}(x)\Lambda_{(6k+2,6k+2,1)/(6k+1)}(x) = -\phi(x \pm i(6k + \frac{9}{2})i)T_{D_{2k-2}}(x)T_{2k}(x)T_{D_{2k}}^\vee(x) \\ = -\phi(x \pm i(6k + \frac{9}{2})i)t_1^{(2)}(x)t_2^{(6)}(x). \end{aligned}$$

Lemma 3 is applied first, then the definitions in (78) and (89) is utilized. Combining these results, we obtain $t_1^{(4)}(x \pm \frac{1}{2L+4}i) = t_1^{(2)}(x)t_1^{(5)}(x) + t_2^{(4)}(x)$.

E.7 the proof for $t_2^{(4)}(x \pm \frac{1}{2L+4}i) = t_1^{(2)}(x \pm \frac{1}{2L+4}i)t_2^{(5)}(x) + t_1^{(4)}(x)t_3^{(4)}(x)$

Here we set $k = \text{odd}$. Since $t_3^{(4)}(x) = T_{B_3}(x)t_2^{(5)}(x)$, the assertion is equivalent to

$$t_2^{(4)}(x \pm \frac{1}{2L+4}i) = t_2^{(5)}(x)(t_1^{(2)}(x \pm \frac{1}{2L+4}i) + t_1^{(4)}(x)T_{B_3}(x)).$$

To prove this, we prepare a few facts.

Lemma 8.

$$\begin{aligned} \frac{1}{\phi(x - (m + \frac{3}{2})i)} \Lambda_{(m,m-1)}(x) &= \frac{1}{\phi(x + (m + \frac{5}{2})i)} \Lambda_{(m,m)/(m-1)}(x + i) \\ \frac{1}{\phi(x - (m + \frac{3}{2})i)} \Lambda_{(m,1)}(x) &= \frac{1}{\phi(x + (m + \frac{5}{2})i)} \Lambda_{(m,m)/(1)}(x + i) \end{aligned}$$

Both of them are easily proved by the $a_2^{(2)}$ property.

Lemma 9.

$$\begin{aligned} &T_{D_{6k+1}}(x)T_{D_{2k}}(x + (4k + 5)i) - T_{D_{6k+3}}(x + 2i)T_{D_{2k-2}}(x + (4k + 3)i) \\ &= \frac{\Lambda_{(2,1)}(x + (6k + 4)i)}{\phi(x + (2k + \frac{11}{2})i)\phi(x + (6k + \frac{1}{2})i)} \times D \end{aligned} \tag{115}$$

where

$$\begin{aligned} D := & \left(T_{6k+1}(x + 2i)\Lambda_{(4k+3,4k+3)/(4k+2)}(x - (2k - 1)i) \right. \\ & \left. - T_{6k+3}(x + 2i)\Lambda_{(4k+1,4k+1)/(4k)}(x - (2k - 3)i) \right). \end{aligned}$$

It is easily checked that the lhs is equal to

$$T_{6k+1}(x + 2i)\mathcal{T}_{(6k+3,6k+2,6k+1)/(4k+3,4k+2)}(x + 2i) - T_{6k+3}(x)\mathcal{T}_{(6k+1,6k,6k-1)/(4k+1,4k)}(x + 4i).$$

The diagram decomposition of this then leads to rhs of (115).

Lemma 10.

$$D = \frac{\phi(x + (2k + \frac{11}{2})i)}{\phi(x - (6k + \frac{1}{2})i)} \Lambda_{(10k,6k+2,6k+1)/(2k,2k)}(x)$$

We use the two decompositions of $\mathcal{T}_{(10k,6k+2,6k+1)/(2k,2k)}(x)$. The comparison of these two leads to

$$\begin{aligned} \Lambda_{(10k,6k+2,6k+1)/(2k,2k)}(x) &= \frac{\phi(x - (6k + \frac{1}{2})i)}{\phi(x + (2k + \frac{3}{2})i)} T_{2k}(x - (8k + 2)i) \Lambda_{(4k-1,1)}(x + (6k + 2)i) \\ &\quad - T_{6k+3} \Lambda_{(4k+1,4k)}(x + (-2k + 2)i). \end{aligned}$$

By the duality, the quantum Jacobi-Trudi formula and Lemma 8, we find

$$\begin{aligned}\Lambda_{(4k-1,1)}(x + (6k+2)i) &= \frac{\phi(x + (2k + \frac{3}{2})i)}{\phi(x + (2k + \frac{11}{2})i)} \Lambda_{(4k+3,4k+3)/(4k+2)}(x - (2k-1)i) \\ \Lambda_{(4k+1,4k)}(x + (-2k+2)i) &= \frac{\phi(x - (6k + \frac{1}{2})i)}{\phi(x + (2k + \frac{11}{2})i)} \Lambda_{(4k+1,4k+1)/(4k+2)}(x - (2k-3)i).\end{aligned}$$

Finally by noticing $T_{2k}(x - (8k+2)i) = T_{6k+1}(x + 2i)$, we prove Lemma 10

The final lemma asserts a relation ,

Lemma 11.

$$\Lambda_{(10k,6k+2,6k+1)/(2k,2k)}(x - (6k+5)i) = \Lambda_{(4k,4k,2k)/(4k-1,1)}(x) = \phi(x + (4k + \frac{5}{2})i) (t_1^{(4)})^\vee(x - \frac{i}{2}).$$

The first equality is due to duality and the second comes from the definition.

Now we prove the relation. We conveniently consider,

$$(t_2^{(4)}(x \pm \frac{i}{2L+4}) - t_1^{(2)}(x \pm \frac{i}{2L+4}) t_2^{(5)}(x))|_{x \rightarrow x + \frac{3i}{2L+4}}$$

and show that it is equal to $t_1^{(4)}(x + \frac{3i}{2L+4}) t_3^{(4)}(x + \frac{3i}{2L+4})$. First we rewrite the difference as

$$t_2^{(5)}(x + \frac{3i}{2L+4}) \left(T_{D_{6k+1}}(x) T_{D_{2k}}(x + (4k+5)i) - T_{D_{6k+3}}(x + 2i) T_{D_{2k-2}}(x + (4k+3)i) \right). \quad (116)$$

then apply Lemma 9. With the expression of $T_{B_3}(x)$ in (24), and the relation $t_3^{(4)}(x) = t_2^{(5)}(x) T_{B_3}(x)$, one concludes that (116) coincides with

$$\frac{t_3^{(4)}(x + \frac{3i}{2L+4})}{\phi(x + (2k + \frac{11}{2})i)} D.$$

Therefore, the relation is equivalent to

$$\frac{D}{\phi(x + (2k + \frac{11}{2})i)} = t_1^{(4)}(x + \frac{3i}{2L+4}). \quad (117)$$

We will show this by rewriting the lhs of (117) , thanks to Lemma 10,

$$\frac{1}{\phi(x - (6k + \frac{1}{2})i)} \Lambda_{(10k,6k+2,6k+1)/(2k,2k)}(x).$$

This can be further rewrite as, with aid of Lemma 11,

$$\frac{\phi(x + (10k + \frac{15}{2})i)}{\phi(x - (6k + \frac{1}{2})i)} (t_1^{(4)})^\vee(x + (6k + 5)i - i\frac{1}{2})$$

which is readily shown to be equal to the rhs of (117) for k odd. The case k even can be treated similarly.

E.8 the proof for $t_1^{(5)}(x \pm \frac{1}{2L+4}i) = t_1^{(3)}t_1^{(4)}t_1^{(6)} + t_2^{(5)}(x)$

We assume k even. The proof for the case k odd is similar. One substitutes $t_1^{(5)}(x) = t_1^{(6)}(x \pm \frac{1}{2L+4}i) - t_2^{(6)}(x)$ and uses the relation $t_2^{(5)}(x) = t_2^{(6)}(x \pm \frac{1}{2L+4})$.

Then the assertion is transformed into an equivalent form,

$$\begin{aligned} t_1^{(3)}(x)t_1^{(4)}(x) &= t_1^{(6)}(x)t_1^{(6)}(x \pm \frac{2}{2L+4}i) \\ &\quad - t_2^{(6)}(x + \frac{1}{2L+4}i)t_1^{(6)}(x - \frac{2}{2L+4}i) - t_2^{(6)}(x - \frac{1}{2L+4}i)t_1^{(6)}(x + \frac{2}{2L+4}i). \end{aligned}$$

We conveniently make a shift in x ,

$$\begin{aligned} t_1^{(3)}(x + \frac{1}{2L+4}i)t_1^{(4)}(x + \frac{1}{2L+4}i) &= t_1^{(6)}(x + \frac{3}{2L+4}i)t_1^{(6)}(x \pm \frac{1}{2L+4}i) \\ &\quad - t_2^{(6)}(x)t_1^{(6)}(x + \frac{3}{2L+4}i) - t_2^{(6)}(x + \frac{2}{2L+4}i)t_1^{(6)}(x - \frac{1}{2L+4}i). \end{aligned} \quad (118)$$

We begin with the following lemma,

Lemma 12.

$$\begin{aligned} t_1^{(3)}(x + \frac{1}{2L+4}i)t_1^{(4)}(x + \frac{1}{2L+4}i) &= t_1^{(6)}(x + \frac{3}{2L+4}i)t_1^{(6)}(x \pm \frac{1}{2L+4}i) \\ &\quad - t_2^{(6)}(x + \frac{2}{2L+4}i)t_1^{(6)}(x - \frac{1}{2L+4}i) - R \end{aligned} \quad (119)$$

where

$$\begin{aligned} R &= \frac{T_{2k}(x)}{\phi(x + (6k + \frac{9}{2})i)} \left(\Lambda_{(6k+2,2k+2)/(1)}(x)t_1^{(6)}(x - \frac{1}{2L+4}i)\phi(x + (6k + \frac{9}{2})i) \right. \\ &\quad \left. - \Lambda_{(4k-1,4k-1)/(4k-2)}(x + (2k+4)i)t_1^{(3)}(x + \frac{1}{2L+4}i) \right). \end{aligned} \quad (120)$$

Proof. Lemma 12

We first note a decomposition of $t_1^{(4)}(x)$,

$$\begin{aligned} t_1^{(4)}(x + \frac{1}{2L+4}i) &= \frac{1}{\phi(x + (6k + \frac{9}{2})i)} T_{2k}(x) \Lambda_{(4k-1,4k-1)/(4k-2)}(x + (2k+4)i) \\ &\quad - T_{2k-2}(x + 2i)t_1^{(6)}(x - \frac{1}{2L+4}i) \end{aligned}$$

where we have used the diagrammatic symmetry,

$$\begin{aligned} t_1^{(6)}(x - \frac{1}{2L+4}i) &= (t_1^{(6)}(x + \frac{1}{2L+4}i))^* \\ &= \frac{1}{\phi(x + (6k + \frac{9}{2})i)} \Lambda_{(4k+1,4k+1)/(4k)}(x + (2k+2)i). \end{aligned}$$

Then the product in the lhs of (119) is rewritten as,

$$\begin{aligned}
& t_1^{(3)}(x + \frac{1}{2L+4}i)t_1^{(4)}(x + \frac{1}{2L+4}i) \\
&= \frac{1}{\phi(x + (6k + \frac{9}{2})i)} T_{2k}(x) \Lambda_{(4k-1, 4k-1)/(4k-2)}(x + (2k+4)i) t_1^{(3)}(x + \frac{1}{2L+4}i) \\
&\quad - T_{6k+3}(x - (8k+2)i) t_1^{(3)}(x + \frac{1}{2L+4}i) t_1^{(6)}(x - \frac{1}{2L+4}i) \tag{121}
\end{aligned}$$

where the duality relation $T_{2k-2}(x + 2i) = T_{6k+3}(x - (8k+2)i)$ is applied. Note that $t_1^{(3)}(x + \frac{1}{2L+4}i) \equiv \Lambda_{(6k+2, 2k)/(1)}(x)$. Then we apply the decomposition rule to the second term in (121),

$$\begin{aligned}
& -T_{6k+3}(x - (8k+2)i) t_1^{(3)}(x + \frac{1}{2L+4}i) \\
&= t_1^{(5)}(x + \frac{P}{2}i - (4k+1)i) - T_{6k+1}(x - (8k+4)i) \Lambda_{(6k+2, 2k+2)/(1)}(x) \\
&= t_1^{(5)}(x + \frac{2i}{2L+4}i) - T_{2k}(x) \Lambda_{(6k+2, 2k+2)/(1)}(x) \\
&= t_1^{(6)}(x + \frac{3i}{2L+4}) t_1^{(6)}(x + \frac{i}{2L+4}) - t_2^{(6)}(x + \frac{2i}{2L+4}) \\
&\quad - T_{2k}(x) \Lambda_{(6k+2, 2k+2)/(1)}(x).
\end{aligned}$$

The first equality follows from the quantum Jacobi-Trudi formula. Then the duality and the established relation in E.5 lead to the last line. By substituting this into (121), one verifies Lemma 12. \square

From Lemma 12 and (118), one only has to show

$$R = t_1^{(6)}(x + i \frac{3}{2L+4}) t_2^{(6)}(x). \tag{122}$$

Our argument consists of two further steps. First we will show a lemma

Lemma 13.

$$\begin{aligned}
R &= \frac{T_{2k}(x)}{\phi(x - (2k + \frac{3}{2})i) \phi(x - (6k + \frac{1}{2})i) \phi(x + (6k + \frac{9}{2})i)} \\
&\quad \times \Lambda_{(L, 1)}(x + (2k+1)i) \left(T_1(x - (10k+5)i) \Lambda_{(2k, 2k)/(2k-1)}(x - (8k+2)i) \right. \\
&\quad \left. - T_0(x - (10k+6)i) \Lambda_{(2k-1, 2k-1)/(2k-2)}(x - (8k+1)i) \right). \tag{123}
\end{aligned}$$

Then the rhs of the above will be shown to be equal to that of (122).

Proof. Lemma 13

The definition of R in (120) is not convenient in applying decomposition rules. We utilize the duality and rewrite

$$\begin{aligned} t_1^{(6)}\left(x - \frac{1}{2L+4}i\right)\phi\left(x + \left(6k + \frac{9}{2}\right)i\right) &= \Lambda_{(8k,4k)}(x - (2k+2)i) \\ \Lambda_{(4k-1,4k-1)/(4k-2)}(x + (2k+4)i) &= \Lambda_{(8k,4k+2)}(x - (2k+2)i). \end{aligned}$$

Then they are located at right positions to apply the quantum Jacobi Trudi formula. The resultant expression reads

$$\begin{aligned} R &= \frac{T_{2k}(x)}{\phi\left(x + \left(6k + \frac{9}{2}\right)i\right)} \\ &\quad \times \left(T_{8k}(x - (2k+1)i)\mathcal{T}_{(8k+1,4k+1,4k)/(2k,2k-1)}(x - 2ki) \right. \\ &\quad \left. - T_{8k+1}(x - (2k+2)i)\mathcal{T}_{(8k,4k,4k-1)/(2k-1,2k-2)}(x + (-2k+1)i) \right) \\ &= \frac{T_{2k}(x)}{\phi\left(x + \left(6k + \frac{9}{2}\right)i\right)} \\ &\quad \times \left(T_1(x - (10k+5)i)\mathcal{T}_{(8k+1,4k+1,4k)/(2k,2k-1)}(x - 2ki) \right. \\ &\quad \left. - T_0(x - (10k+6)i)\mathcal{T}_{(8k,4k,4k-1)/(2k-1,2k-2)}(x + (-2k+1)i) \right) \end{aligned}$$

where the duality is applied in the last equality.

The "height 3" diagrams are decomposed into smaller pieces due to the tableaux rule, see fig. 17.

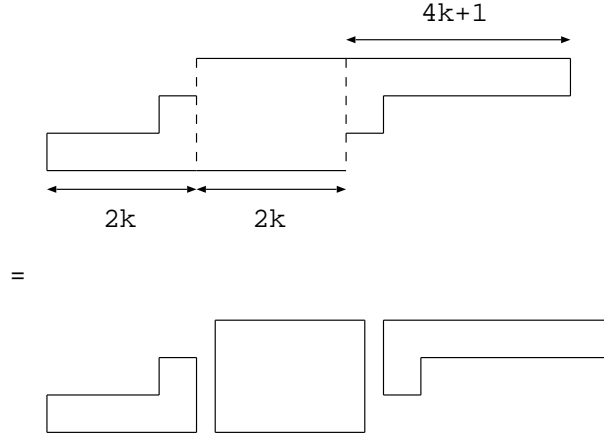


Figure 17: The decomposition of the "height 3" diagram corresponding to $\mathcal{T}_{(8k+1,4k,4k-1)/(2k,2k-1)}$

Accordingly, R is represented by

$$\begin{aligned} R &= \frac{T_{2k}(x)\Lambda_{(4k+1,1)}(x+(2k+1)i)}{\phi(x+(6k+\frac{9}{2})i)\phi(x-(2k+\frac{3}{2})i)\phi(x-(6k+\frac{1}{2})i)} \\ &\quad \times \left(T_1(x-(10k+5)i)\Lambda_{(2k,2k)/(2k-1)}(x-(8k+2)i) \right. \\ &\quad \left. - T_0(x-(10k+6)i)\Lambda_{(2k-1,2k-1)/(2k-2)}(x-(8k+1)i) \right). \end{aligned}$$

Thus the lemma is established. \square

The final step starts from rewriting the first term in the bracket of (123) in Lemma 13 as,

$$\begin{aligned} &\frac{\Lambda_{(1,1)}(x-(10k+5)i)}{\phi_2(x-(10k+5)i)}\Lambda_{(2k,2k)/(2k-1)}(x-(8k+2)i) \\ &= \frac{\phi(x-(10k+\frac{7}{2})i)}{\phi(x-(10k+\frac{15}{2})i)}\Lambda_{(2k+1,2k+1,1)/(2k)}(x-(8k+4)i) \\ &\quad + T_0(x-(10k+6)i)\Lambda_{(2k-1,2k-1)/(2k-2)}(x-(8k+1)i). \end{aligned}$$

The second term in the rhs coincides with that in the bracket of (123). Thus

$$\begin{aligned} R &= \frac{T_{2k}(x)t_1^{(6)}(x+\frac{3i}{2L+4})}{\phi(x-(6k+\frac{1}{2})i)\phi(x-(10k+\frac{15}{2})i)} \\ &\quad \times \Lambda_{(2k+1,2k+1,1)/(2k)}(x-(8k+4)i) \end{aligned}$$

where $\phi(x-(10k+\frac{7}{2})i) = \phi(x+(6k+\frac{9}{2})i)$ and the definition of $t_1^{(6)}$ is used. Finally we apply Lemma 3 to the above and reach the expression (122). Thereby we prove the functional relation.

F A result for an exceptional case

We sketch the result for exceptional cases, $L = 3 \sim 6$.

For $L = 3, 4, 6$, the Y system is neatly described by

$$Y_j(x \pm \frac{L-2}{2L+4}) = \prod_{j \sim \ell} \Xi_\ell(x) \quad (j = 1, \dots, r)$$

where the corresponding Dynkin diagrams are those for E_r , and $r = 8, 7, 6$, respectively.

The solutions of Y in terms of transfer matrices have been reported in [22] for $L = 3$ and [23] for $L = 4, 6$.

The case $L = 5$, corresponding to $M_{5,6} + \phi_{1,2}$ takes a little bit complicated as announced in [73]. Below, we shall summarize the result then supplement outline of the proof as promised there.

In this case, there are more breathers in the system than the cases we discussed above. We, therefore need to introduce more sl_2 origin objects.

$$T_{B_1}(x) := T_1(x) \quad (124)$$

$$T_{B_3}(x) := \Lambda_{(8,1)}(x + \frac{13}{14}i)/\phi(x - \frac{12}{7}i) \quad (125)$$

$$T_{B_5}(x) := \Lambda_{(15,8,8)/(7,7)}(x)/\phi(x \pm \frac{3}{2}i) \quad (126)$$

$$T_{B_7}(x) := \Lambda_{(15,15,8,8)/(14,7,7)}(x + \frac{11}{14}i)/(\phi(x - \frac{12}{7}i)\phi(x \pm \frac{9}{7}i)) \quad (127)$$

$$T_{B_2}(x) := T_7(x) \quad (128)$$

$$T^{(6)}(x) := \Lambda_{(8,7)/(6)}(x + \frac{25}{14}i) \quad (129)$$

then the following relations hold.

$$\begin{aligned} T_{B_1}(x \pm \frac{3}{14}i) &= T_0(x \pm \frac{11}{14}i) + \phi(x - \frac{12}{7}i)T_{B_3}(x) \\ T_{B_3}(x \pm \frac{3}{14}i) &= T_0(x)T_0(x \pm \frac{8}{14}i) + T_{B_1}(x)T_{B_5}(x) \\ T_{B_5}(x \pm \frac{3}{14}i) &= T_0(x \pm \frac{3}{14}i)T_0(x \pm \frac{5}{14}i) + T_{B_3}(x)T_{B_7}(x) \\ T_{B_2}(x \pm \frac{3}{14}i) &= T_0(x \pm \frac{1}{14}i) + T^{(6)}(x) \end{aligned}$$

For a magnon-like $t-$ system we assume,

$$t_1^{(1)}(x + \frac{i}{14})t_1^{(1)}(x - \frac{i}{14}) = t_2^{(1)}(x) + t_1^{(3)}(x)g_1^{(1)}(x) \quad (130)$$

$$t_2^{(1)}(x + \frac{i}{14})t_2^{(1)}(x - \frac{i}{14}) = t_1^{(1)}(x)t_3^{(1)}(x) + t_2^{(3)}(x)g_2^{(1)}(x) \quad (131)$$

$$t_3^{(1)}(x + \frac{i}{14})t_3^{(1)}(x - \frac{i}{14}) = t_2^{(1)}(x)t_4^{(1)}(x) \quad (132)$$

$$t_1^{(2)}(x + \frac{i}{14})t_1^{(2)}(x - \frac{i}{14}) = t_2^{(2)}(x) + t_1^{(3)}(x)g_1^{(2)}(x) \quad (133)$$

$$t_2^{(2)}(x + \frac{i}{14})t_2^{(2)}(x - \frac{i}{14}) = t_1^{(2)}(x)t_3^{(2)}(x) + t_2^{(3)}(x)g_2^{(2)}(x) \quad (134)$$

$$t_3^{(2)}(x + \frac{i}{14})t_3^{(2)}(x - \frac{i}{14}) = t_2^{(2)}(x)t_4^{(2)}(x) \quad (135)$$

$$t_1^{(3)}(x + \frac{i}{14})t_1^{(3)}(x - \frac{i}{14}) = t_2^{(3)}(x) + t_1^{(1)}(x)t_1^{(2)}(x)t_1^{(4)}(x) \quad (136)$$

$$t_2^{(3)}(x + \frac{i}{14})t_2^{(3)}(x - \frac{i}{14}) = t_2^{(1)}(x)t_2^{(2)}(x)t_2^{(4)}(x) \quad (137)$$

$$t_1^{(4)}(x + \frac{i}{14})t_1^{(4)}(x - \frac{i}{14}) = t_2^{(4)}(x) + t_1^{(3)}(x) \quad (138)$$

$$t_2^{(4)}(x + \frac{i}{14})t_2^{(4)}(x - \frac{i}{14}) = t_2^{(3)}(x) \quad (139)$$

$$g_1^{(a)}(x \pm \frac{i}{14}) = g_2^{(a)}(x), \quad a = 1, 2$$

Remark: They are obtained from the T-system for D_4 , by requiring $t_3^{(3)} = t_3^{(4)} = 0$.

The identification between Y and T is given by

$$\begin{aligned}
Y_{B_1} &= \phi(x - \frac{12}{7}i)T_{B_3}(x)/T_0(x \pm \frac{11}{14}i) \\
Y_{B_3} &= T_{B_1}(x)T_{B_5}(x)/(T_0(x)T_0(x \pm \frac{4}{7}i)) \\
Y_{B_5} &= T_{B_3}(x)T_{B_7}/(T_0(x \pm \frac{3}{14}i)T_0(x \pm \frac{5}{14}i)) \\
Y_{B_2} &= T^{(6)}(x)/T_0(x \pm \frac{1}{14}i) \\
Y_{K_1}(x) &= \frac{t_2^{(1)}(x)}{t_1^{(3)}(x)g_1^{(1)}(x)} \\
Y_{K_2}(x) &= \frac{t_2^{(2)}(x)}{t_1^{(3)}(x)g_1^{(2)}(x)} \\
Y^{(1)}(x) &= \frac{t_2^{(3)}(x)}{t_1^{(1)}(x)t_1^{(2)}(x)t_1^{(4)}(x)} \\
Y^{(2)}(x) &= \frac{t_2^{(4)}(x)}{t_1^{(3)}(x)}.
\end{aligned}$$

And the explicit solution is asserted as follows. The following choice of $t_{1,2}^{(a)}(x)$ solves the kink T-system

$$t_1^{(1)}(x) = T^{(6)}(x) \quad (140)$$

$$t_1^{(2)}(x) = T_{B_7}(x) \quad (141)$$

$$t_1^{(3)}(x) = \Lambda_{(12,8,7)/(5,4)}(x) \quad (142)$$

$$t_1^{(4)}(x) = \Lambda_{(5,1)}(x + \frac{15}{14}i)/\phi(x - \frac{13}{2}i + \frac{15}{14}i) \quad (143)$$

$$t_2^{(1)}(x) = T_{B_5}(x)T_{B_2}(x \pm \frac{i}{7}) \quad (144)$$

$$t_2^{(2)}(x) = T_{B_5}(x \pm \frac{i}{7})T_{B_2}(x) \quad (145)$$

$$t_2^{(3)}(x) = T_{B_5}(x \pm \frac{i}{14})T_{B_2}(x \pm \frac{i}{14}) \quad (146)$$

$$t_2^{(4)}(x) = T_{B_5}(x)T_{B_2}(x) \quad (147)$$

with additional constraints,

$$\begin{aligned}
t_3^{(1)}(x) &= t_2^{(3)}(x), \\
T_{B_3} &= \frac{t_3^{(2)}(x)}{t_2^{(3)}(x)} \\
g_1^{(1)}(x) &= T_0(x), \quad g_1^{(2)}(x) = T_0(x \pm \frac{2i}{7}).
\end{aligned}$$

By these choice the above Y satisfy the $Y-$ system proposed in [25],

$$\begin{aligned}
Y_{B_1}(x \pm \frac{3}{14}i) &= \Xi_{B_3}(x) \\
Y_{B_3}(x \pm \frac{3}{14}i) &= \Xi_{B_1}(x)\Xi_{B_5}(x) \\
Y_{B_5}(x \pm \frac{3}{14}i) &= \Xi_{B_3}(x)\Xi_{K_2}(x \pm \frac{2}{14}i)\Xi_{K_1}(x)\Xi^{(1)}(x \pm \frac{1}{14}i)\Xi^{(2)}(x) \\
Y_{B_2}(x \pm \frac{3}{14}i) &= \Xi_{K_1}(x \pm 2)\Xi^{(1)}(x \pm \frac{1}{14}i)\Xi_{K_2}(x)\Xi^{(2)}(x) \\
Y_{K_2}(x \pm \frac{1}{14}i) &= \Xi_{B_5}(x)\mathcal{L}^{(1)}(x) \\
Y_{K_1}(x \pm \frac{1}{14}i) &= \Xi_{B_2}(x)\mathcal{L}^{(1)}(x) \\
Y^{(1)}(x \pm \frac{1}{14}i) &= \mathcal{L}^{(2)}(x)\mathcal{L}_{K_2}(x)\mathcal{L}_{K_1}(x) \\
Y^{(2)}(x \pm \frac{1}{14}i) &= \mathcal{L}^{(1)}(x).
\end{aligned}$$

We first remark a few lemmas concerning about equivalent expressions for transfer matrices

Lemma 14. $T_{B_5}(x)$ has the following two equivalent expressions in addition to (126).

$$T_{B_5}(x) = T_{D_2}(x) = \frac{1}{\phi(x \pm \frac{3}{2}i)} \Lambda_{(8,8,1)/(7)}(x + \frac{12}{7}i).$$

The first equality has already appeared in (25). The second is shown by the duality.

Lemma 15. $T_{B_7}(x)(= t_1^{(2)}(x))$ is also written as follows.

$$T_{B_7}(x) = \frac{1}{\phi(x + \frac{22}{14}i)} \Lambda_{(4,3,1)/(2)}(x - \frac{31}{14}i)$$

To prove this, we utilize $\mathcal{T}_{(15,15,8,8)/(14,7,7)}(x)$. The quantum Jacobi-Trudi formula and the duality relation conclude,

$$\begin{aligned}
\mathcal{T}_{(15,15,8,8)/(14,7,7)}(x) &= \Lambda_{(15,15,8,8)/(14,7,7)}(x) \\
&+ T_0(x)T_0(x - 2i)(T_1(x + 17i)T_4(x - i) - T_0(x + 16i)T_3(x)). \quad (148)
\end{aligned}$$

On the other hand, the same quantity is given by

$$\mathcal{T}_{(15,15,8,8)/(14,7,7)}(x) = \phi(x + \frac{i}{2})\phi(x + \frac{13i}{14})T_7(x - 11i)\Lambda_{(8,8)/(7)}(x + 10i) \quad (149)$$

thanks to the semi-standard condition. Again, by the quantum Jacobi-Trudi formula and the duality relation, $\Lambda_{(8,8)/(7)}(x+10i) = T_1(x-7i)T_2(x+\frac{3}{7}i) - T_0(x-\frac{8}{7}i)T_1(x-2i)$. Using this expression, as well as with some rearrangement, we find

$$\begin{aligned} T_7(x-11i)\Lambda_{(8,8)/(7)}(x+10i) &= T_1(x-7i)T_{D_2}(x-i) - T_0(x-\frac{8}{7}i)\Lambda_{(2,1)}(x) \\ &\quad + T_0(x-i)(T_4(x-i)T_1(x-7i) - T_0(x-\frac{8}{7}i)T_3(x)). \end{aligned}$$

Substitute this into (149), compare the resultant expression with (148) and we have,

$$\Lambda_{(15,15,8,8)/(14,7,7)}(x) = \phi(x+\frac{i}{2})\phi(x+\frac{13i}{14})(T_1(x-7i)T_{D_2}(x-i) - T_0(x-\frac{8}{7}i)\Lambda_{(2,1)}(x)).$$

By the representation of $T_1(x-7i)$ by 2×1 table, the diagrammatical rule immediately leads to

$$\Lambda_{(15,15,8,8)/(14,7,7)}(x) = \frac{d_{B_7}(x-\frac{11}{14}i)}{\phi(x+\frac{11}{14}i)}\Lambda_{(4,3,1)/(2)}(x-3i),$$

where $d_{B_7}(x)$ specifies the denominator in (127). This proves the lemma after a shift in x and the simplification in the coefficient.

Lemma 16. $t_1^{(3)}(x)$ can be also represented by

$$t_1^{(3)}(x) = \frac{1}{\phi(x \pm \frac{3}{2}i)}\Lambda_{(7,7,5,1)/(6,2)}(x + \frac{12}{7}i).$$

Just as in the proof of Lemma 15, two expressions for $\mathcal{T}_{(12,8,7)/(5,4)}(x)$ leads to

$$\begin{aligned} t_1^{(3)}(x) = \Lambda_{(12,8,7)/(5,4)}(x) &= \frac{1}{\phi(x \pm \frac{3}{2}i)}(\Lambda_{(5,1)}(x+8i)\Lambda_{(5,5)/(4)}(x+16i) \\ &\quad - \phi(x \pm \frac{3}{2}i)T_7(x)T_{D_2}(x)). \end{aligned} \tag{150}$$

The product $\Lambda_{(5,1)}(x+8i)\Lambda_{(5,5)/(4)}(x+16i)$ decomposes as follows.

$$\begin{aligned} (\Lambda_{(5,1)}(x+8i)\Lambda_{(5,5)/(4)}(x+16i)) &= (\Lambda_{(5,1)}(x-4i)\Lambda_{(5,5)/(4)}(x+4i))_{x \rightarrow x + \frac{12}{7}i} \\ &= \Lambda_{(7,7,5,1)/(6,2)}(x + \frac{12}{7}i) + T_2(x + \frac{12}{7}i)\Lambda_{(8,8,1)/(7)}(x + \frac{12}{7}i) \\ &= \Lambda_{(7,7,5,1)/(6,2)}(x + \frac{12}{7}i) + T_7(x)T_{B_5}(x)\phi(x \pm \frac{3}{2}i) \end{aligned} \tag{151}$$

where we have used Lemma 14 in the last equality. Using (151) in (150) and remembering $T_{B_5}(x) = T_{D_2}(x)$, one easily establishes the lemma.

Lemma 17. *The following equality can be easily verified,*

$$\Lambda_{(6,6,4,3,1)/(5,3,2)}(x) = \phi(x \pm \frac{3}{14}i) T_{B_5}(x \pm \frac{i}{7} + \frac{12}{7}i).$$

The diagrammatic decomposition yields,

$$\Lambda_{(6,6,4,3,1)/(5,3,2)}(x) = \frac{1}{f_2(x)} \Lambda_{(3,3,1)/(2)}(x \pm 5i).$$

The $m = 3$ case of Lemma 3 and $T_{B_5}(x) = T_{D_2}(x)$ then validates the lemma..

With these preparations, we prove the magnon-like t system.

Proof of (130)

With (140), (129) and using the duality and the quantum Jacobi-Trudi formula, we can express the product $t_1^{(1)}(x \pm \frac{1}{14}i)$ using only $T_0(x)$ and $T_2(x)$. Similarly $t_1^{(3)}$ can be rewritten by $T_0(x)$, $T_2(x)$ and $T_4(x)$, according to (142). Then it is immediately seen,

$$T_0(x)t_1^{(3)}(x) - t_1^{(1)}(x \pm \frac{1}{14}i) = T_2(x \pm \frac{11}{7}i) T_{D_2}(x).$$

Then the equality $T_{B_5}(x) = T_{D_2}(x)$, $T_2(x + \frac{12}{7}i) = T_7(x)$ and the definition of $t_2^{(1)}(x)$ in (144) concludes (130).

Proof of (131)

Consider the product $\Lambda_{(4,3,1)/(2)}(x - 4i) \Lambda_{(4,4,2)/(3,1)}(x + 4i)$. which is equal to

$$\phi(x \pm \frac{3}{14}i) t_1^{(2)}(x \pm \frac{1}{14}i + \frac{12}{7}i) \quad (152)$$

due to Lemma 15.

As is usual, the diagrammatical argument leads to

$$\Lambda_{(4,3,1)/(2)}(x-4i) \Lambda_{(4,4,2)/(3,1)}(x+4i) = \phi(x \pm \frac{3}{2}i) \phi(x \pm \frac{5}{2}i) \Lambda_{(7,7,5,1)/(6,2)}(x) + T_2(x) \Lambda_{(6,6,4,3,1)/(5,3,2)}(x).$$

Then we apply Lemma 16 and Lemma 17 to the first and the second term in the rhs, respectively, to reach

$$\phi(x \pm \frac{3}{14}i) (t_1^{(3)}(x + \frac{12}{7}i) T_0(x \pm \frac{2}{7}i + \frac{12}{7}i) + T_{B_2}(x + \frac{12}{7}i) T_{B_5}(x \pm \frac{1}{7}i + \frac{12}{7}i)). \quad (153)$$

By equating (152) and (153), we show the validity of (131) .

Proof of (133)

This is actually equivalent to (150). Note that $\Lambda_{(5,1)}(x + 8i) = \phi(x + \frac{3}{2}i) t_1^{(4)}(x + \frac{1}{14}i)$ and that the diagrammatic symmetry leads to $\Lambda_{(5,5)/(4)}(x - 8i) = \phi(x - \frac{3}{2}i) t_1^{(4)}(x - \frac{1}{14}i)$.

Note also $T_7(x) = T_{B_2}(x)$. Then one easily verifies (133) using $t_2^{(4)}(x)$ in (147).

Proof of (136)

This is the final nontrivial relation. This relation can be simply shown by using the result for the A_{4k+1} case. We simply put $k = 1$ and identify $t_1^{(1)}, t_1^{(2)}, t_1^{(3)}, t_1^{(4)}, t_2^{(3)}, g_1^{(1)}, g_1^{(2)}$ here with $t_1^{(3)}, t_1^{(4)}, t_1^{(5)}, t_1^{(6)}, t_2^{(5)}, t_1^{(1)}, t_1^{(2)}$ there and use the duality $T_2 = T_7^\vee$.

All remaining relations can be checked easily. Thus the above argument completes the proof of the magnon-like t system of the dilute A_5 model .

G Numerical Results for the dilute A_8 model in regime 2

We supplement some numerical data supporting the conjecture of the analyticity of Y functions in section 11.1. Throughout this appendix, we choose $\beta = 0.4$ and $J = 1$.

The solution to the Bethe ansatz equation, corresponding to the largest eigenvalue of QTM, assumes the form of two strings. We list the explicit locations of roots for $N = 10$, $q = 0$.

BAE Roots $q = 0$	
0.13548013966460354	$\pm 0.4464809553245548 i$
0.03263577725129405	$\pm 0.4935687693509952 i$
0.002550182914375612	$\pm 0.4961489632802383 i$
-0.02495383965703369	$\pm 0.4946627475810687 i$
-0.09400161546158932	$\pm 0.47389905045124336 i$

Their imaginary parts are approximately equal to $\pm \frac{1}{2}$, irrespective of L, N, q, β . See figure 18 .

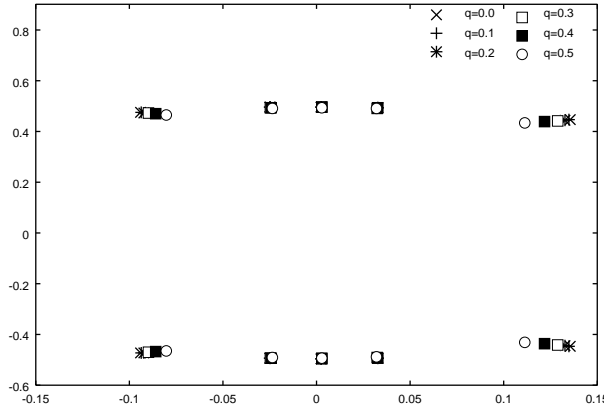


Figure 18: The Bethe ansatz roots for $N = 10$ for $q = 0, 0.1, 0.2, 0.3, 0.4, 0.5$. Their location changes only slightly.

The zeros for symmetric fusion QTM, T_m , ($m = 1, \dots, 7$), are plotted in fig. (19)-fig. (22). These figures clearly show that the simple-minded choice of Y in 17 is not appropriate: the choice requires T_m should be analytic in the strip $\Im x \in [-1, 1]$. (Or the arguments can be simultaneously shifted by half period so that strip is $\Im x \in [0.8, 1.8] \cup [-1.8, -0.8]$) Obviously, neither choice of strip results set of T_m free from zeros. (Especially, T_3 AND T_5 break the analyticity in both strips.) Therefore, the transformation of Y system to TBA is not legitimate.

The difference in the argument x appearing in the breather T , $sl_3 T$ and magnon-like t is much smaller than unity, which is crucial.

$T_{B_1}(x)$ is identified with $T_1(x)$. The functional relation then implies that it should be analytic within $\Im x \in [-\frac{3}{10}, \frac{3}{10}]$. This can be easily checked from the figure 19. Among other

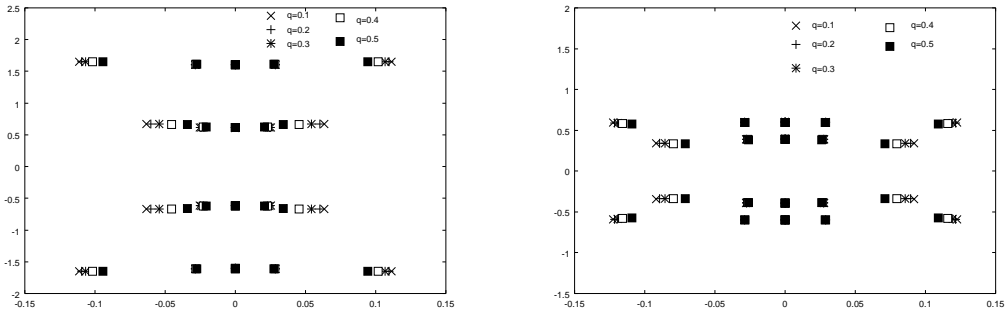


Figure 19: Zeros of $T_1(x)$ (left) and $T_2(x)$ (right) for $N = 10$ and $q = 0.1, 0.2, 0.3, 0.4, 0.5$.

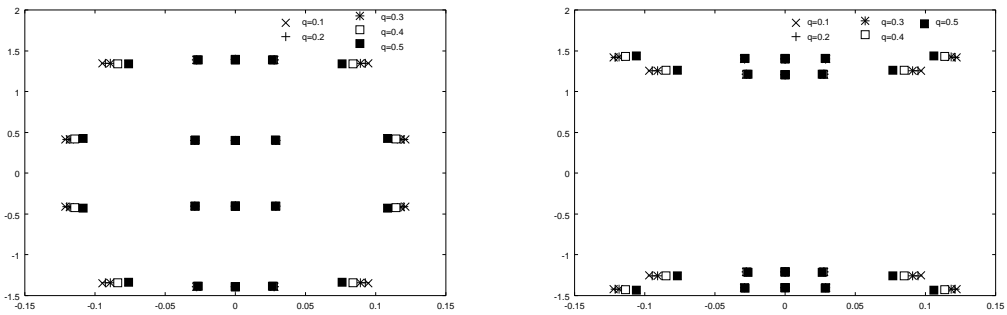


Figure 20: Zeros of $T_3(x)$ (left) and $T_4(x)$ (right) for $N = 10$ and $q = 0.1, 0.2, 0.3, 0.4, 0.5$.

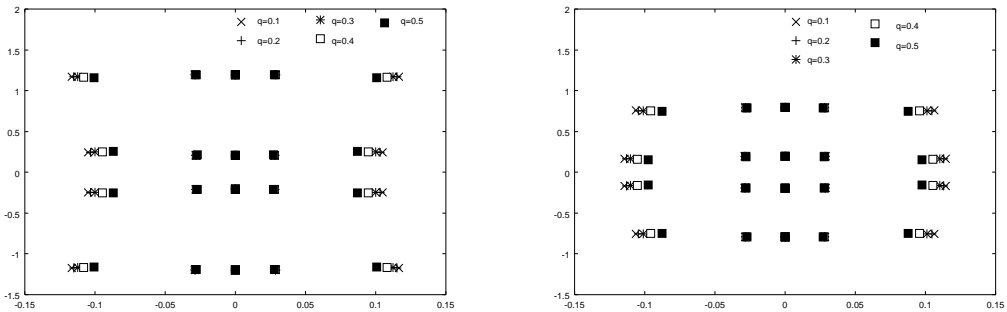


Figure 21: Zeros of $T_5(x)$ (left) and $T_6(x)$ (right) for $N = 10$ and $q = 0.1, 0.2, 0.3, 0.4, 0.5$.

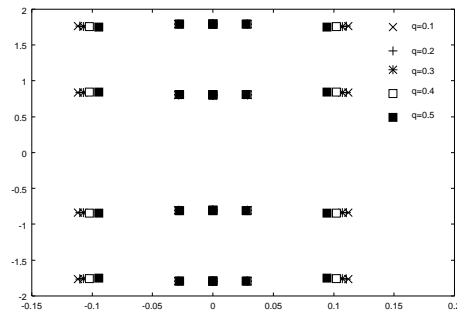


Figure 22: Zeros of $T_7(x)$ for $N = 10$ and $q = 0.1, 0.2, 0.3, 0.4, 0.5$.

T_m , $T_4(x)$ and $T_2(x + \frac{9}{5}i)$ are identified with $t_1^{(1)}(x)$ and $t_2^{(3)}(x)$. Their ANZC property in wider strip than $\Im x \in [-\frac{1}{5}, \frac{1}{5}]$ is clearly seen.

The breather related QTM, $T_{B_3}(x)$ is equal to $t_1^{(7)}(x)$, and $T_{B_5}(x)(= T_{D_2}(x))$ is $t_2^{(4)}(x)$, thus the information on their zeros is significant. Especially the latter appears frequently in the solution of other $t_m^{(a)}$, ($m = 2, 3$).

Their zeros are shown in fig. (23)

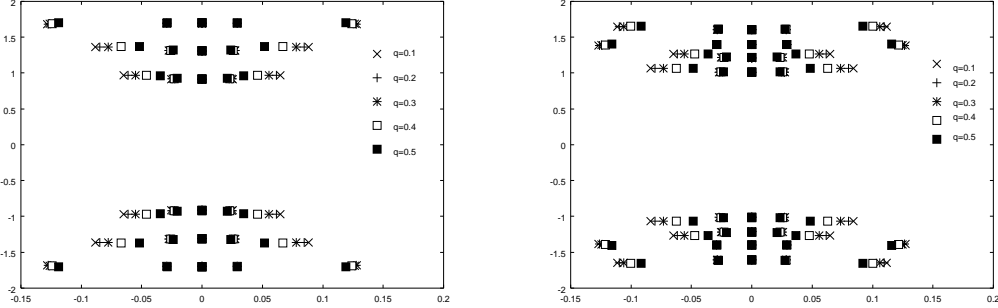


Figure 23: Zeros of $T_{B_3}(x)$ (left) and $T_{B_5}(x)(= T_{D_2})$ (right) for $N = 10$ and $q = 0.1, 0.2, 0.3, 0.4, 0.5$.

The remaining zeros of QTM to be specified are those for $t_1^{(0)}(x)$, $t_1^{(2)}(x)$, $t_1^{(3)}(x)$ and $t_1^{(4)}(x)$. They are depicted in fig. (24) and fig.(25), respectively.

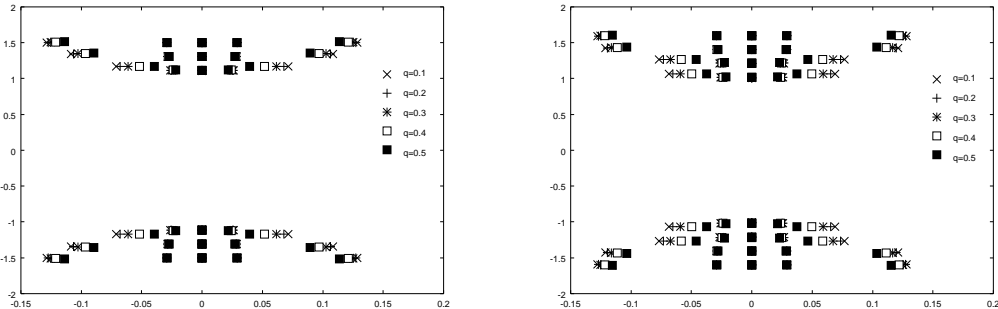


Figure 24: Zeros of $t_1^{(0)}(x)$ (left) and $t_1^{(2)}(x)$ (right) for $N = 10$ and $q = 0.1, 0.2, 0.3, 0.4, 0.5$.

By combining the above data on zeros, one can verify that all Y and $1 + Y$ possess no zeros or singularities from QTM in their own strips. Only trivial zeros (or singularity) of order N exists for Y_{B_1} simply coming from normalization factor $\phi^V(x)$ (or $T_0(x)$).

H The kernel matrices for $L = 5, 7$

For $L = 5$, we define the order as

$${}^t(\widehat{\log}Y_{B_1}, \widehat{\log}Y_{B_3}, \widehat{\log}Y_{B_5}, \widehat{\log}Y_{B_2}, \widehat{\log}Y_{K_1}, \widehat{\log}Y^{(1)}, \widehat{\log}Y^{(2)})$$

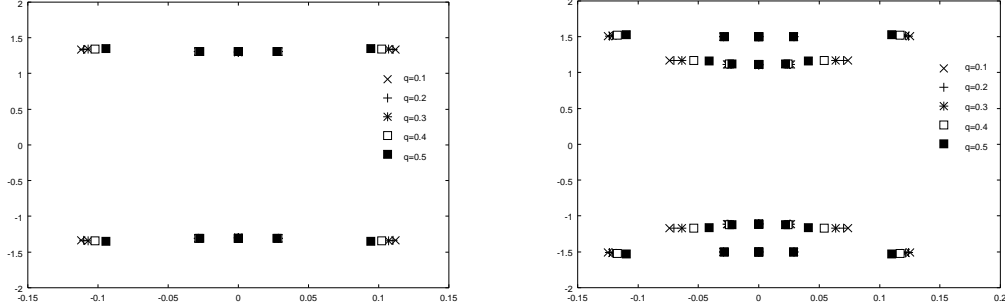


Figure 25: Zeros of $t_1^{(3)}(x)$ (left) and $t_1^{(4)}(x)$ (right) for $N = 10$ and $q = 0.1, 0.2, 0.3, 0.4, 0.5$.

then

$$\widehat{M} = \begin{pmatrix} 2\text{ch}\frac{3}{14}k & -1 & 0 & 0 & 0 & 0 & 0 & 0 & 0 \\ -1 & 2\text{ch}\frac{3}{14}k & -1 & 0 & 0 & 0 & 0 & 0 & 0 \\ 0 & -1 & 2\text{ch}\frac{3}{14}k & 0 & -1 & -2\text{ch}\frac{2}{14}k & -2\text{ch}\frac{1}{14}k & , -1 \\ 0 & 0 & 0 & 2\text{ch}\frac{3}{14}k & -2\text{ch}\frac{2}{14}k & -1 & -2\text{ch}\frac{1}{14}k & , -1 \\ 0 & 0 & 0 & -1 & 2\text{ch}\frac{1}{14}k & 0 & 0 & 0 \\ 0 & 0 & -1 & 0 & 0 & 2\text{ch}\frac{1}{14}k & 0 & 0 \\ 0 & 0 & 0 & 0 & 0 & 0 & 2\text{ch}\frac{1}{14}k & 0 \\ 0 & 0 & 0 & 0 & 0 & 0 & 0 & 2\text{ch}\frac{1}{14}k \end{pmatrix}$$

$$\widehat{K}_0 = \begin{pmatrix} 0 & 1 & 0 & 0 & 0 & 0 & 0 & 0 \\ 1 & 0 & 1 & 0 & 0 & 0 & 0 & 0 \\ 0 & 1 & 0 & 0 & 1 & 2\text{ch}\frac{2}{14}k & 2\text{ch}\frac{1}{14}k & , 1 \\ 0 & 0 & 0 & 0 & 2\text{ch}\frac{2}{14}k & 1 & 2\text{ch}\frac{1}{14}k & , 1 \\ 0 & 0 & 0 & 1 & 0 & 0 & -1 & 0 \\ 0 & 0 & 1 & 0 & 0 & 0 & -10 & 0 \\ 0 & 0 & 0 & 0 & -1 & -1 & 0 & -1 \\ 0 & 0 & 0 & 0 & 0 & 0 & -1 & 0 \end{pmatrix}.$$

For $L = 7$, we define the order as

$${}^t(\widehat{\log}Y_{B_1}, \widehat{\log}Y_{B_3}, \widehat{\log}Y_0^{(1)}, \widehat{\log}Y_0^{(2)}, \widehat{\log}Y_1^{(1)}, \widehat{\log}Y_1^{(2)}, \widehat{\log}Y_1^{(3)}, \widehat{\log}Y_1^{(4)}, \widehat{\log}Y_1^{(5)}, \widehat{\log}Y_1^{(6)},)$$

then

$$\widehat{M} = \begin{pmatrix} 2\text{ch}\frac{5}{18}k & -1 & 0 & 0 & 0 & 0 & 0 & 0 & 0 & 0 \\ -1 & 2\text{ch}\frac{5}{18}k & 0 & -2\text{ch}\frac{1}{18}k & 0 & -1 & 0 & 0 & 0 & 0 \\ 0 & 0 & 2\text{ch}\frac{4}{18}k & -1 & 0 & 0 & 0 & 0 & 0 & 0 \\ 0 & -1 & -1 & 2\text{ch}\frac{4}{18}k & 0 & 0 & 0 & 0 & 0 & 0 \\ 0 & 0 & 0 & 0 & 2\text{ch}\frac{1}{18}k & 0 & -1 & 0 & 0 & 0 \\ 0 & 0 & 0 & 0 & 0 & 2\text{ch}\frac{1}{18}k & 0 & -1 & 0 & 0 \\ 0 & 0 & 0 & 0 & -1 & 0 & 2\text{ch}\frac{1}{18}k & 0 & -1 & 0 \\ 0 & 0 & 0 & 0 & 0 & -1 & 0 & 2\text{ch}\frac{1}{18}k & -1 & 0 \\ 0 & 0 & 0 & 0 & 0 & 0 & -1 & -1 & 2\text{ch}\frac{1}{18}k & -1 \\ 0 & 0 & 0 & 0 & 0 & 0 & 0 & 0 & -1 & 2\text{ch}\frac{1}{18}k \end{pmatrix}$$

$$\widehat{K}_0 = \begin{pmatrix} 0 & 1 & 0 & 0 & 0 & 0 & 0 & 0 & 0 & 0 \\ 1 & 0 & 0 & 2\text{ch}\frac{1}{18}k & 0 & 1 & 0 & 0 & 0 & 0 \\ 0 & 0 & 0 & 1 & -2\text{ch}\frac{3}{18}k & 0 & -2\text{ch}\frac{2}{18}k & -1 & -2\text{ch}\frac{1}{18}k & -1 \\ 0 & 1 & 1 & 0 & 0 & -2\text{ch}\frac{3}{18}k & -1 & -2\text{ch}\frac{2}{18}k & -2\text{ch}\frac{1}{18}k & -1 \\ 0 & 0 & -1 & 0 & 0 & 0 & 1 & 0 & 0 & 0 \\ 0 & 0 & 0 & -1 & 0 & 0 & 0 & 1 & 0 & 0 \\ 0 & 0 & 0 & 0 & 1 & 0 & 0 & 0 & 1 & 0 \\ 0 & 0 & 0 & 0 & 0 & 1 & 0 & 0 & 1 & 0 \\ 0 & 0 & 0 & 0 & 0 & 0 & 1 & 1 & 0 & 1 \\ 0 & 0 & 0 & 0 & 0 & 0 & 0 & 0 & 1 & 0 \end{pmatrix}.$$

References

- [1] G.E. Andrews, R.J. Baxter and P.J. Forrester, J. Stat. Phys. **35** (1984) 193 .
- [2] S.O.Warnaar, B. Nienhuis and K. A. Seaton, Phys. Rev. Lett. **69**(1992) 710.
- [3] S.O.Warnaar, B. Nienhuis and K. A. Seaton, Int. J. Nod. Phys. **B 7** (1993) 3727.
- [4] A.B. Zamolodchikov, Adv. Stud. Pure. Math. **19** (1989) 641.
- [5] A.B. Zamolodchikov, Int. J. Mod. Phys. **A 4** (1989) 4235.
- [6] M. Henkel and H. Saleur, J. Phys. **A 22** (1989) L513.
- [7] P.G. Lauwers and V. Rittenberg, Phys. Lett. B **233** (1989) 197.
- [8] I.R. Sagdeev and A. B. Zamolodchikov, Mod. Phys. Lett. **B3** (1989) 1375.
- [9] G. von Gehlen, Nucl. Phys. **B330** (1990) 741.
- [10] V.P. Yurov and Al. B. Zamolodchikov, Int.J. Mod. Phys. **A6** (1991) 4556.

- [11] P. Dorey, "Hidden Geometrical Structures in Integrable Models" in *integrable quantum field theories*, NATO Advanced Study Seies, Physics V.310, eds. L. Bonuro et al (Plenum, New York, 1993)
- [12] G. Delfino and G. Musssardo, Nucl Phys. **B455** (1995) 724.
- [13] M.T. Batchelor, V. Fridkin and Y.K. Zhou, J. Phys. A, J. Phys. **A29** (1996) L61.
- [14] M.T. Batchelor and K.A. Seaton, J. Phys. **A 30** (1997) L479.
- [15] M.T. Batchelor and K.A. Seaton, Nucl. Phys. **B520** (1998) 697.
- [16] C. Korff and K.A. Seaton, Nucl.Phys. **B636** (2002) 435.
- [17] S.O.Warnaar, P.A. Pearce, B. Nienhuis and K. A. Seaton, J. Stat. Phys **74** (1994) 469.
- [18] B. McCoy and P. Orrick, Phys. Lett. **A 230** (1997) 24.
- [19] V.V. Bazhanov, O. Warnaar and B. Nienhuis, Phys. Lett. **B 322** (1994) 198.
- [20] U. Grimm and B. Nienhuis, "Scaling Properties of the Ising Model in a Field", in: *Symmetry, Statistical Mechanical Models and Applications*, Proceedings of the Seventh Nankai Workshop (Tianjin 1995), edited by M.L. Ge and F.Y. Wu, World Scientific, Singapore (1996), pp.384.
- [21] U. Grimm and B. Nienhuis, Phys. Rev. **E 55** (1997) 5011.
- [22] J. Suzuki, Nucl Phys **B528** (1998) 683.
- [23] J. Suzuki, Progress in Math. **191** (2000) 217.
- [24] P. Dorey, A. Pocklington and R. Tateo, Nucl. Phys. **B661** 425.
- [25] P. Dorey, A. Pocklington and R. Tateo, Nucl. Phys. **B661** 464.
- [26] F. A. Smirnov, Int. J. Mod. Phys. **A6** (1991) 1407.
- [27] L. Chim and A. Zamolodchikov, Int. J. Mod. Phys. **A 7** (1992) 5317.
- [28] A. Koubek, M. J. Martins and G. Mussardo, Nucl. Phys. **B368** (1992) 591.
- [29] A. Koubek, Int. J. Mod. Phys. **A9**(1994) 1909.
- [30] P. Dorey, R. Tateo and K.E. Thompson, Nucl. Phys. **B470** (1996) 317.
- [31] Al.B. Zamolodchikov, Phys. Lett **B 253** (1991) 391
- [32] A. Kuniba and T. Nakanishi, Mod. Phys. Lett. **A7** (1992) 3487.

- [33] R. Tateo, Int. J. Mod. Phys. **A10** (1995) 1357.
- [34] P.P. Kulisk, N. Yu. Reshetikhin and E. K. Sklyanin, Lett. Math. Phys. **5** (1981) 393.
- [35] A. Klümper and P. A. Pearce, Physica **A183**(1992) 304.
- [36] A. Kuniba, T. Nakanishi and J. Suzuki, Int. J. Mod. Phys. **A9** (1994) 5215, ibid 5267.
- [37] Y. Hara, M. Jimbo, H. Konno, S. Odake and J. Shiraishi, J. Math. Phys. **40** (1999) 3791.
- [38] U. Grimm, P.A. Pearce and Y.K. Zhou, Physica **A 222** (1995) 261
- [39] V.V. Bazhanov and N. Yu Reshetikhin, J.Phys. **A23** (1990) 1477.
- [40] A. Kuniba and J. Suzuki, Comm. Math. Phys. **173** (1995) 225.
- [41] J. Suzuki, Phys. Lett. **A195** (1994) 190.
- [42] Z. Tsuboi, J. Phys.**A 30** (1997) 7975.
- [43] A.G. Izergin and V. E. Korepin, Comm. Math. Phys. **79** (1981) 303.
- [44] M. Suzuki, Phys. Rev.**B.31** (1985) 2957.
- [45] T. Koma, Prog. Theoret. Phys. **78**(1987) 1213.
- [46] M. Suzuki and M. Inoue, Prog. Theor. Phys. **78** (1987) 787.
- [47] J. Suzuki, Y. Akutsu and M. Wadati, J. Phys. Soc. Japan **59** (1990) 2667.
- [48] M. Takahashi, Phys. Rev. **B 43** (1991) 5788, see also vol. 44 p. 12382.
- [49] A. Klümper, Ann. Physik **1** (1992) 540.
- [50] A. Klümper, Z. Phys. **B 91** (1993) 507.
- [51] G. Jüttner, A. Klümper and J. Suzuki, Nucl. Phys. **B512**(1998) 581.
- [52] A. Kuniba, K. Sakai and J. Suzuki, Nucl Phys **B525** 597.
- [53] K. Sakai and Z. Tsuboi, Int. J. Mod. Phys. **A15** (2000) 2329.
- [54] T.R. Klassen and E. Melzer, Nucl. Phys. **B350**(1991) 635.
- [55] Y.K. Zhou, unpublished note
- [56] I. Krichever, O. Lipan, P. Wiegmann and A. Zabrodin, Comm. Math. Phys. **188** (1997) 267
- [57] R.M. Ellem and V.V. Bazhanov Nucl.Phys. **B647** (2002) 404.

- [58] R. Kedem, T.R. Klassen, B.M. McCoy and E. Melzer, Phys.Lett. **B307** (1993) 68-76.
- [59] S. Dasmahapatra, R. Kedem, T.R. Klassen, B.M. McCoy and E. Melzer, Int.J.Mod.Phys. **B7** (1993) 3617.
- [60] A. Berkovich, Nucl.Phys. **B431** (1994) 315.
- [61] E. Melzer, Lett.Math.Phys. **31** (1994) 233.
- [62] A. Berkovich and B.M. McCoy, Lett.Math.Phys. **37** (1996) 49 .
- [63] S. O. Warnaar, J. Stat. Phys.**82** (1996) 657.
- [64] S. O. Warnaar, J. Stat. Phys.**84** (1996) 49.
- [65] S.V. Kerov, A. N. Kirillov and N. Y. Reshetikhin, J. Sov. Math. **41**(1988) 916.
- [66] A. N. Kirillov and N. Y. Reshetikhin, J. Sov. Math. **41**(1988) 925.
- [67] G. Hatayama, A. Kuniba, M. Okado, T. Takagi and Y. Yamada, Contemporary Math. **248** (1999) 243.
- [68] G. Hatayama, A. Kuniba, M. Okado, T. Takagi and Z.Tsuboi, Prog.Math.Phys. **23** (2002) 205.
- [69] A. Schilling, "Rigged configurations and the Bethe Ansatz" (math-ph/0210014).
- [70] A. Berkovich, B.M. McCoy and P.A. Pearce , Nucl.Phys. **B519** (1998) 597 .
- [71] A. Berkovich and B.M. McCoy, "The perturbation $\phi_{2,1}$ of the $M(p, p + 1)$ models of conformal field theory and related polynomial character identities" (math.QA/9809066).
- [72] S.O. Warnaar and P.A. Pearce, J.Phys. **A27** (1994) L891.
- [73] J. Suzuki, J. Phys. **37** (2004) 511.